2009

The Neural Circuitry Of Social Behavior In C. elegans

Evan Z. Macosko

THE NEURAL CIRCUITRY OF SOCIAL BEHAVIOR IN *C. ELEGANS*

A Thesis Presented to the Faculty of

The Rockefeller University

in Partial Fulfillment of the Requirements for

the degree of Doctor of Philosophy

by

Evan Z. Macosko

June 2009

THE NEURAL CIRCUITRY OF SOCIAL BEHAVIOR IN *C. ELEGANS*

Evan Z. Macosko, Ph.D.

The Rockefeller University 2009

Most animal species, from simple invertebrates to complex mammals, require behavioral mechanisms to communicate with and respond to conspecifics, whether to mate, to assess predatory danger, or evaluate the nutritional quality of the surrounding environment. Understanding the molecular and cellular underpinnings of these social behaviors remains a central challenge in neurobiology. I used the nematode *C. elegans* as a model system to study the genetics and neural circuitry that underlie social behavior.

First, I evaluated the behavioral responses of *C. elegans* to a nematode extract (deathmone), which served as a model for alarm pheromones in other animal species (chapter 2). Worms showed acute avoidance of deathmone, and reduced their exploration when cultivated on it, a behavior termed "dwelling." I combined chemical analysis, laser ablation studies, and genetic studies to identify the sensory neurons and molecular signaling pathways that promote dwelling in response to deathmone.

Second, I investigated the neuronal substrates responsible for social feeding, a behavior in which certain strains of *C. elegans* display high lomocotory speeds, accumulate on the border of bacterial food lawns, and aggregate into groups. A low activity or null allele of the neuropeptide y receptor homologue *npr-1* promotes social feeding, while a high activity form—which is found in the wild-type *N2* strain—promotes solitary behavior[1]. Expression of a high-activity *npr-1* cDNA specifically in the interneuron RMG converted

npr-1 loss-of-function mutants from social feeders into solitary ones. The RMG neurons are gap junctional hubs that electrically couple the sensory neurons URX, ASH, and ADL—all previously implicated in social feeding—and the pheromone-sensing neuron ASK, suggesting that social feeding and pheromone responses may be related. Indeed, *npr-1* social feeders are attracted to ascarosides, while *N2* solitary feeders are repelled, a behavioral difference that is dependent on RMG function. Calcium imaging of ASK and its postsynaptic partner AIA demonstrated that RMG promotes signaling from ASK to AIA. Taken together, these data provide a common neural circuitry for social behaviors in *C. elegans*, and offer some insights into the molecular mechanisms of their regulation.

Acknowledgments

Graduate school has been a time of great personal and intellectual growth that would not have been possible without advice, encouragement, and support from many people. I thank my thesis committee members, Jeffrey Friedman, Samie Jaffrey, Michael Young, and Bruce McEwen. My first rotation in Jeff's lab was an important scientific training ground, and the laboratory environment he created was both friendly and rigorous. Samie has been a continuous source of personal and professional support since I start my rotation with him in medical school. It was from him that I learned some of the most important principles of experimental design, and the magical ratio of diet to regular coke that maximizes taste while minimizing calories. Both Bruce and Mike have provided thoughtful insights into my work during our discussions.

Cori Bargmann has been a fantastic mentor and advisor. Her rare combination of creativity and encyclopedic knowledge has served as an illustrative example of how to do rigorous and innovative science. Each interaction with her left me thoughtful, engaged, and motivated, always welcome feelings, especially amidst those occasional moments of frustrated despair that are an essential part of the graduate school experience. She was always available with intellectual and personal support, yet she allowed me the freedom to try, to fail, to re-evaluate, and ultimately to assemble a body of scientific data of which I am very proud.

I am also grateful to Cori for the educational and supportive lab environment she has created. The people I have worked with were not just inspiring colleagues but have become good friends. I thank my baymates, Evan Feinberg and Greg Lee, for all of the

invigorating hilarity we fomented. It was not only fun, but also therapeutic during those times of experimental monotony. Evan also created Cre-Lox plasmids that were important for my work, while Greg's rare aesthetic intuition was indispensable during the creation of figures. I am tremendously grateful to Sreekanth Chalasani for his time, thoughts, and advice, especially during the summer months of 2008 when I was learning functional calcium imaging from him. His unique sense of humor, though often difficult to decipher, was also a perpetual spirit-lifter. I thank Navin Pokala for some great conversations, both about science and politics, and for his help in adapting tetanus toxin to use in *C. elegans*. Manuel Zimmer has provided helpful guidance, especially with regards to oxygen-related experiments. Patrick McGrath and Makoto Tsunuzaki were both great sources of scientific advice, and conversations I had with them were crucial in determining my path of scientific inquiry. Bluma Lesch and Andres Bendesky have been great friends and colleagues. Early on in the lab, I received some patient and through guidance from Massimo Hilliard and Yun Zhang, for which I am very grateful. I have been thankful to work with Christian Woods, our lab manager, whose thoughtfulness and creativity have made the lab incredibly efficient and pleasant. He also throws a great Christmas party.

I have been fortunate to have great collaborators in Rebecca Butcher and her postdoctoral supervisor Jon Clardy. Rebecca and I first met when I was an undergraduate in Stuart Schreiber's lab, before we serendipitously found ourselves working together to purify and characterize behaviorally active molecules from *C. elegans*. In addition, I thank Piali Sengupta, who kindly shared unpublished results with us that helped inform my own experimental designs.

I have been deeply grateful for having a cadre of supportive friends here in New York City during my graduate career. Though essential to one's sanity, it can be hard to both physically and mentally leave the lab. John Raskin, Adam Ruder, and Jonah Westerman have helped me to enjoy the city, and remain conversant in matters non-scientific. Lastly, I want to thank my family for all of their help. My fiancée Candace has been a steadfast and unconditional source of support for me, for which I am deeply grateful. And my parents, whose advice, encouragement, and care have been essential to my happiness these past three years.

Table of Contents

List of Tables

List of Figures

Chapter 1*:*

Introduction

In order to survive and reproduce, animals must be able to perceive and interact with other individuals in their species. Social behavior—which we can define as any activity that involves cooperation in a group of conspecific individuals[1]—is not restricted to the elaborately structured arthropod colonies of ants and bees, or the hierarchical societies of primates such as chimpanzees. Rather, it is a direct consequence of evolutionary pressures experienced by every animal: competition for nutritional resources, avoidance of predation and harmful environmental conditions, and selection of a mating partner. Even sea anemones, which are capable of asexual reproduction and feed in isolation, display aggressive behaviors towards conspecifics[2] and possess chemical means of signaling alarm to each other[3]. Understanding the purpose of social behavior, its adaptive consequences, and its neural underpinnings are thus important goals in biology.

Social behavior is a phenomenon of nervous systems, which receive and process complex stimuli to effect adaptive behavioral outputs. Given the pervasiveness of sociality, might there be common, shared neural mechanisms whereby different animal species produce and regulate social behavior? By studying social behavior in a simple, well-defined system, can we arrive at some organizing principles underlying sociality? This has been the focus of my graduate studies. I have sought to harness the genetic and anatomical strengths of the nematode *Caenorhabditis elegans* to understand, at the level of neuronal and genetic interactions, how social behavior works.

Social behaviors can be grouped according to whether they afford individual animals an advantage in one of four categories: (1) resource exploitation (foraging) (2) mate finding, (3) predation protection, and (4) environmental protection. For each of the four categories, I will provide an example from a classical social system, and then describe potentially related phenomena in *C. elegans*.

1. Exploitation of resources. Bark beetles have a well-studied aggregation phenomenon[4] in which an individual, having found a new plant food source, secretes pheromones that attract other beetles, who help to digest away plant resin that obstructs feeding. Without aggregation, beetle foraging is seriously impaired[5]. Interestingly, these same chemical signals also serve as kairomones, attracting predators to the feeding site[6]. Is the pheromone a true social signaling compound, promoting cooperation amongst beetles, or a metabolic byproduct, sensed by predators and conspecifics alike, that has both adaptive and maladaptive consequences? Such questions illustrate how definitional ambiguities can persist, even after thorough examination of potential social behaviors like aggregation phenomena. Theoretical approaches can be used to suggest adaptive advantages to particular behaviors, as has been done for bark beetle aggregation[5]. Alternatively, a more detailed understanding of the anatomical and molecular underpinnings of pheromone production and sensation systems can suggest answers. For example, highly specialized glandular production of a pro-social pheromone with no other apparent function is likely to have evolved for an adaptive purpose.

C. elegans displays an aggregative behavior known as social feeding in which certain strains, prefer to accumulate on the edge of bacterial lawns and feed in tight groups[7]. Although the presence of bacterial food is required for this behavior, no

resource exploitation advantage, akin to that seen in beetle aggregation, has been noted. Interestingly, a comprehensive meta-study of aggregation phenomena in nonsocial arthropods found that insects which feed on microbes, or on microbially predigested plant matter, are far more likely to aggregate than those that feed on living plants[8]. Aggregating adults could help to inoculate plant matter with microcrobes in order to improve environmental conditions for larvae. *C. elegans*, whose diet is entirely microbial and is naturally found in environments rich in decaying plant matter[9], could employ social feeding for similar purposes.

2. Mating. Nearly all animal species engage in sexual reproduction[10]; consequently, an innumerable number of social behaviors are devoted to the identification and selection of an appropriate mate. Fire ants provide a good example. During nuptual flights, female ants initiate the mating process by secreting volatile odors that attract males[11]. The nuptual flights themselves begin when members of the colony secrete other odors that promote male excitability. Interestingly, these same compounds are also used as alarm pheromones to begin the coordination of group defensive maneuvers[12], suggesting that disparate behavioral phenomena within a species may pass through common intermediates.

Mating behavior in *C. elegans* has been well-studied[13]. The species consists of two sexes: a hermaphrodite and a male. To bear progeny, hermaphrodites can either be self-fertilized or cross-fertilized by males. Males, when encountering a hermaphrodite, execute a multi-step copulation program that requires input from sensory neurons[14]. The finding of potential mates involves attraction of males to specific compounds called ascarosides that are secreted by hermaphrodites[15,16]. These same compounds participate

in the developmental decision to form a dauer larva[17,18,19] in which, under conditions of crowding, high temperature, and low food availability, young larvae enter an alternative developmental progression into a non-reproductive form that is resistant to a variety of environmental stresses. This indicates that, like fire ants, worms utilize the same chemicals to initiate very different physiological and behavioral processes.

3. Predation. Avoidance of predation through social behavior is seen across the animal kingdom, but is perhaps best exemplified by schooling in fish. When the threat of predation is elevated, as evaluated primarily by chemical and visual cues[20], individual teleost fishes assemble into highly coordinated groups that can execute a variety of defensive maneuvers including avoidance, in which the school swims away from the predator, flash expansion, in which the school disassembles with individuals swimming chaotically in random directions, and the fountain effect, where a school divides in half around a predator, reassembling behind it[21]. These behaviors are all designed to confuse the predator, and reduce the predation threat to individual members of the school. *C. elegans* social behavior has not been studied from the perspective of predation; my examination of the subject appears in Chapter 2.

4. Environmental protection. Finally, social behavior can exist in order to ameliorate environmental conditions for the individual members of a species. Honeybees, for instance, possess an impressively elaborate means of stabilizing the temperature of their hives[1]. During the cold winter months, honeybees aggregate into groups, in which individuals in the center produce heat through metabolic activity, while bees on the edges of the aggregates serve as insulation. On the other hand, when the

external temperature is high, the bees engage in coordinated wing flapping that aerates the hive, cooling its members.

Aggregation of *C. elegans* may all play a role in environmental optimization. *C. elegans* has a strong preference for intermediate oxygen levels of 8-12% over atmospheric oxygen[22]. The social feeding of *C. elegans* occurs at atmospheric oxygen levels (21%), and the oxygen concentration in the interior of worm aggregates is much lower than 21% due to local consumption[22]. These observations suggest that worms both produce and seek out regions of lower oxygen, suggesting that they, like honeybees, use aggregation as a means of improving their environment.

In order to truly understand social behaviors like those described above, the behaviors must be examined at the cellular and molecular levels. Many of the classic social behavior paradigms that have been studied by zoologists, entomologists, and ecologists are of limited use in such studies, because the relevant organisms are not experimentally tractable. New genomic tools, however, are starting to become available to address this deficiency. For example, gene expression analyses of the honeybee *Apis mellifera* have resulted in numerous insights into potential mechanisms governing complex social behaviors. Young adult honeybees perform tasks in the hive, such as brood care, while older adults leave the hive to gather food. Expression of the gene *foraging (for)*, which encodes a cGMP-dependent protein kinase originally identified in the fruit fly *Drosophila melanogaster* as a regulator of fly foraging behavior[23], increases when honeybees leave the hive to forage, and pharmacological activation of *for* can induce premature foraging in young adult bees[24]. Other studies have used whole-genome expression profiling to identify new candidate genes that affect honeybee social

behaviors[25]. Such endeavors offer the beginnings of a molecular understanding of complex social behaviors.

The molecular study of social behavior in vertebrates has focused extensively on neuropeptides, which can function as neurotransmitters at synapses, or as hormones, acting at receptors on distant neurons[26]. In particular, vasopressin and oxytocin, two structurally related neuropeptides, have been implicated in a diverse array of social behaviors, including pair bonding, sexual behavior, pup nursing, and social trust[27,28]. The availability of genetic knockout and rescue techniques in the mouse *Mus musculus* has allowed researchers to evaluate the requirement of vasopressin or oxytocin for the various behaviors they elicit[29,30], and understand where they act in the mouse brain[31]. These studies provide the foundation for neural circuit mapping of social behavior in very large and complex nervous systems.

In order to achieve a finer understanding of how neural circuitry is used for social behavior, simpler, better defined, and more genetically tractable systems are needed. In this endeavor, the fruit fly *Drosophila* has proven informative. Fruit fly mating behavior has been an area of intense molecular, cellular, and behavioral study[32]. The male fly, when sensing a receptive female, emits a courtship song produced by wing vibration; the female responds by reducing her speed and opening her vaginal plate for copulation[33]. Both of these steps involve decisions that are informed by chemical and aural stimuli emitted by potential mating partners. The pheromone *cis*-vaccenyl acetate (cVA), produced specifically by male flies, was originally isolated as a volatile that promotes aggregation in both females and males[34]. cVA is transferred to females during mating, which makes mated females less attractive to males. In the presence of cVA from either

males or mates females, male courtship is inhibited, and when the receptor for cVA, OR67d, is deleted, male flies inappropriately court other males[35]. By contrast, OR67d deletion in females results in a decrease in receptivity to courtship[35], indicating that cVA functions are sexually dimorphic.

The availability of transgenic, genomic, and other molecular tools in *Drosophila* have allowed researchers to gain a detailed understanding of the pathways that control cVA detection and responses. Additional molecules required for sensation of cVA have been identified[36,37,38], while a genetically encoded neuronal tracer was used to observe sexual dimorphisms in the anatomy of neurons downstream of the OR67d-expressing cells[39].

Downstream of mating pheromones, the *fruitless (fru)* gene, a transcription factor that directs sex specification in the nervous system, has been invaluable in understanding the circuitry underlying sexual dimorphisms in *Drosophila* behavior. The *fru* gene is expressed in approximately 2000 neurons in the fly nervous system[40], which are obvious candidates for controlling sex-specific behaviors like male singing. A female that inappropriately expresses the male-specific isoform of *fru* shows singing behavior that is otherwise restricted to males[41]. A specific subset of 20 *fru*(+) neurons made to express the male-specific *fru* isoform in females was subsequently found to be sufficient to induce singing[42]. These experiments indicate the importance of classical regulators, like transcription factors, in the biological control of social behavior.

To fully appreciate the significance of social behavior, it must be integrated into an understanding of the functions of the entire nervous system. For instance, elicitation of many social behaviors requires specific environmental stimuli, such as the temperature

control methods of the honeybee. How do different social behaviors interact with each other, and how do non-social stimuli affect social phenotypes? To address such questions, a simple, well-defined system like *C. elegans* is desirable.

The genetic advantages of *C. elegans* are many[43]: worms complete a reproductive cycle in about three days, and produce 300 eggs when self-fertilized. The hermaphrodite can reproduce without mating, enabling the efficient propagation of mutant strains that are deficient in locomotion or mating behavior. Animals can be cultivated on *E. coli* grown on an agar medium, and strains are easily frozen, remaining viable for decades[44]. Moreover, transgenesis is technically straightforward[45], allowing for targeted expression of desired genes to particular tissues. RNAi mediated knockdown of gene expression was pioneered in *C. elegans*[46], although it often remains cumbersome in neurons[47]. In addition to these genetic tools, the lineages of each cell have been delineated[48] and the neural connectivity solved from electron microscopy (EM) of serial section[49]. The nervous system is thus a well defined, known entity, with individual cell classes that can be reliably identified in different individuals based on their fixed positions along the animal.

These advantages have been used to explore the cellular and molecular bases of numerous behaviors. The first systematic study of *C. elegans* behavior elucidated a circuit for mechanosensation and locomotion by destroying individual neurons, characterizing the defects[50], and then isolating mutants defective in responses that required a single sensory cell type[51]. These seminal studies have yielded numerous important biological discoveries, including the cloning and characterization of multiple subunits of a touch receptor and the identification of "command" interneurons that

control backward or forward locomotion through the direction of motoneurons. Since then, sensory neurons and transduction molecules have been identified for a wide variety of behaviors[52], including chemotaxis[53], thermotaxis[54,55], and male mating[56]. Further studies revealed that the worm's nervous system was capable of executing forms of plasticity, such as mechanosensory habituation[57], olfactory adaptation[58], and aversive learning[59].

A variety of approaches have been used to gain greater insight into these individual behaviors. Quantitative analyses have been applied to thermotaxis[60] and chemotaxis[61], and a mechanistic model has been proposed for the latter based upon chemotaxis in bacterial organisms[62]. Calcium imaging[63,64] and electrophysiological methods[65,66] have been employed to examine the activity of individual neurons in response to fixed stimuli, while chemical fractionation and purification have been used to isolate behaviorally active compounds that attract males to hermaphrodites[16]. Recently, microfluidic devices were employed to carefully control worm movement and sensory stimulation during calcium imaging[67,68] and behavioral studies[69].

Can the approaches available in this system be used to examine social behavior? To date, studies of social behavior in *C. elegans* have focused on social feeding and mating, both of which have been briefly described above. The first goal of my graduate work was to expand our knowledge of *C. elegans* social behavior: are there other behavioral responses elicited by worm pheromones? A very common, and evolutionarily ancient, response to conspecifics occurs in the context of danger, when animals release alarm signals, especially when stressed or injured. In Chapter 2, I examine behavioral responses to an extract of injured worms, and follow up extensively on one of these

behaviors, in which animals reduce their local exploration in response to this alarm cue (termed dwelling). I present data on the molecular composition of the pheromone that elicits *C. elegans* dwelling, and the genetic pathways that are involved in the perception and processing of the pheromone cue.

A basic but often formidable task in the study of social behavior is the rigorous demonstration that an observed biological phenomenon is, in fact, social. When bats exit their caves together, forming a swarm thousands or millions large, are they each responding to a common external cue (i.e. sunset) or are they cooperating to lower their chance of predation[70]? The identification of a chemical or visual cue to which other conspecifics respond is a powerful means of demonstrating sociality. In Chapter 3, I investigate social feeding in detail, and re-evaluate the extent to which it can be described as social. A polymorphism in the neuropeptide Y receptor homologue *npr-1* had been found to control social feeding[7]. To uncover where *npr-1* acts in the *C. elegans* nervous system, I rescued the gene cell-specifically in the loss-of-function background. These studies on social feeding, and the subsequent neuronal circuitry they exposed, are presented. Intriguingly, I found that the circuitry governing social feeding and pheromone responses overlap extensively, and provide evidence that the two behaviors may be functionally related.

Finally, in Chapter 4, I describe my reverse genetic approaches to studying social behavior. As described above, the neuropeptides vasopressin and oxytocin have long-established roles in social behavior. I present my behavioral experiments with a *C. elegans* vasopressin/oxytocin peptide homologue and some of its candidate receptors.

My work defines overlapping "social behavior circuits" in *C. elegans* that mediate an array of behavioral responses. The insights gleaned from these circuits may offer lessons for the study of behaviors (particularly social ones) in other organisms.

Chapter 2:

Behavioral Responses to C. elegans Alarm Pheromone

One of the most common chemosensory social behaviors is the alarm response, in which a frightened or injured animal releases compounds that induce defensive behaviors in conspecifics. Alarm pheromones have been found in a wide range of animals, including rats[71], fish[72], many insects[73], sea urchins[74], and anemones[3]. The best-studied example is the Schreckstoff system in ostariophysans, a superorder of fish that constitutes 28% of all known fish species[75]. These fish possess a specialized pouch in the dermis which, when the skin is damaged, causes the release of a complex array of substances, collectively termed "Schreckstoff" (German for "scary stuff") that induce behavioral responses in nearby animals. While one component of Schrekstoff, a hypoxanthine derivative, appears to be common to almost all of the fish species in this superorder, behavior is fine-tuned to conspecifics through the addition of other, unique chemical compounds to the mixture. Fish that sense Schreckstoff engage in a variety of behavioral responses, the most common being movement away from a high concentration of the pheromone and long-term downregulation of activity[75]. The adaptive advantage of the Schreckstoff production system is unknown. Possibilities include (1) kin selection, since related fish will be protected by sensing Schreckstoff and escaping; (2) the alarm pheromone may attract additional predators to the site of attack, who compete with the attacker and enable the prey to escape in the commotion; (3) some species will school in the presence of Schreckstoff, distracting the predator to allow the prey to escape by hiding in a crowd of conspecifics. The adaptive advantage of the Schreckstoff response

is clearer: acute escape from the predator and reduced exposure to predators through defensive suppression of activity.

Pharmacological studies have implicated the neurotransmitters serotonin, norepinephrine, and GABA in the regulation of anti-predation responses in fish, suggesting that these behaviors may share an underlying basis with anxiety and fear behaviors[75]. In addition, genetic knockout studies have identified roles for certain neuroendocrine modulators, such as oxytocin, in anti-predator responses[76]. However, a genetic understanding of how heightened awareness of predation risk is balanced by other stimuli, and how these fear-associated behaviors confer added fitness, is not well understood in any system.

There is evidence that *C. elegans* responds to compounds secreted by conspecific hermaphrodites. The growth medium from a culture of hermaphrodites is attractive to *C. elegans* males[15], but repulsive to other hermaphrodites (J.Q. White, unpublished). Male attraction requires the TRP channel OSM-9 and the male-specific CEM neurons[77], but nothing has been published on the genetics or circuitry of hermaphrodite repulsion.

Recently, a family of sugar derivatives called ascarosides was found to be the primary compounds in hermaphrodite growth medium that attract males[16]. Ascarosides were previously found to mediate the *C. elegans* developmental decision to form a dauer larva,[17,18,19] in which, under conditions of crowding, high temperature, and low food availability, young larvae enter an alternative developmental progression into a non-reproductive form that is resistant to a variety of environmental stresses.

I asked whether *C. elegans* displays an alarm pheromone response, focusing on two behavioral assays: (1) assessment of acute avoidance of the chemical substance; and (2) influence of the substance on the worm's exploratory behavior.

Results

Characterization of an endogenous acute repellent

An injured worm, or a filtrate of boiled or sonicated worms (termed "deathmone") induces avoidance behaviors in *C. elegans* (J.H. Thomas, unpublished data). I prepared deathmone by boiling a slurry of *C. elegans* and passing the released liquid through a 0.2 μm filter. This filtrate was then used in the drop test, in which liquid is loaded into a small capillary tube, and dropped in front of the path of a forward-moving animal (Figure 2-1A). If the animal reverses upon encountering the spot, it is scored as having avoided the dropped substance. In the drop test, wild-type N2 animals showed robust avoidance of 100-fold diluted deathmone (Figure 2-1B). In agreement with previous studies (J.H. Thomas, unpublished) I found that the TRP channel OSM-9, which is important for the avoidance of many other substances, was essential for this behavior. *osm*-9 is expressed in approximately 30 cells, including the ASH sensory neurons, considered the *C. elegans* nociceptive neurons, which are required for acute avoidance of many noxious substances and were previously shown to be required for deathmone acute avoidance (J.H Thomas, unpublished). The *osm-9* mutant defect was rescued by expression of *osm-9* specifically in ASH, indicating that deathmone is another nociceptive stimulus.

Are ascarosides responsible for the acute avoidance? One member of the ascaroside family of compounds (C7, Figure 2-1C) had been isolated at the time I

conducted these experiments[17]. I asked whether C7 might be the active component of deathmone that generates ASH-mediated acute avoidance. Drop tests with C7 revealed a strong repellent activity (Figure 2-1D), but this avoidance was only partially *osm-9* dependent. Furthermore, the partial *osm-9* defect could not be rescued in ASH, indicating that the acute avoidance induced by deathmone is mediated by other compounds, not C7. These compound(s) have yet to be identified, but they could include one of the other ascarosides—to date, the list includes C3, C5, C6, and C9.

The modulation of exploratory behavior by deathmone

Overall movement during animal foraging can take two general strategies: exploration of a wide area (hereafter, "roaming") and restriction to a local area (hereafter, "dwelling"). The decision to roam or to dwell requires the integration of past experiences, such as food availability and access to mating partners, with current sensory information, such as the detection of toxins, chemicals, and nutrients[78]. Low quality food and the absence of mating opportunities increase an animal's motivation to roam, while nutrient abundance generally promotes a dwelling state.

C. elegans, when well-fed, has been shown to alternate between roaming and dwelling states[79]. When placed on a uniform lawn of bacterial food, individual animals will engage in 5-10 minute bouts of long forward locomotion, interspersed between variable periods of low activity. Sensory cues modulate the frequency of roaming periods, which are more common on low quality food sources[80]. Mutants defective in many classes of sensory neurons roam less than wild-type animals, while the cyclic GMP-dependent protein kinase mutant *egl-4* roams more than wild-type[79]. The specific

sensory neurons that are important for regulating roaming and dwelling states have not been identified, nor has genetic analysis of the behavior been further developed. In addition, little is known about sensory cues that alter the frequency and duration of roaming periods. Theoretical and empirical studies of other organisms have established that risk of predation inversely correlated with a suppression of movement[78]. Therefore, the threat of predation induces dwelling behavior in prey animals.

I asked whether deathmone regulated roaming and dwelling behavior. The roaming rate of *C. elegans* in the presence of deathmone was measured by growing single L4-stage larvae overnight on individual agar plates containing deathmone and bacterial food. After 17 hours, the area of tracks the animal made was measured and compared to worms grown in the absence of deathmone (Figure 2-2A). When exposed to deathmone, animals showed a consistent reduction in the area they explored, restricting their movement to a small region near the location they were originally placed (Figure 2-2B).

Identification of Active Compounds in Deathmone

I further purified the deathmone filtrate to determine the chemical nature of the active components for inhibition of exploration. Fractionation over a solid C18 reverse-phase column showed activity was strongest in the 25% and 50% elutions (data not shown). Deathmone was analyzed in collaboration with Rebecca Butcher in Jon Clardy's lab, which recently identified several chemical components of dauer pheromone, including several ascarosides (Figure 2-2C and data not shown). One of the compounds, the C6 ascaroside, was found to be concentrated in behaviorally active fractions of deathmone. Artificially synthesized C5, C6, C7, or C9 ascarosides induced dwelling, like

deathmone (Figure 2-2C). A fifth ascaroside, C3, had minimal dwelling activity. These chemical assays suggest that dwelling behavior is activated by dauer pheromone components.

Quantification of absolute amounts of ascaroside in the active deathmone fraction indicated, however, that the ascarosides could not account for the entire activity. Deathmone produced robust dwelling when diluted at least 1000-fold. Our collaborators found that the total ascaroside concentration in deathmone was around 1 uM. Yet, C6 produced consistent dwelling activity only at concentrations above 100 nM (Figure 2-2D). This ~100-fold difference suggests that additional compounds exist in the deathmone mixture that enhance ascaroside activity. Our collaborators performed NMR spectroscopy on the active deathmone fraction, and found that an additional indole-containing small molecule was present (data not shown). This compound was likely to be tryptophan or a related derivative, such as serotonin.

To determine whether tryptophan or serotonin could be indole-containing enhancers of dwelling, I performed the exploratory assay with combinations of ascarosides and either serotonin or tryptophan. Both of these compounds had little dwelling activity by themselves, but enhanced the activity of some ascarosides (Figures 2-2D and 2-2E). Tryptophan-like molecules are present in micromolar amounts in active deathmone fractions (R. Butcher), sufficiently high concentrations to account for the deathmone enhancement. Therefore, ascarosides may act in concert with tryptophan and/or its derivatives to induce dwelling.

The utilization of multiple classes of small molecules in alarm pheromone signaling is common. For example, in the Schrekstoff of fish, a single compound, which

is produced across many species of fish, can induce a behavioral response at sufficiently high concentrations. However, the potency of the compound can be enhanced by the additional presence of other chemicals, which are produced by smaller subsets of fish. This allows fish to contextualize danger, and fine-tune their behavioral response appropriately. Inspired by the fish example, I prepared a deathmone extract from a distantly related nematode, *Pristionchus pacificus*, which is separated from *C. elegans* by 200 million years of evolution. This preparation was active in the roaming and dwelling assay (Figure 2-2F), suggesting that deathmone, like Schrekstoff in fish, may share common chemical components in different species. A dilution series of PS512 deathmone has not been conducted. The active compounds in PS512 deathmone have not been chemically characterized, although ascarosides do not appear to be present at high concentrations (R. Butcher, unpublished results).

Cell ablation studies of deathmone-induced dwelling

Many chemosensory neurons regulate dauer formation, and therefore these are candidates to sense ascarosides[81]. The sensory neurons ADF, ASG, and ASI prevent dauer formation, while under favorable conditions ASJ is crucial for allowing larvae to exit the dauer state and resume development towards reproductive adulthood[82]. The TGF-β ligand gene *daf-7*, which prevents dauer formation, is expressed strongly in ASI and regulated by dauer pheromone, further confirming the role of this neuron in dauer formation[83]. Laser ablations in a genetically sensitized background (the mutant *daf-11*), indicate that ASJ and ASK neurons promote dauer formation, antagonizing ADF, ASG,

and ASI[84]. Together, these studies implicate multiple neurons in dauer pheromone (ascaroside) sensation.

Are the same neurons important for behavioral responses to ascarosides? To determine the chemosensory pathways that mediate deathmone-induced dwelling, I used laser ablation to kill individual sensory neurons. The primary sensory organs of *C. elegans* are the two amphids, which are associated with twelve pairs of ciliated neurons. I found that sensitivity to deathmone was completely abolished the mutants *che-2* and *osm-6* that lack a functional amphid as well as the other sensory structures (data not shown). I laser-ablated individual pairs of amphid neurons (10 of the total 12) to identify specific cells responsible for deathmone sensation in the dwelling assay.

Ablation of ASI resulted in a dramatic phenotype, causing the animals to dwell constitutively in the absence of deathmone (Figure 2-3A). Ablation of AWB or ASH caused a general reduction in roaming, although these animals were still sensitive to deathmone. Conversely, ADL-, ASK-, or AWC-ablated animals showed an overall increase in roaming rate that was also deathmone sensitive. Ablation of ASJ induced minor increases in roaming on deathmone that were not statistically significant. Ablation of the neuron ADF yielded high variability in roaming. Other tested neurons did not have any phenotype (Figure 2-3A).

Examination of the *C. elegans* wiring diagram[49] revealed that ASI is presynaptic to many other amphid neurons (Figure 2-3B, Table 2-1) including three that promote dwelling: ASK, AWC, and ADL. I ablated ASI together with each of these three neurons to determine whether any of them could be downstream of ASI. Only ASK was epistatic to ASI: doubly ablated animals had increased basal roaming and, unlike ASI-killed

animals, were sensitive to deathmone (Figure 2-3C). By contrast, AWC+ASI and ADL+ASI animals resembled ASI-killed animals, and did not regulate roaming activity in response to deathmone. These data suggest that ASI may exert its effect in part by inhibiting ASK.

There are four interneurons in the worm that receive a large portion of the amphid's synaptic output: AIA, AIB, AIY, and AIZ[85]. All of these neurons have been implicated in chemotaxis or related behaviors[86,68,53,87]. I asked whether ablation of any of these four neurons results in an exploratory defect. Ablation of AIA mildly reduced basal roaming, but sensitivity to deathmone was unaffected (Figure 2-3D). AIB-killed animals had no phenotype. Ablation of AIY caused animals to dwell constitutively, irrespective of the presence of deathmone. By contrast, AIZ-killed worms roamed excessively, both on and off deathmone. AIY synapses heavily onto AIZ; these ablation studies might suggest that those synapses are inhibitory, and that these two neurons function in a linear pathway to direct exploratory behavior.

Two other interneurons, RIA and RIB, were also tested for exploratory behavior. RIA receives synapses from many classes of neuron, including the AIY and AIZ interneurons, as well as the sensory neurons ASH, AWB, and AWC, all of which are known to impact roaming behavior. Ablation of either RIA or RIB did not have a strong phenotype on deathmone, although RIA ablation did suppress basal roaming (Figure 2-3D).

Two additional interneurons, AVA and AVB, were examined for their roles in roaming and dwelling. These neurons receive input from both sensory and interneuron cell types, and form extensive synapses onto motoneurons. They are described as

"command interneurons," because their output is believed to dictate the physical movements of the animal. Several studies have shown that the AVA neurons are required for reversal behavior, while the AVB cells control forward locomotion[50,88]. In the roaming assay, AVA or AVB ablations did not appear to cause a phenotype, either in basal exploration or dwelling in response to deathmone. Killing AVE, another command interneuron, also did not affect on exploratory behavior (data not shown).

ASI and TGF-β Signaling

Since ASI ablation resulted in a strong constitutive dwelling phenotype, I examined mutants of genes that affect this cell. *daf-7*, a secreted TGF-β homolog expressed specifically in the sensory neuron ASI, showed a dwelling phenotype identical to an ASI ablation (Figure 2-4A**)**. The secreted DAF-7 likely acts through its receptor DAF-1, since *daf-1* and *daf-7* null mutants resemble each other (Figure 2-4A). Expression of *daf-1* under cell specific promoters could provide information about where in the nervous system DAF-7 is acting. Rescue of *daf-1* under the pan-neuronal promoter *tag-168* resulted in rescue of basal roaming and deathmone-induced dwelling. Recently, it was found that both *daf-1* and *daf-7* display feeding and fat storage abnormalities[89]. These *daf-1* defects could be rescued by expression of *daf-1* specifically in the RIM and RIC interneurons, implicating them as targets for the DAF-7 peptide[89]. I asked whether the tyraminergic RIM and octopaminergic RIC neurons might also be the targets of DAF-7 targets in roaming behavior. Rescue of *daf-1* in the RIM and RIC neurons caused an increase in basal roaming, but did not restore regulation by deathmone (Figure 2-4A).

These results suggest that DAF-1 acts in a different neuron to promote dwelling in the presence of ascarosides.

Does ASI release other factors to promote roaming besides *daf-7*? Like its constitutive dauer formation phenotype, the dwelling behavior of *daf-7* could be suppressed by the downstream SMAD transcription factor *daf-3*. To determine whether secretion of *daf-7* was completely responsible for deathmone-induced dwelling, I killed ASI in a *daf-7; daf-3* mutant background. These animals also dwelled, suggesting that ASI releases both DAF-7 and other signals that promote roaming (Figure 2-4B). The additional signal released by ASI to promote roaming may be a neurotransmitter, or a neuropeptide. Currently, the neurotransmitters used by ASI are not known, although glutamate, the worm's primary excitatory neurotransmitter, is a good candidate. All known glutamate signaling involves the vesicular glutamate transporter EAT-4. *eat-4* mutants had a partial defect in deathmone-induced dwelling that was not rescued by specific expression in ASI (data not shown). In addition, I tested null alleles of several neuropeptides known to be expressed in ASI. These mutants were largely phenotypically normal, although *nlp-7* did show a small decrease in basal roaming (Figure 2-4B). Therefore, the additional factor(s) released by ASI that mediate exploratory behavior, and in particular, the dwelling in response to deathmone, remain unknown.

EGL-4 Acts in the Dauer Sensory Neurons to Promote Dwelling

By screening existing mutants, I have identified many that roamed excessively on deathmone, including mutants deficient in oxygen preference, serotonin signaling, and chemosensation (Table 2-2). I also found many mutants that showed a reduction in the

basal roaming rate. In total, more than 100 mutants were tested. However, only two mutants were identified that resulted in complete, constitutive roaming, regardless of the presence of deathmone: the cGMP-dependent protein kinase *egl-4* and the neuropeptide Y receptor homologue *npr-1* (Figure 2-5 and Chapter 3). The uniqueness of this constitutive roaming phenotype suggested that the sites of action of these genes could be particularly important for the behavior. In this section, I describe my efforts to rescue *egl-4*. Discussion of *npr-1* rescue appears in Chapter 3.

The *egl-4* gene has been implicated in several sensory transduction functions, including chemotaxis mediated by the AWC neuron[90,91]. Furthermore, *egl-4* mutants roam excessively[79]. A previous study found that expression of *egl-4* in a large subset of amphid sensory neurons could rescue the roaming phenotype, but the individual neurons required were not determined[79]. Six isoforms of *egl-4* have been identified (Figure 2-5A)[92]. I expressed 4 of the 6 isoforms under the control of a pan-neuronal promoter to examine their relative effectiveness at rescuing basal exploratory behavior[1]. The *egl-4f* isoform showed the strongest rescue, probably due to the absence of the N-terminal regulatory domain, leading to constitutive activity (Figure 2-5B). Because of the historical difficulty of rescuing *egl-4*[79], I used this strong *egl-4f* isoform in subsequent experiments.

I expressed *egl-4f* under a variety of heterologous promoters, and examined the roaming behavior of these transgenic lines in the presence and absence of deathmone. A bicistronic expression plasmid was used to co-express soluble GFP and therefore identify the neurons expressing *egl-4f*. Expression of *egl-4f* in ASI, ASJ, and ASK using the *gcy-*

[1] Since egl-4 roams so strongly, I examined exploratory behavior after only 6 hours, rather than the usual 18-20.

27 promoter restored a degree of deathmone sensitivity to *egl-4* mutants. It also partially rescued the basal roaming phenotype of *egl-4*. Adding expression in ASH and ADL using the *nhr-79* promoter resulted in improved rescue. These results indicate that *egl-4* acts in the sensory neurons implicated in dauer formation to promote dwelling, and further supports the hypothesis derived from the laser ablation experiments that deathmone is sensed and interpreted by ASI, ASJ, and ASK.

Discussion

The circuit analysis described above provides some information about the neurons that control deathmone-induced dwelling. The sensory neurons implicated in dauer formation—especially ASI but also, to some extent, ASJ and ASK—appear important to sensation of deathmone. ADL and AWC also play roles, while AWB and ASH, like ASI, appear to promote basal exploratory behavior. Among ASI, ASJ, and ASK, which are most important for the behavior? My laser ablation studies suggest that ASI acts at least partly through ASK to regulate roaming. However, it is difficult to dissect the individual contributions of these three neurons, because activity of a single neuronal pair can be strongly influenced by the others. This is especially true for ASI, which expresses certain genes that can be regulated by mutations in ASK-specific genes (Sengupta lab, unpublished data). I attempted to express *egl-4f* under an ASI-specific promoter, but, despite injection of the construct at high concentrations, was never able to observe GFP expression in ASI. ASK expression is not sufficient to rescue *egl-4* (Figure 2-5C). An ASJ-specific rescue of *egl-4* was not tested. Therefore, it remains possible that ASJ is the

crucial *egl-4* neuron. Taken together with laser ablation experiments, it appears likely that all three neurons contribute to the regulation of roaming behavior.

The *egl-4* gene has previously been implicated as a regulator of TGF-β signaling[90], because the *egl-4* chemotaxis defects could be suppressed by *daf-3*. \ However, *egl-4* and *daf-7* display opposite phenotypes, and a *daf-3* mutation in the *daf-7* background results in enhanced dwelling. From these epistatic relationships, it is difficult to explain *egl-4* roaming simply as a function of enhanced ASI activity. Further genetic and transgenic studies would be needed to fully appreciate the role of EGL-4 in regulating exploratory behavior, and the dwelling response to deathmone.

The relevant synaptic output of the dauer neurons for this behavior is not clear. They are mostly presynaptic to AIA and AIB[85], but ablation of these neurons and did not affect roaming (Figure 2-3D). ASI does synapse onto AIY and AIZ, so they could be part of the relevant output. Alternatively, the contributions of ASI, ASJ, and ASK to deathmone-induced dwelling could be mediated by neuropeptide release, which can be extrasynaptic[89].

From these results, it is impossible to determine whether particular cells are directly involved in deathmone sensation, or instead affect other sensory processes that increase, or decrease, roaming. For example, ablation of the AWC sensory neuron causes increased roaming on and off of deathmone. AWC is known to sense food-related odors[68], and animals lacking the AWC neurons exhibit less turning behavior than wild-type when removed from food[22]. The AWC ablation phenotype in the exploratory behavior assay, therefore, could be a consequence of the animal's impaired food perception, or a direct deathmone response. Furthermore, sensory neurons are known to

be affected by internal state changes—ASI, for example, responds to caloric restriction[93]. Calcium imaging, in which changes in cellular calcium are examined while presenting a particular stimulus, is a useful method for determining whether a cell is directly responsive to a chemical. In Chapter 3, I use calcium imaging to show ASK neurons likely sense ascarosides directly.

Corollary: Deathmone may be an ecologically relevant signal

Is *C. elegans* exposed to deathmone in the wild, and if so, are these chemicals associated with elevated predatory danger? Answering this question can help illuminate the core functions of any genes or neurons that are identified as mediators of the behavior. I have obtained a predatory nematode, *Mononchoides gaugleri*, that was isolated from agricultural topsoil in New Jersey[94]. This animal uses a sharp buccal tooth to incise the cuticle of its prey and release its inner contents (Figure 2-3E**)**; in addition, it can also consume bacteria if nematode prey are absent. *M. gaugleri* was found to readily kill *C. elegans* of all developmental stages on normal agar cultivation plates; in addition, *C. elegans* showed consistent and rapid avoidance of injured and dead conspecifics on plates with *M. gaugleri* (data not shown). This is the first direct demonstration, to my knowledge, of *C. elegans* undergoing predation. Due to the difficulty of raising *M. gaugleri* under standard laboratory conditions[2], little further data was gathered on this predator-prey interaction. However, I believe that further investigation is warranted, as such interactions could provide fertile ground for uncovering novel *C. elegans* behaviors.

[2] Despite numerous attempts (bleaching of gravid adults, treatment with antibiotics), I found it impossible to generate a sterile culture of *M. gaugleri*. The microorganism that co-cultured with the predatory nematode was pathogenic to *C. elegans*, and altered behavior.

Table 2-1. Number of synaptic connections between designated neuron pairs and other amphid neurons. Data taken from White et al[9].

Cell name	# Confirmed Synapses to Other Amphid Cells
ASI	**11**
ADL	5
ASE	3
AWB	3
ASJ	2
AWA	2
ADF	1
AWC	0
AFD	0
ASK	0
ASG	0
ASH	0

Table 2-2. Exploratory behavior in a variety of mutants, grouped according to function in the nervous system.

Chemosensory machinery

Gene Name	Molecular Identity; Known Functions	Phenotype
che-2	Ciliary development; amphid function	Dweller (+++)
gpa-2	GPCR signaling; dauer formation	Dweller (++)
gpa-3	GPCR signaling; dauer formation	Dweller (+)
gpa-6	GPCR signaling	Wild-type
gpa-9	GPCR signaling	Wild-type
gpa-10	GPCR signaling	Wild-type
gpa-14	GPCR signaling	Wild-type
gpa-1; gpa-2; gpa-3	GPCR Signalling; Dauer formation	Dweller (+++)
osm-9	TRP Channel; chemotaxis	Roamer (+)
ocr-2	TRP Channel; chemotaxis	Roamer (++)
egl-4	cGMP-dependent protein kinase; chemotaxis	Roamer (++)
cmk-1	Calcium/calmodulin-dependent protein kinase I (CaMK1)	Roamer (++)
crh-1	cyclic AMP-response element binding protein (CREB) homologue	Wild-type

Neuropeptide Signaling

Gene Name	Molecular Identity; Known Functions	Phenotype
npr-1	Neuropeptide Y receptor homologue; social feeding/hyperoxia avoidance	Roamer (+++)
npr-2	Neuropeptide FF homologue	Dweller (++)
npr-9	Galanin receptor homologue	Dweller (++)
F54D7.3	Gonadotropin releasing hormone receptor homologue	Wild-type
F14F4.1	Vasopressin V1R receptor homologue	Wild-type
nlp-1	ASI-expressed neuropeptide	Wild-type
nlp-5	ASI-expressed neuropeptide	Dweller (+)
nlp-7	ASI-expressed neuropeptide	Dweller (+)
nlp-18	ASI-expressed neuropeptide	Wild-type
nlp-24	ASI-expressed neuropeptide	Dweller (+++)
flp-1[3]	FMRFamide neuropeptide	Roamer (+++)
flp-18	FMRFamide neuropeptide	Roamer (+)
flp-21	FMRFamide neuropeptide	Wild-type
ins-1	Insulin-like peptide	Wild-type
daf-28	Insulin-like peptide; dauer formation	Wild-type
daf-2	Insulin receptor; dauer formation	Wild-type

[3] The *flp-1(yn2)* also leads to a deletion in *daf-10*, resulting in defective cilia formation; based on results with *che-2*, however, this would be expected to result in dwelling, not roaming.

daf-7	ASI-expressed TGF-beta homologue; dauer formation	Dweller (+++)
egl-21	Neuropeptide maturation (cleavage); locomotion, egg-laying	Dweller (+++)

Catecholamine Neurotransmission

Gene Name	Molecular Identity; Known Functions	Phenotype
cat-1	Vesicular monoamine transporter; all serotonin-associated behaviors	Roamer (++)
tph-1	Serotonin synthesis; all serotonin-associated behaviors	Dweller (+++)
ser-1	Serotonin receptor	Wild-type
mod-1	Serotonin receptor; infection-related behaviors	Wild-type
mod-5	Serotonin reuptake	Dweller (+)
cat-2	Dopamine synthesis; dopamine behaviors	Wild-type
cat-4	Serotonin and dopamine biosynthesis	Roamer (+)
tdc-1	Tyramine synthesis; reversal and egg-laying behaviors	Dweller (+)
tbh-1	Octopamine synthesis	Wild-type
ser-1	Putative serotonin receptor	Wild-type
ser-2	Putative tyramine receptor	Dweller (+)
amx-1	Putative monoamine oxidase	Wild-type
amx-2	Putative monoamine oxidase	Dweller (+)
gcy-12	Membrane guanylyl cyclase	Dweller (++)
gcy-35	Soluble guanylate cyclase	Wild-type

Glutamate Neurotransission

Gene Name	Molecular Identity; Known Functions	Phenotype
eat-4	Glutamate transporter; pharyngeal pumping, chemosensation	Roamer (++)
nmr-1	Glutamate receptor	Wild-type
glr-1	Glutamate receptor	Wild-type
glr-6	Glutamate receptor	Roamer (++)
mgl-1	Group II metabotropic glutamate receptor; pharyngeal pumping	Dweller (+)
mgl-2	Group I metabotropic glutamate receptor; head movement and tap reflexes	Dweller (+)
glc-3	Glutamate-sensitive chloride channel	Wild-type

Additional mutants

Gene Name	Molecular Identity; Known Functions	Phenotype
gta-1	GABA transaminase	Wild-type
exp-1	Excitatory GABA receptor	Wild-type
snf-11	GABA transporter	Wild-type
sra-11	7 transmembrnae receptor expressed in interneurons	Dweller (+)
daf-22	Uncloned gene involved in dauer pheromone synthesis	Wild-type
ttx-3	LIM homeodomain protein required for AIY interneuron differentiation	Dweller (+++)
hen-1	LDL-receptor homologue expressed in AIY interneurons	Dweller (+)
daf-12	steroid hormone receptor	Wild-type

Figure 2-1. a, Diagram of the drop test assay[95] (see methods). **b**, Deathmone is an acute repellent in the drop test assay. Deathmone was tested at 1:1000 dilution, except in "1:1" where undiluted deathmone was used. Asterisk, different from N2 ($P < 0.05$ by Bonferroni's t-test). Error bars indicate standard deviation from the mean (s.d.). **c,** Chemical structure of the C7 ascaroside[17]. **d**, C7 ascaroside induces acute avoidance Error bars indicate standard deviation from the mean (s.d.).

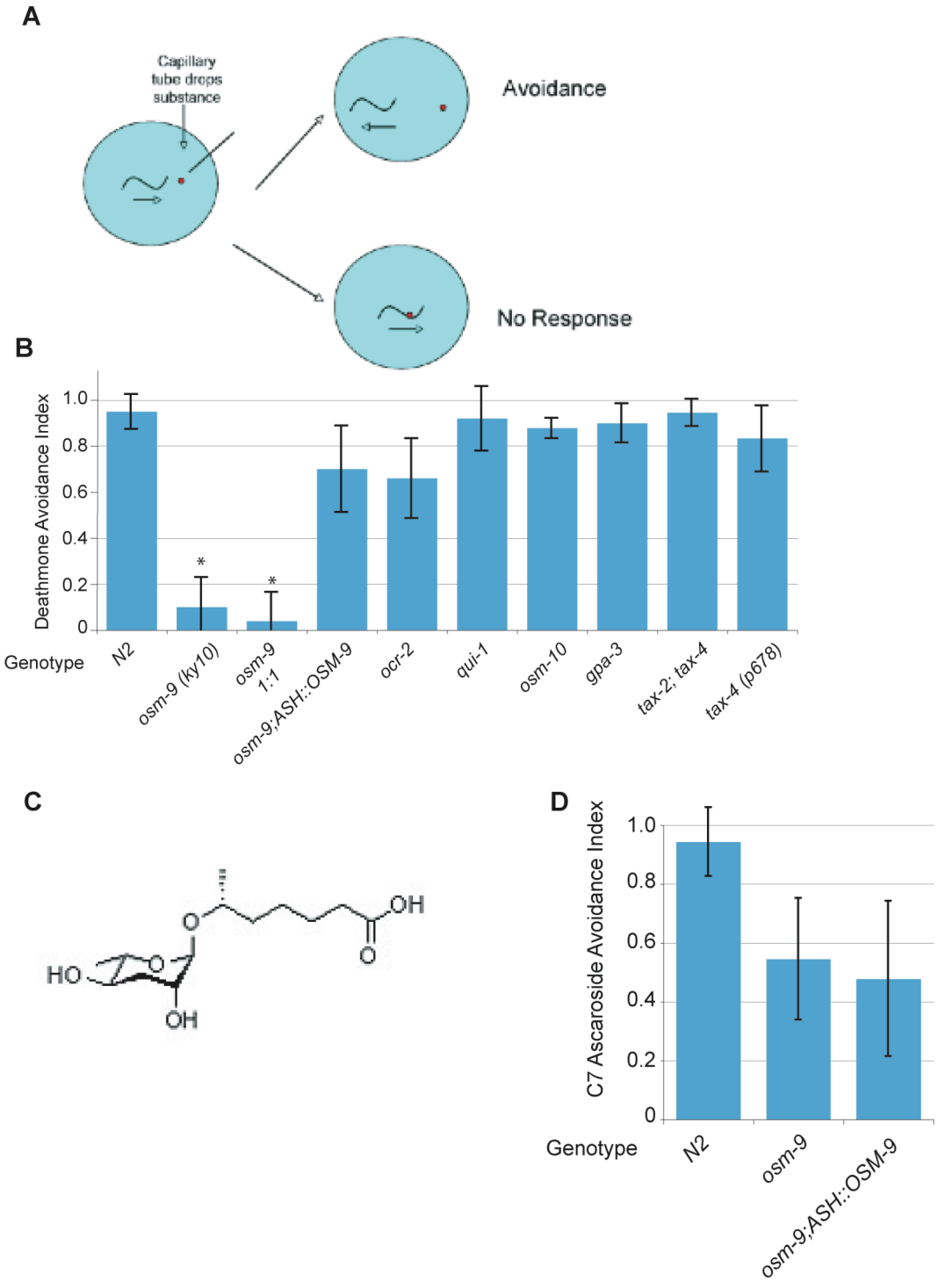
A
Capillary tube drops substance
Avoidance
No Response
B
Deathmone Avoidance Index
1.0
0.8
0.6
0.4
0.2
0
*
*
Genotype
N2
osm-9 (ky10)
osm-9 1:1
osm-9;ASH::OSM-9
ocr-2
qui-1
osm-10
gpa-3
tax-2; tax-4
tax-4 (p678)
C
HO
O
O
OH
OH
D
C7 Ascaroside Avoidance Index
1.0
0.8
0.6
0.4
0.2
0
Genotype
N2
osm-9
osm-9;ASH::OSM-9

Figure 2-1

Figure 2-2. **a,** Diagram of the exploration assay. Single L4s are picked to individual plates seeded overnight with baterial food. Tracks are observed 17-20 hours later (see methods). **b,** Deathmone induces an inhibition of exploratory behavior. Asterisk, different from deathmone (-) animals ($P < 0.05$ by student's t-test). Error bars indicate standard deviation from the mean (s.d.). **c.** Chemical structures of C3, C5, C6, and C9 ascarosides[18,19]. Error bars indicate standard error of the mean (s.e.m). **d,** L-tryptophan (100 μM) enhances the dwelling activity of ascarosides. Asterisk, different from control, tryptophan (-) animals ($P < 0.05$ by Bonferonni's t-test). Double asterisk, $P < 0.05$ by student's t-test. Error bars indicate standard error of the mean (s.e.m). **e**, Serotonin (100 μM) enhances the swelling activity of C9 ascaroside. Asterisk, different from control, serotonin (-) animals ($P < 0.05$ by Bonferonni's t-test). Error bars indicate standard error of the mean (s.e.m). **f**, Deathmone prepared from *Pristonchus punctatus* strain PS512 also possesses dwelling activity.

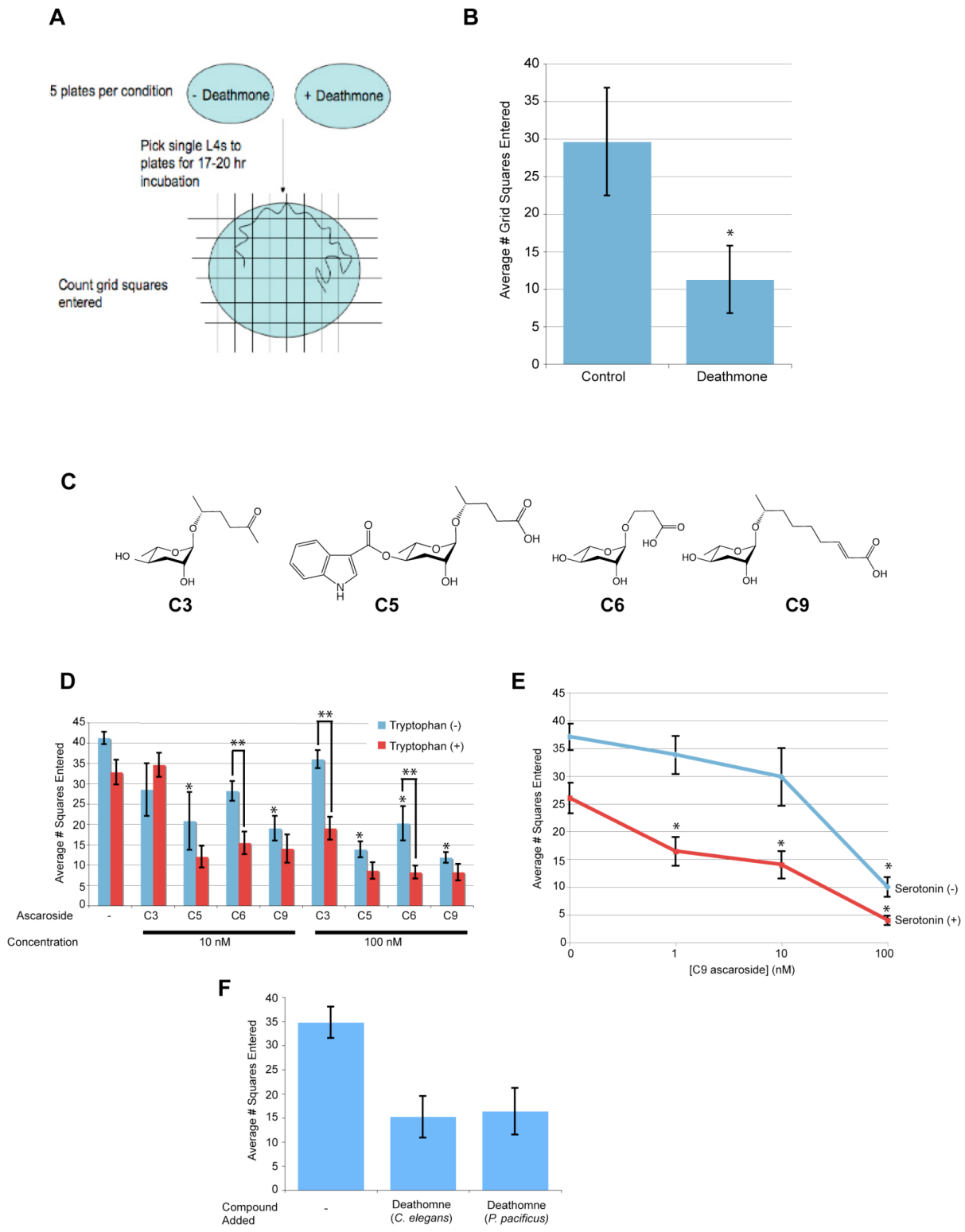
A
5 plates per condition
- Deathmone
+ Deathmone
Pick single L4s to plates for 17-20 hr incubation
Count grid squares entered
B
Average # Grid Squares Entered
Control
Deathmone
C
C3
C5
C6
C9
D
Average # Squares Entered
Tryptophan (-)
Tryptophan (+)
Ascaroside
Concentration
10 nM
100 nM
E
Average # Squares Entered
Serotonin (-)
Serotonin (+)
[C9 ascaroside] (nM)
F
Average # Squares Entered
Compound Added
Deathomne (C. elegans)
Deathomne (P. pacificus)

Figure 2-2

Figure 2-3. Laser ablation analysis of deathmone-induced dwelling behavior. **a,** Ablation of sensory neuron pairs in the amphid. Asterisk, different from mock ablated, deathmone (+) animals ($P < 0.05$, Dunnett test). Error bars indicate standard deviation of the mean (s.d). Double asterisk, different from mock ablated, deathmone (-) animals ($P < 0.05$, Dunnett test). **b**, Diagram of ASI postsynaptic sensory targets[49]. **c,** Ablation of ASI and its downstream sensory neuron targets. Asterisk: Different from ASI ablated, deathmone (-) animals ($P < 0.05$, student's t-test) and ASI+ASK deathmone (+) animals ($P < 0.05$, student's t-test). Error bars indicate standard error of the mean (s.e.m). **d**, Ablation of interneurons downstream of amphid sensory neurons. Asterisk, different from mock ablated, deathmone (+) animals ($P < 0.05$, Dunnett test). Double asterisk, different from mock ablated, deathmone (-) animals ($P < 0.05$, Dunnett test). Error bars indicate standard deviation of the mean (s.d).

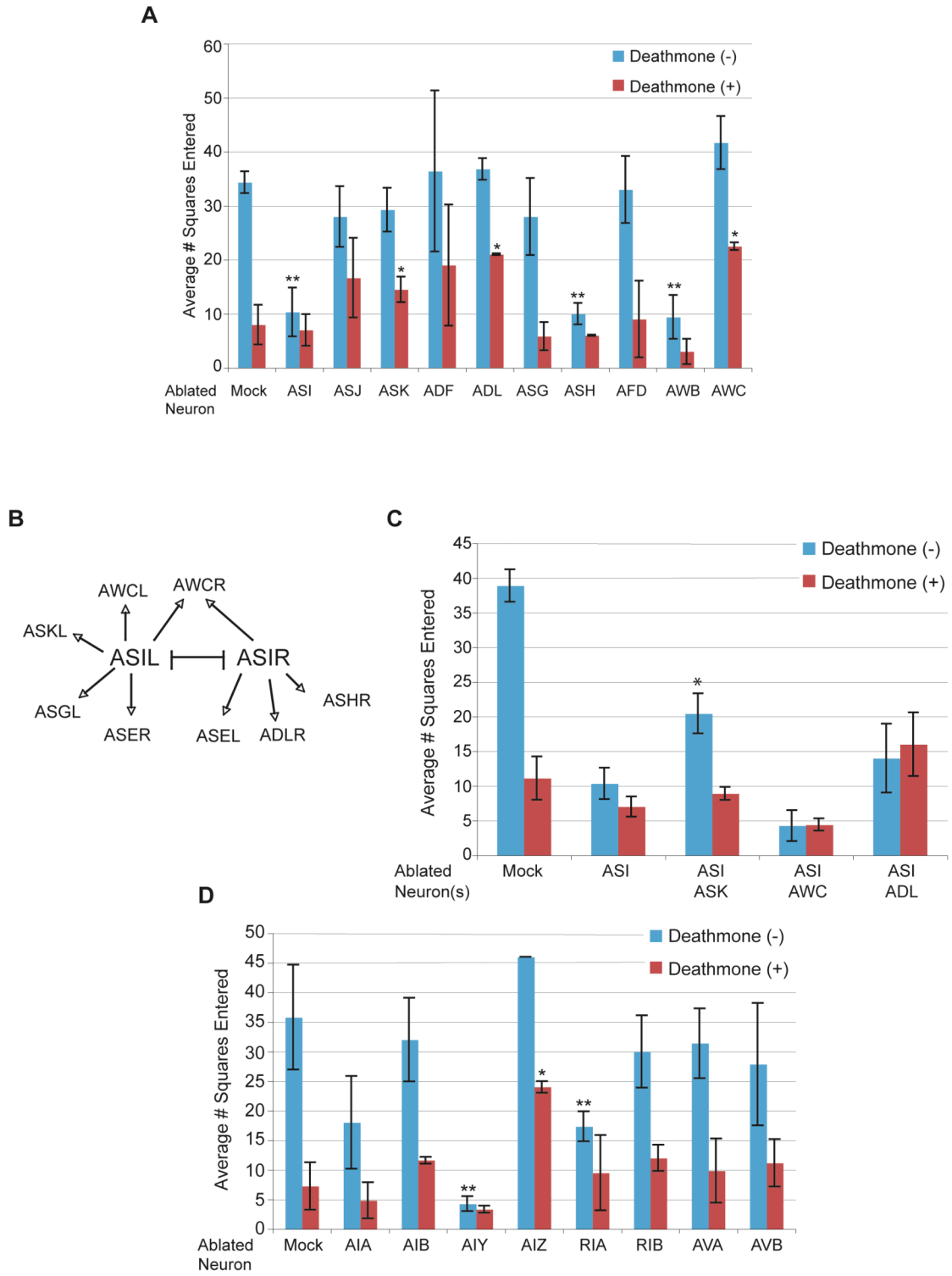
A
Deathmone (-)
Deathmone (+)
Average # Squares Entered
Ablated Neuron
Mock
ASI
ASJ
ASK
ADF
ADL
ASG
ASH
AFD
AWB
AWC
B
AWCL
AWCR
ASKL
ASIL
ASIR
ASHR
ASGL
ASER
ASEL
ADLR
C
Deathmone (-)
Deathmone (+)
Average # Squares Entered
Ablated Neuron(s)
Mock
ASI
ASI ASK
ASI AWC
ASI ADL
D
Deathmone (-)
Deathmone (+)
Average # Squares Entered
Ablated Neuron
Mock
AIA
AIB
AIY
AIZ
RIA
RIB
AVA
AVB

Figure 2-3

Figure 2-4. Multiple ASI signals promote exploratory behavior. **a,** Rescue of *daf-1* under a pan-neuronal and the *tdc-1* promote restore dwelling in the absence of deathmone. Asterisk, different from N2 deathmone (-) animals ($P < 0.05$, Dunnett test). **b**, Ablation of ASI in *daf-3; daf-7* mutants results in constitutive dwelling, indicating that other pro-roaming factors are released from ASI. Asterisk, different from *daf-7* deathmone (-) animals ($P < 0.05$ by student's t-test). Double asterisk, different from *daf-7;daf-3* deathmone (-) animals ($P < 0.05$ by student's t-test).

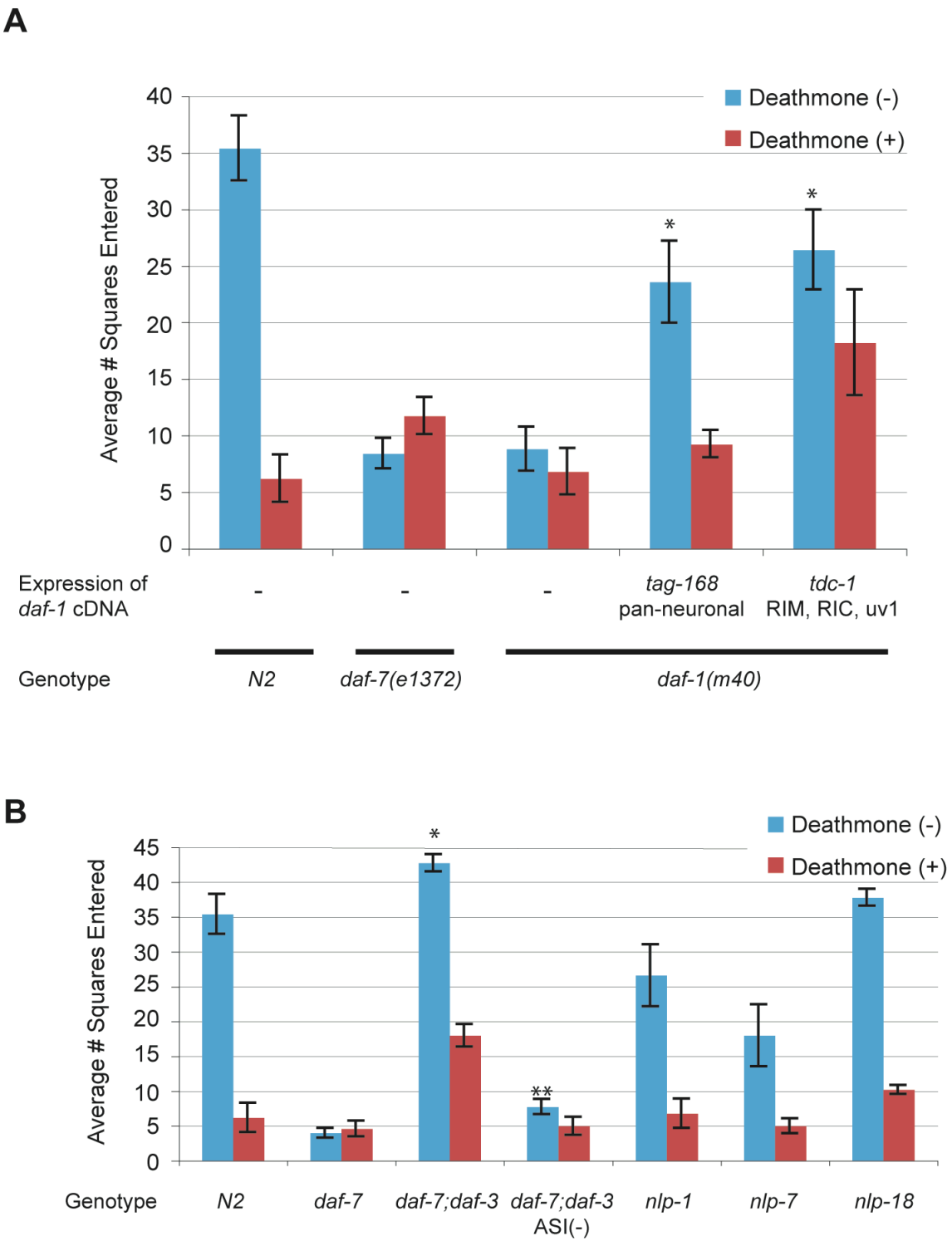
A
Deathmone (-)
Deathmone (+)
Average # Squares Entered
40
35
30
25
20
15
10
5
0
*
*
Expression of daf-1 cDNA
-
-
-
tag-168 pan-neuronal
tdc-1 RIM, RIC, uv1
Genotype
N2
daf-7(e1372)
daf-1(m40)
B
Deathmone (-)
Deathmone (+)
Average # Squares Entered
45
40
35
30
25
20
15
10
5
0
*
**
Genotype
N2
daf-7
daf-7;daf-3
daf-7;daf-3 ASI(-)
nlp-1
nlp-7
nlp-18

Figure 2-4

Figure 2-5. **a,** Organization of the *egl-4* genetic locus[92]. **b,** Pan-neuronal expression of different *egl-4* splice forms in the *egl-4* mutant. Asterisk, different from *egl-4* mutant ($P < 0.05$ by Dunnett's t-test). **c,** Expression of *egl-4* in a subset of amphid sensory neurons rescues the exploratory behavior defect. Asterisk, different from *egl-4* deathmone (-) animals ($P < 0.05$ by Dunnett's t-test). Double asterisk, $P < 0.05$ by student's t-test. Error bars indicate standard deviation from the mean (s.d). **d**, Left, picture of a *Mononchoides* predator aggregate feeding on an injured *C. elegans* hermaphrodite on a standard growth plate. Right, picture of a mononchid predator feeding on nematode prey[92].

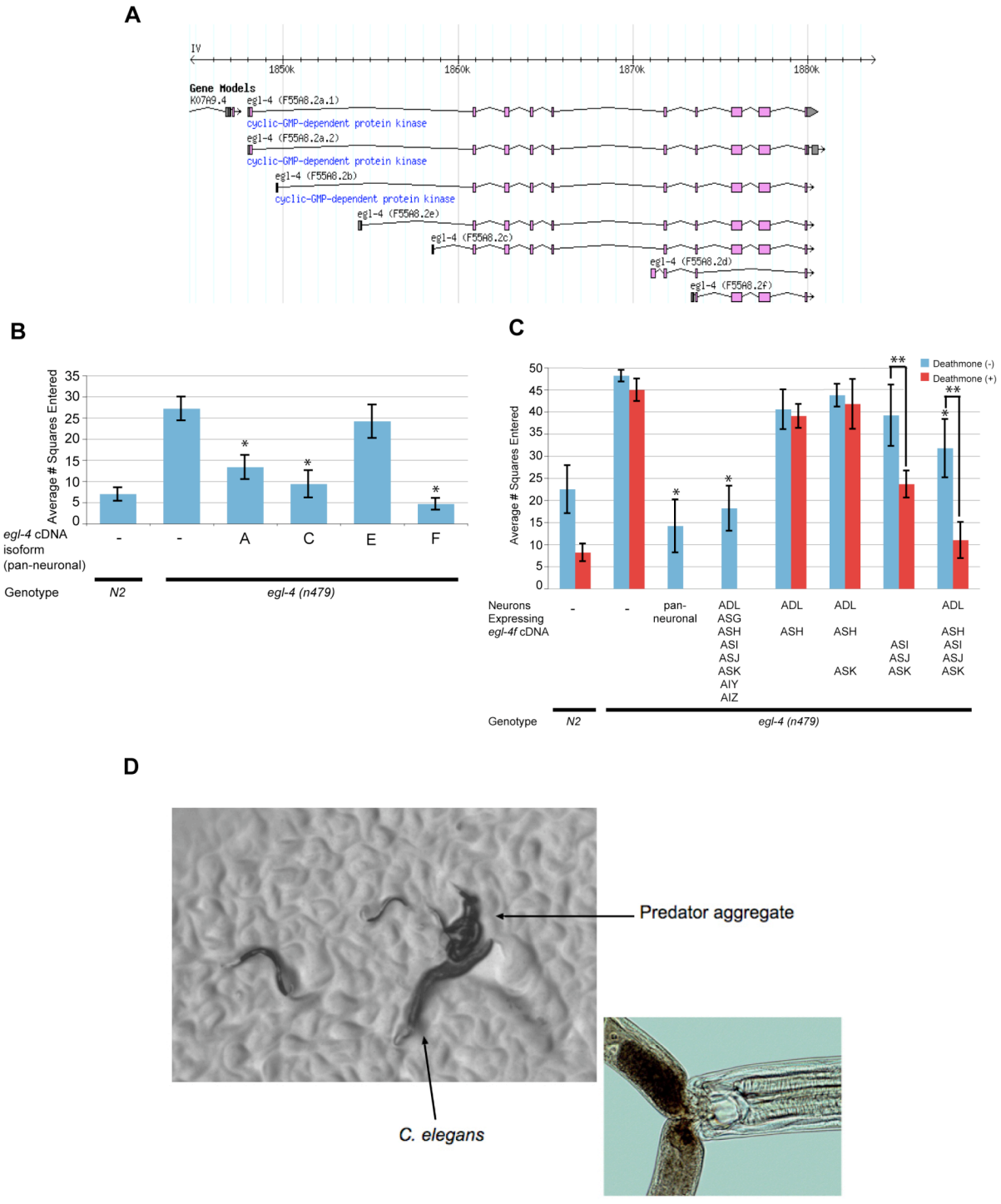
A
IV
1850k
1860k
1870k
1880k
Gene Models
K07A9.4
egl-4 (F55A8.2a.1)
cyclic-GMP-dependent protein kinase
egl-4 (F55A8.2a.2)
cyclic-GMP-dependent protein kinase
egl-4 (F55A8.2b)
cyclic-GMP-dependent protein kinase
egl-4 (F55A8.2e)
egl-4 (F55A8.2c)
egl-4 (F55A8.2d)
egl-4 (F55A8.2f)
B
Average # Squares Entered
egl-4 cDNA isoform (pan-neuronal)
-
-
A
C
E
F
Genotype
N2
egl-4 (n479)
C
Average # Squares Entered
Deathmone (-)
Deathmone (+)
Neurons Expressing egl-4f cDNA
-
-
pan-neuronal
ADL ASG ASH ASI ASJ ASK AIY AIZ
ADL ASH
ADL ASH ASK
ASI ASJ ASK
ADL ASH ASI ASJ ASK
Genotype
N2
egl-4 (n479)
D
Predator aggregate
C. elegans

Figure 2-5

Chapter 3:

npr-1, Social Feeding, and Pheromone Chemotaxis

Introduction

The regulated aggregation behavior of *C. elegans,* a simple animal with only 302 neurons, is an attractive system for circuit analysis of social behavior. Many naturally isolated *C. elegans* strains aggregate into feeding groups consisting of dozens of animals, although other strains, including the laboratory strain N2, are solitary feeders[96]. Aggregating strains show other behavioral changes compared to solitary feeders: they accumulate on the border of a bacterial lawn (bordering) and move rapidly on food (Figure 3-1A). Aggregation, bordering, and rapid movement are coordinately controlled by the neuropeptide Y receptor homologue NPR-1[7]. Solitary strains have a high-activity form of NPR-1 with a valine at amino acid residue 215, whereas aggregating strains have a low-activity form of NPR-1 with phenylalanine at residue 215; wild-type *N2* worms with a loss-of-function mutation in *npr-1* are hyper-social[7,97]. Neuropeptide control of aggregation provides an interesting analogy to mammalian social behavior, which is regulated by the neuropeptides oxytocin and vasopressin[98].

In addition to genetic regulation by *npr-1,* aggregation is sensitive to environmental signals. It is stimulated by URX sensory neurons that detect environmental oxygen[22], and ASH and ADL sensory neurons that sense noxious stimuli[99]. Attraction to low-oxygen environments promotes accumulation at the lawn border and feeding in groups, which have low oxygen levels compared to the open lawn[22,100]. Population density, food availability[99], and environmental stressors[101] also modulate aggregation behavior.

Results

NPR-1 acts in RMG to control social feeding

In an attempt to better understand the neural circuitry mediating social feeding, I determined where NPR-1 acts in the nervous system to promote the behavior. A previous report using a genomic *npr-1* fragment identified the oxygen-sensing URX neuron as a site of *npr-1* action, but behavioral rescue was incomplete, with rescue of aggregation, partial rescue of bordering, and no rescue of rapid movement[102]. To identify additional neurons in which NPR-1 promotes solitary behavior, I first established that a full-length *npr-1* cDNA expressed from the endogenous *npr-1* promoter rescued solitary behavior in the strong loss of function mutant *npr-1 (ad609)* (Figure 3-1B). Because promoter expression patterns in *C. elegans* can vary depending on the exact fragment used[103], the expression vector employed[104], and the presence of introns[105], I used a bicistronic mRNA to express both *npr-1* and GFP, and identified GFP-positive neurons in each rescued line with solitary behavior (see methods). Of the 11-13 pairs of head neurons expressing GFP in *npr-1::npr-1::GFP* rescued lines (Table 3-1), those observed most frequently were AQR, ASG, AUA, RIG, RMG, SMBD, and URX. To determine which cells were responsible for the behavioral rescue, I expressed the *npr-1* cDNA and GFP under other characterized promoters (Figure 3-1B). Only promoters driving expression in the inter/motor neuron RMG showed robust rescue of aggregation, bordering, and locomotion speed (Figure 3-1B).

Next, I asked whether RMG expression of *npr-1* is sufficient to suppress aggregation. No RMG-specific promoter is known, so I utilized an intersectional strategy developed by another graduate student in our lab, Evan Feinberg, to drive *npr-1*

expression only in the cells that express both *flp-21* and *ncs-1* (Table 3-1), using Cre-mediated recombination between LoxP sites. In one transgene, the *ncs-1* promoter drove expression of the nCre recombinase; in a second transgene, the *flp-21* promoter was separated from GFP or *npr-1* cDNAs by transcriptional stop sequences and mRNA cleavage sequences, flanked by LoxP sites. When *ncs-1::nCre* and *flp-21::LoxStopLox::GFP* strains were crossed together, nCre recombination excised the transcriptional stop and mRNA cleavage sequences, and the intersection between *ncs-1* and *flp-21* generated strong and consistent GFP expression only in RMG and the M2 pharyngeal neurons (Figure 3-2A). I next inserted the *npr-1* cDNA into the *flp-21::LoxStopLox* plasmid (Figure 3-2A), and injected the plasmid into *npr-1 (ad609)* animals with or without *ncs-1::nCre*. In *npr-1* animals expressing both *flp-21*::*LoxStopLox*::*npr-1* and *ncs-1::nCre*, aggregation, bordering, and high speed on food were strongly suppressed (Figure 3-2B). M2 is synaptically isolated from the neurons implicated in these behaviors, so RMG-specific expression of *npr-1* can block aggregation and related behaviors.

In mammals, neuropeptide Y receptors generally inhibit neurotransmitter release[106,107]. To ask whether NPR-1 suppresses aggregation by inhibiting or by activating RMG, I killed RMG in wild-type and *npr-1* animals using a laser microbeam, anticipating an effect on the genotype(s) in which RMG is normally active. Killing RMG in *npr-1(lf)* eliminated aggregation, bordering, and rapid movement (Figures 3-2C, 3-2D), whereas killing RMG in solitary wild-type animals had no effect (Figure 3-2D). These results show that RMG neurons stimulate aggregation-related behaviors in *npr-1* mutants, and suggest that NPR-1 inhibits RMG activity in solitary strains.

RMG links multiple sensory neuron classes required for social behavior

Inspection of the *C. elegans* wiring diagram revealed that RMG is the hub of a gap junction network connecting seven classes of neurons, including the oxygen-sensitive URX neurons and the nociceptive ASH and ADL neurons previously implicated in aggregation behavior[102] (Figure 3-3A). To determine whether RMG is generally required for chemosensation by associated sensory neurons, I tested RMG-ablated *npr-1* animals for their avoidance of high osmolarity, a behavior mediated by ASH[108]. No significant defect was observed (Figure 3-3B), indicating that RMG is not essential for all functions of associated sensory neurons, but selectively required for aggregation and related behaviors.

Among the other neurons electrically coupled to RMG, the ASK neurons were of particular interest, given their role in ascaroside sensation[84]. In addition, ASK has recently been implicated in male attraction to hermaphrodite pheromones[16]. The role of ASK was probed using a *tax-4* mutation that affects sensory transduction: *tax-4* encodes a cyclic GMP-gated transduction channel expressed in ASK and other sensory neurons (Table 3-1), but not in RMG[55,109]. *tax-4*; *npr-1(lf)* double mutants are strongly suppressed for aggregation and related behaviors[102], and rescue of these behaviors requires *tax-4* expression in at least two classes of neurons: URX and an unknown sensory neuron[102]. I asked whether ASK might be the unknown sensory neuron. Indeed, simultaneous rescue of *tax-4* in URX and ASK resulted in near-complete restoration of aggregation and related behaviors in *tax-4; npr-1(lf)* double mutants (Figure 3-3C). Rescue was also observed upon expression of *tax-4* in URX and ASJ neurons, which

synapse onto ASK (Figure 3-3C). Thus ASK and ASJ promote aggregation and related behaviors.

The predicted connectivity of RMG suggests two alternative circuit models: 1) RMG could modify the activity of electrically connected sensory neurons, all of which have chemical synapses; or 2) RMG could integrate sensory input through gap junctions and stimulate aggregation using its own chemical synapses. RMG forms synapses onto multiple interneurons that control forward and backward locomotion[85,88,50] and forms neuromuscular junctions with head muscles (Figure 3-3A). To ask whether the synaptic output of RMG promotes aggregation, I used the Cre/Lox system to express the light chain of tetanus toxin (TeTx) in RMG of *npr-1(lf)* mutants. TeTx silences synaptic transmission by cleaving the vesicle fusion protein synaptobrevin at a glutamine(Q)-phenylalanine(F) peptide bond that is conserved from worms to mammals[110,111,112]. Aggregation and related behaviors were partially suppressed by TeTx expression in RMG (Figure 3-3D). Co-expression of TeTx with a cleavage-resistant *C. elegans* synaptobrevin (Q68V)[110] mutant significantly suppressed the RMG::TeTx effect in *npr-1 (ad609)* animals, confirming that TeTx acts via synaptobrevin cleavage (Figure 3-3E). Aggregation was also suppressed by expression of TeTx in the ASK and ASJ sensory neurons, a second line of evidence linking these neurons to aggregation behaviors, and TeTx expression in both RMG and ASK/ASJ had additive effects (Figure 3-3D). Silencing or killing URX neurons suppresses aggregation[102,113] but TeTx expression in URX neurons had little effect unless the other neurons were silenced (Figure 3-3D). These results suggest that both RMG and ASK/ASJ synaptic output contribute to aggregation behaviors, a hybrid of the two circuit models proposed above.

Since synaptic inhibition of RMG and coupled sensory neurons suppressed aggregation in *npr-1(lf)* strains, I asked whether stimulation of these cells in solitary wild-type animals might be sufficient to drive aggregation. Neurons were activated by expressing a constitutively active protein kinase C homolog of *C. elegans* (*pkc-1(gf)*). Expression of *pkc-1(gf)* in most RMG-coupled neurons elicited aggregation, bordering, and high speed in solitary strains, a near-complete transformation of their behavior (Figure 3-4A). Expression in subsets of neurons had partial effects suggesting contributions from RMG, URX, ASK/ASJ, and possibly other cells (Figure 3-4A). Like the behavior of *npr-1(lf)* strains, the *pkc-1(gf)*-induced behaviors were suppressed by killing RMG neurons (Figure 3-4C). Thus simultaneous activation of RMG and sensory neurons by *pkc-1(gf)* can drive aggregation and related behaviors.

The *pkc-1(gf)* allele has previously been shown to promote synaptic release at the neuromuscular junction[114], as well as neuropeptide release[115], and may have additional excitatory properties[116]. How does *pkc-1(gf)* promote social feeding in solitary *N2* animals? Expression of *pkc-1(gf)* in AQR, PQR, and URX using the *gcy-36* promoter resulted in bordering behavior (Figure 3-4B). If *pkc-1(gf)* acts by promoting synaptic release, then co-expression of TeTx in these three neurons should suppress the bordering phenotype. Indeed, TeTx expression in AQR, PQR, and URX did reduce the bordering phenotype of *gcy-36::pkc-1(gf)* animals (Figure 3-4B), indicating that *pkc-1(gf)* activates these neurons by promoting synaptic release.

Pheromone responses are altered in *npr-1* mutants

The dual involvement of ASK in aggregation and male attraction to hermaphrodites[16] prompted an examination of pheromone responses in aggregating strains. Ascarosides are attractive to males, but repulsive to solitary hermaphrodites, suggesting that they promote sex-specific attraction for mating[16,18,77] (and see Chapter 2). Ascarosides are constitutively secreted by all stages of *C. elegans,* providing a plausible source of an aggregation signal. Behavioral attraction to ascarosides was assayed using an equimolar cocktail of three ascarosides (Figure 3-5A). As reported, solitary wild-type hermaphrodites were repelled by ascarosides; by contrast, *npr-1(lf)* hermaphrodites were attracted to low levels of ascarosides, with responses resembling those of males (Figure 3-5C). Expression of *npr-1* in RMG restored pheromone avoidance to *npr-1(lf)* hermaphrodites, linking this behavior to the RMG circuit (Figure 3-5C).

Attraction to pheromones was absent in *tax-4; npr-1(lf)* double mutants, suggesting that one or more *tax-4*-expressing sensory neurons detect ascarosides (Figure 3-5D). Rescue of *tax-4* in ASK neurons restored ascaroside attraction to *tax-4; npr-1(lf)* strains, providing evidence that ASK is a relevant pheromone sensor (Figure 3-5D). Silencing the ASK and ASJ neurons with TeTx eliminated ascaroside attraction, as did silencing RMG (Figure 3-5E). The correlation between the cellular requirements for pheromone attraction and aggregation supports the hypothesis that these two behaviors are functionally related.

How is avoidance of pheromone mediated in wild-type *N2* animals? Avoidance of pheromones was absent in *tax-4* mutants. Expression of *tax-4* under the *gcy-27* promoter, which showed expression in ASI, ASK, and occasionally ASJ, restored pheromone

avoidance to *tax-4* animals (Figure 3-5F). ASI-specific *tax-4* expression yielded mild avoidance. By contrast, expression of *tax-4* in ASK specifically caused pheromone attraction. These data indicate that ASI is the main *tax-4*-expressing sensory neuron mediating avoidance, perhaps in cooperation with ASJ and/or ASK.

To better understand the contributions of the individual components of the ascaroside cocktail, I tested chemotaxis to each separately, as well as to C5, an additional member of the ascaroside family that was not included in the mixture. Wildtype animals avoided the C6 and C9 ascarosides, but were mildly attracted to C3 (Figure 3-5G). By contrast, *npr-1(lf)* worms showed significant defects in their responses to C6, C9 (Figure 3-5G). Attraction was strongly enhanced when C3 was paired with either C6 or C9, an affect that is dependent on ASK (Figure 3-5H).

Sensory properties of ASK were examined directly by monitoring sensory-evoked calcium transients with the genetically-encoded calcium indicator G-CaMP[117]. In both wild-type and *npr-1(lf)* animals, ASK responded to ascaroside cocktails (100 pM -1 μM) with a rapid diminution of fluorescence suggesting decreased calcium levels; fluorescence recovered upon ascaroside removal (Figure 3-1A). The rapid response in ASK neurons supports their identification as ascaroside-sensing neurons; the calcium decrease suggests that ASK uses a hyperpolarizing mode of sensory transduction[68,118]. At attractive nanomolar ascaroside concentrations, ASK calcium responses were reliably greater in *npr-1* animals than in wild type, with a greater calcium decrease upon ascaroside addition and a greater rebound following ascaroside removal (Figure 3-1A).

Ascaroside responses were next monitored in the major synaptic targets of ASK, the AIA interneurons. G-CaMP was expressed under an AIA-selective promoter and

calcium signals were followed in the AIA process of *npr-1(lf)* mutants. The ascaroside cocktail elicited a large increase in G-CaMP fluorescence in AIA, suggesting depolarization (Figure 3-6C). The AIA response was greatly diminished and slightly delayed in animals whose ASK neurons were killed with a laser, suggesting that ASK sensory input is a major source of ascaroside signals in AIA (Figures 3-6D). The inversion of calcium signals (decrease in ASK, increase in AIA) indicates that ASK forms inhibitory synapses onto AIA. Ascaroside-induced AIA calcium signals were also diminished when the RMG neurons were killed, with a three-fold reduction in average response magnitude (Figure 3-6D). RMG-ablated animals responded both less frequently and less strongly (Figure 3-6E). An RMG ASK double ablation resembled an ASK ablation alone, indicating that RMG and ASK work through a common process to affect AIA (Figure 3-6D). As RMG does not have any direct connections onto the AIA interneurons, these results suggest that RMG may exert its effects by modulating the ASK-to-AIA connection (Figure 3-6F).

AIA calcium responses were also examined in wild-type *N2* animals. A reduction in the magnitude of the response was seen compared with *npr-1(lf)* animals (Figure 3-6G). *N2* animals showed less frequent responses than *npr-1*, but when responses were present, they were often quite strong (Figure 3-6H). It is therefore unclear how the response of N2 to pheromone addition differs from that of *npr-1*. *N2* and *npr-1* strains were also tested for their AIA responses to the removal from pheromone after a 20 minute incubation (see Methods). Both strains similarly increased calcium when pheromone was removed (Figures 3-6I, 3-6J), indicating that AIA possesses both an “on” response to pheromone addition and an “off” response to its removal.

A screen for social feeding suppressors

The identification of RMG as the site of action of NPR-1 suggests that social feeding is controlled by a gap junctional network of sensory neurons linked through RMG. The process by which social feeding is controlled in RMG must therefore involve a host of genes, none of which (besides *npr-1*) is presently unknown. Table 3-2 contains a comprehensive list of the genes known to be involved in social feeding, based upon the ability of mutants to suppress the behavior in an *npr-1* background. All of these mutants disrupt sensory signal transduction. In fact, the only known non-sensory gene that controls social feeding is *npr-1* itself.

I sought to identify additional *npr-1* suppressors that do not affect sensory transduction, using a two-tiered forward genetic screen. First, *npr-1(lf)* L4 larvae were mutagenized with EMS, and 3 F1 adult progeny were placed on individual plates that had been seeded with a set amount of bacteria to produce a standardized circular lawn. Three days later, the plates were examined for solitary animals. Under these conditions, *npr-1(lf)* mutants are almost entirely on the border, with most aggregating. Therefore, any animals observed to be feeding in the center of the lawn were likely to be mutants. One individual solitary animal from each growth plate was picked to a fresh plate. The progeny of these clones was again examined for aggregation to eliminate false positives. A total of 80 individual clones were confirmed to be bona fide *npr-1* suppressors out of 12,000 genomes screened.

Next, these mutants were tested for their responses to oxygen. Jesse Gray[22] and Manuel Zimmer (unpublished) have shown that *N2* and *npr-1(lf)* animals display

qualitatively different changes in their speed when shifted to 10% oxygen and back to 21%. Specifically, *npr-1* slows dramatically upon the oxygen downshift, and speeds up when returned to 21% (Figure 3-7A). When RMG was killed in *npr-1(lf)* mutants, the oxygen response profile was inverted: they sped up in low oxygen, and remained slow for several minutes when shifted back to 21% (Figure 3-7A). *N2* animals behave similarly to RMG ablations, reducing their speed transiently when shifted back to 21% oxygen (Figure 3-7B). By contrast, many of the sensory transduction mutants that suppress *npr-1*—such as *tax-4* and the soluble guanylate cyclase mutants *gcy-36* and *gcy-35*—show a completely flat speed profile in this assay. That is, they do not slow either when shifted to low oxygen, or when shifted back to high oxygen.

The 80 social feeding suppressors were tested for their responses to oxygen, seeking mutants that respond like *N2* or an RMG cell-kill. Of the 80 mutants tested, only three mutants displayed an *N2*-like oxygen response, slowing when shifted from 10% to 21%. The double mutant *npr-1;ky891* behaved like N2 (Figure 3-7C), while *npr-1;ky893* displayed features akin to RMG-ablated animals (Figure 3-7D), including a mild speed increase in low oxygen, and a prolonged slowing response upon upshift from 10% to 21% oxygen. A third allele, *npr-1;ky890*, had an N2 behavioral profile (not shown).

The *ky891* allele was mapped to a 555 kilobase (kb) region on the far right of chromosome II, using single nucleotide polymorphism (SNP) mapping (see methods). Of the 18 fosmids spanning the interval that were microinjected, only one rescued social feeding (data not shown). There are three full genes on this fosmid; only one, *arl-3*, is expressed in neurons. Sequencing of *arl-3* in *ky891* revealed a single G-to-A mutation that converted the aspartic acid at position 170 to a glycine. A knockout allele of *arl*-3,

tm1703, phenocopied *ky891* when crossed to *npr-1* (Figure 3-7E), and the two alleles failed to complement each other (data not shown). These data demonstrate that the molecular lesion in *ky891* responsible for suppressing social feeding is in *arl-3*.

arl-3 encodes an ADP ribosylation factor-like GTPase that is conserved in vertebrate and invertebrate genomes. The ARL-3 of mammals was shown to bind to PDEδ[119], a prenyl-binding protein that interacts with the rod-specific phosphodiesterase PDE6[120]. Loss of PDEδ results in the absence of GIRK1 and PDE6 from the photoreceptor outer segments[121]. The PDEδ homolog in *C. elegans* is *pdl-1*. A null mutation in *pdl-1* partially suppressed the social feeding of *npr-1* (Figure 3-7E). These data suggest that *arl-3* in *C. elegans*—like its homolog in mice—may be involved in the proper trafficking and organization of gene products in the ciliated processes of sensory neurons. Consequently, its role in social feeding was not investigated further.

The *ky893* allele was mapped to a 590 kb interval on the right of chromosome IV, using SNP mapping. *ky893;npr-1* mutants were observed to have a visible egg-laying (*egl*) defect. Examination of the interval revealed a known *egl* mutant, *egl-21*, a carboxypeptidase E responsible for the production of mature neuropeptides[122]. Sequencing of the *egl-21* coding region in *ky893* revealed a G-to-A mutation that converted the glutamate at position 329 to a lysine. An existing reduction-of-function allele of *egl-21*, *n411*, phenocopied *ky893*, suppressing social feeding in the *npr-1* background (data not shown). These data indicate that the suppression of social feeding by *ky893* is the result of a lesion in *egl-21*.

Where does *egl-21* act in the nervous system to control social feeding? To answer this question, I drove expression of *egl-21* in various subsets of neurons in the social

feeding circuit. Pan-neuronal rescue of *egl-21* restored bordering and aggregation (Figure 3-7F). Preliminary results indicate that social feeding can be partially restored by rescue in the ASI, ASJ, and ASK neurons (not shown).

Discussion

A model for aggregation behavior can be assembled from these studies of *npr-1* rescue and the affected neurons. Solitary animals ignore oxygen in the presence of food, and are repelled by ascarosides produced by other animals. In *npr-1(lf)* animals, two sensory cues drive aggregation: oxygen-sensing URX neurons promote accumulation at the lawn border, and ascaroside-sensing ASK neurons promote attraction to other animals (or neutralize repulsion mediated by other neurons). RMG stimulates these activities of URX and ASK; in the case of ASK, calcium imaging suggests that the synaptic connection between ASK and AIA interneurons is strengthened when RMG is active. The morphological gap junctions linking RMG to URX, ASK, and the aggregation-promoting ASH and ADL neurons suggest an anatomical route for sensory integration. Electrical coupling could activate RMG when O_2 levels are high (URX) and nociceptive cues are present (ASH, ADL), leading to increased ASK-to-AIA signaling and attraction to ascarosides. Other neurons in the circuit may change their signaling properties as well, including the less-characterized AWB, IL2, and RMH neurons. Validation of this hypothesis awaits direct evidence for electrical coupling of the neurons; gap junctions can be tightly regulated, and the RMG gap junctions are at present only morphologically defined.

It was previously shown that social feeding could be partially suppressed by expressing *npr-1* in URX under *gcy-32* or *flp-8* promoters[102]. I did not observe strong suppression using any of the three tested URX-expressing promoters: *gcy-32, flp-8,* or *gcy-35*. Two possible explanations for this incongruity are: 1) The published rescue employs an intron-containing genomic fragment of *npr-1*, whereas we used an *npr-1* cDNA. Some introns in *C. elegans* act as tissue-specific or nonspecific transcriptional enhancers[105]. Therefore the *npr-1* genomic constructs may have directed some expression in RMG; in addition, some fragments of the *flp-8* promoter, which was more potent in the published report, are occasionally expressed in RMG[123]. 2) The published genomic clone may result in higher *npr-1* expression in URX than the cDNA clone. Social feeding can be partially suppressed by silencing or killing URX[102,113], and the reported partial suppression is consistent with silenced URX neurons. Whether the higher or lower levels of *npr-1* are more physiological is unclear, but it is a concern that transgenes can be toxic when expressed at high levels, even when they drive "inert" molecules such as GFP. In any case, the effects of RMG *npr-1* expression described here are much stronger than the reported effects of URX expression.

NPR-1 appears to inhibit RMG function in solitary strains, perhaps by inhibiting electrical coupling between RMG and connected sensory neurons, or perhaps by inhibiting RMG excitability or synaptic release. A model in which NPR-1 inhibits gap junctions that link sensory pathways has analogies with dopamine action in the mammalian retina, where gap junctions link rod and cone visual pathways to increase light sensitivity at night; during the day, dopamine inhibits these electrical connections to increase spectral and spatial resolution[124]. Several environmental cues that regulate

aggregation, such as oxygen levels[22] and exposure to ethanol[101], are known to affect gap junctional coupling[125,126], but further studies will be required to elucidate the mechanism of NPR-1 action. The NPR-1 ligand FLP-21 is expressed in RMG neurons as well as URX, ASH, ASJ, and ASK neurons that promote aggregation[97]. Its expression pattern suggests that FLP-21 could be an autocrine signal from RMG that acts on NPR-1 receptors on the same neuron, or a paracrine signal that coordinates activity levels across cell types.

The regulation of RMG by *npr-1* addresses a puzzling feature of the sensory circuit, which is that URX and ASH sensory neurons generate comparable strong chemosensory behaviors in social and solitary strains[113], yet only promote aggregation in social strains. The chemosensory avoidance function of ASH does not rely on RMG or *npr-1;* instead, it relies upon glutamatergic chemical synapses between ASH and movement command interneurons[127,128]. The differential regulation of chemical synapses and gap junctions has the potential to expand or restrict neuronal function in interesting ways. Within the *C. elegans* wiring diagram, gap junction distributions are highly skewed. Most neurons have only a few gap junctions, but seventeen classes of neurons are gap junction hubs that link seven or more classes of neurons[129]. This circuit motif could perform a characteristic computation.

Neuropeptide signaling systems regulate diverse behavioral processes; for example, Neuropeptide Y signaling in mammals influences aggression[130], circadian rhythmicity[131], sexual behavior[132], and feeding behaviors[133,134]. Neuropeptide Y receptors of both vertebrates and invertebrates are widely expressed in the nervous system, and the *npr-1* gene of *C. elegans* is expressed in about 10% of all neurons. Yet,

for three different *C. elegans* behaviors—high locomotion on food, bordering on a bacterial lawn, and aggregation—NPR-1 action converges on a single cell type, the inter/motor neuron RMG. This observation suggests that the sites of neuropeptide action may be more focal than would be expected from their broad receptor expression: there may be central behavioral sites for neuropeptide receptor function, along with peripheral expression in neurons with modulatory roles.

High oxygen is clearly necessary in laboratory conditions for social feeding, but pheromone attraction—or lack of repulsion—likely assists in helping animals form aggregates. There are many examples from other animals where a non-social cue is a necessary prerequisite for social behavior. Snakes, for example, require seasonal changes in temperature to aggregate[135], but likely use cues from conspecifics, such as pheromones[136], to drive aggregation. Although ascaroside responses are altered in *npr-1* animals, it still remains unproven that these pheromones, like high oxygen, promote aggregation. More detailed behavioral assays, using carefully controlled microenvironments[137], will help elucidate the relative contributions of these different stimuli.

This work indicates a central functional role in social feeding for a previously unstudied class of neuron, RMG. So far, no other genes have been found that function in RMG to regulate behavior. At present, I have used transcriptional reporters to find four genes that are expressed reasonably specifically in RMG: *npr-1*, *ncs-1*, *flp-21*, and *glb-6*. *flp-21* is a putative ligand of *npr-1*, as described above. An *ncs-1* null mutant does not suppress social feeding in *npr-1(lf)* animals (data not shown). No *glb-6* alleles exist, and hence the role of this gene in social feeding is unknown. The goal of my forward genetic

screen was to identify additional factors that act in RMG by isolating mutants with behavioral profiles similar to N2 or RMG-killed animals. Two mutants were cloned from this screen: one, *arl-3*, is likely to be involved in sensory transduction. The other, *egl-21*, an enzyme involved in the production of mature neuropeptides, was found to likely act in the pheromone sensing neurons ASI, ASJ, and ASK, and probably not in RMG. Although the discovery of the *egl-21*-dependent neuropeptides that affect social feeding will likely be informative, the screen failed to identify RMG-acting genes. Perhaps additional behavioral phenotypes are needed to distinguish between mutants acting in sensory cells and those acting in interneurons like RMG. A more detailed comparative analysis of N2 and other social feeding suppressors could help generate the behavioral tools required to meet this challenge.

Table 3-1. Expression patterns of constructs used in Chapter 3. In all figures, lines labeled "RMG" were made using the intersectional cre-lox strategy described in Figure 3-2A.

FIGURE 3-1	
Construct Name	***Expression Pattern***
npr-1::npr-1 SL2 GFP	AUA (96.3%), RMG (78.57%), ASG (78.57%), RIG (71.42%), SMBD (71.42%), AQR (71.42%), URX (64.2%), ASE (57.14%), 4-5 neurons anterior to the nerve ring, body motor neurons, 2-4 tail neurons.
gcy-32::npr-1 SL2 GFP	AQR, PQR, URX
flp-8::npr-1 SL2 GFP	URX, AUA
ncs-1::npr-1 SL2 GFP	ADL, AFD, AIY/AVK, ASE, ASG, ASI, AVE, AWB, AWC, BAG, RMG, 1 tail cell, 1 additional cell anterior to the nerve ring
flp-21::npr-1 SL2 GFP	RMG (100%), ASJ (100%), URA? (100%), URX (88.9%), M2 pharyngeal neuron (88.9%), FLP? (77.8%), ASK (77.8%), ASH (33.3%), ASG (22.2%), ASI (22.2%), ADF (22.2%), unidentified tail cells
FIGURE 3-3 and 3-5	
Construct Name	***Expression Pattern***
gcy-36::tax-4 SL2 GFP	AQR, PQR, URX
srh-11:tax-4 SL2 GFP	ASJ
sra-9::tax-4 SL2 GFP	ASK
str-3::tax-4 SL2 GFP	ASI
gcy-36::TeTx	AQR, PQR, URX
srh-11::TeTx+sra-9::TeTx	ASJ, ASK
FIGURE 3-4	
gcy-36::pkc-1(gf) SL2 GFP	AQR, PQR, URX
gcy-27::pkc-1(gf) SL2 GFP	ASI, ASJ, ASK
flp-21::pkc-1(gf) SL2 GFP	ADF, ASG, ASH, ASJ, ASK, URA, FLP?, M2 pharyngeal neuron, RMG

Table 3-2. List of known suppressors of *npr-1* social feeding.

Suppressor Gene Name	Known Function	Reference
osm-9/ocr-2	TRP channel subunits; sensory transduction	De Bono et al., 2002[99]
tax-2/tax-4	Cyclic nucleotide-gated cation channel subunits; sensory transduction	Coates and de Bono, 2002[102]
odr-4/odr-8	Membrane proteins involved in proper localization of seven transmembrane proteins to sensory cilia	De Bono et al., 2002[99]
daf-11	Guanylate cyclase; sensory transduction	Tremain et al, unpublished data
gcy-35/gcy-36	Soluble guanylate cyclases; sensory transduction	Gray et al., 2004[22]
lim-4	Homeodomain-containing protein required for proper neuronal development	Tremain et al, unpublished data
M01F1.7	Phosphatidylinositol transfer protein; sensory transduction	Macosko and Lee, unpublished data

1 de Bono, M. et al., Social feeding in Caenorhabditis elegans is induced by neurons that detect aversive stimuli. Nature 419, 899 (2002).

2 Coates, J. C. and de Bono, M., Antagonistic pathways in neurons exposed to body fluid regulate social feeding in Caenorhabditis elegans. Nature 419, 925 (2002).

3 Gray, J.M. et al., Oxygen sensation and social feeding mediated by a C. elegans guanylate cyclase homologue. Nature 430, 317 (2004).

Figure 3-1. Selective expression of NPR-1 suppresses aggregation and related behaviors in *npr-1* mutants. **a,** A standard assay showing the solitary behavior of 150 wild type N2 animals (left image) and aggregation behavior of 150 *npr-1(ad609)* animals (right image). **b,** Behavioral phenotypes of *npr-1(ad609)* animals expressing an *npr-1* cDNA under a pan-neuronal promoter (*tag-168),* its endogenous promoter (*npr-1*), URX promoters (*gcy-32* and *flp-8*) and RMG promoters (*ncs-1, sax-7,* and *flp-21*). Additional promoter sets are shown at the far right. For aggregation and bordering, the average fraction of 3 or more behavioral assays was used; for speed on food, the average speed was calculated from tracking 20 animals for 10 minutes. Full promoter expression patterns are in Supplemental Table 1. Error bars indicate standard deviation (s.d.). Asterisk, different from *npr-1(ad609)* ($P < 0.01$, Bonferroni's multiple comparison test).

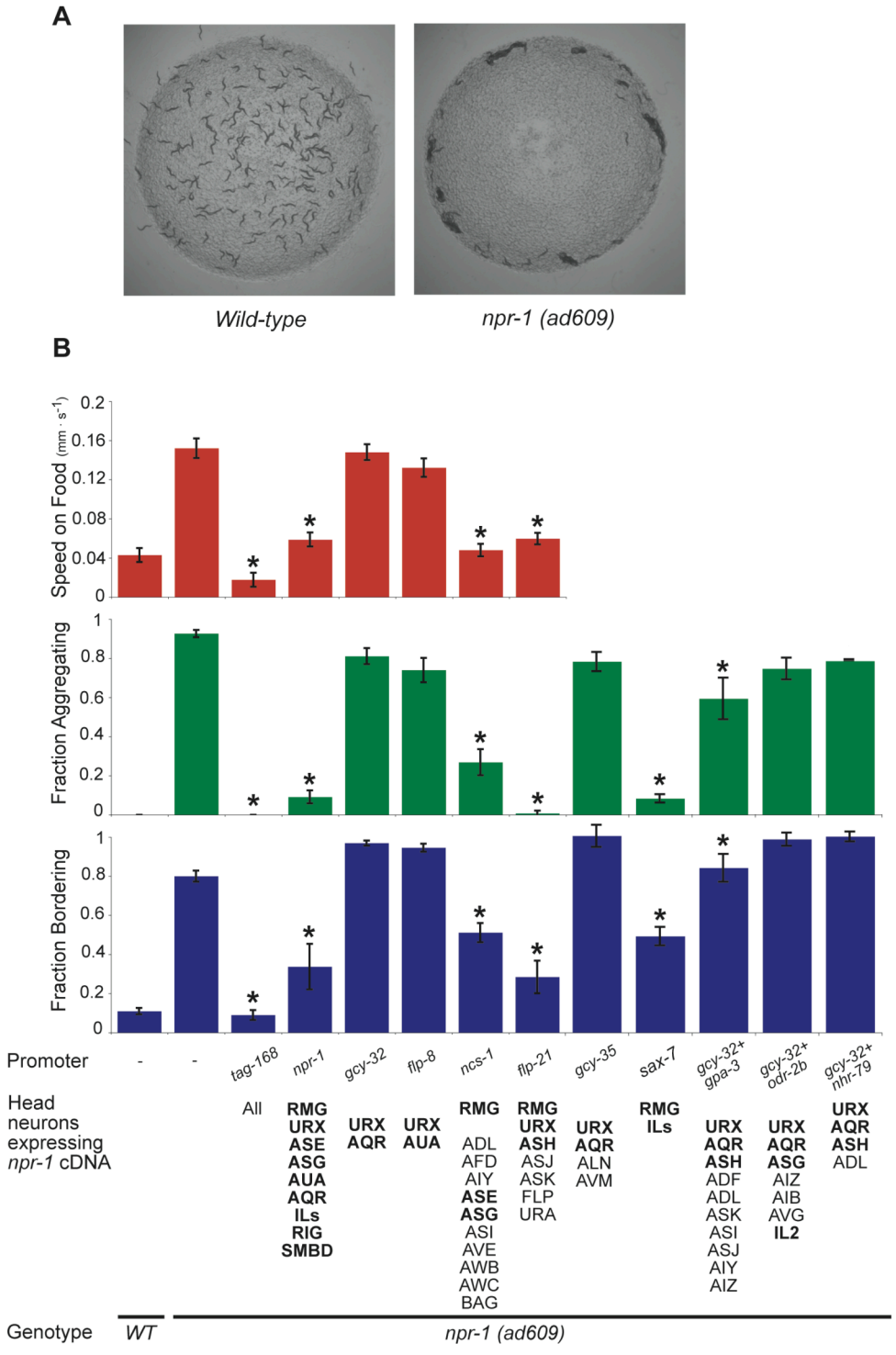
A
Wild-type
npr-1 (ad609)
B
Speed on Food (mm · s-1)
0.2
0.16
0.12
0.08
0.04
0
Fraction Aggregating
1
0.8
0.6
0.4
0.2
0
Fraction Bordering
1
0.8
0.6
0.4
0.2
0
Promoter
-
-
tag-168
npr-1
gcy-32
flp-8
ncs-1
flp-21
gcy-35
sax-7
gcy-32+ gpa-3
gcy-32+ odr-2b
gcy-32+ nhr-79
Head neurons expressing npr-1 cDNA
All
RMG URX ASE ASG AUA AQR ILs RIG SMBD
URX AQR
URX AUA
RMG ADL AFD AIY ASE ASG ASI AVE AWB AWC BAG
RMG URX ASH ASJ ASK FLP URA
URX AQR ALN AVM
RMG ILs
URX AQR ASH ADF ADL ASK ASI ASJ AIY AIZ
URX AQR ASG AIZ AIB AVG IL2
URX AQR ASH ADL
Genotype
WT
npr-1 (ad609)

Figure 3-1

Figure 3-2. Inhibition of RMG by NPR-1 is sufficient to suppress social behavior. **a,** Top, schematic of the Cre/Lox strategy used to express *npr-1* specifically in RMG. A LoxP-flanked *LacZ* sequence containing a transcriptional stop, three repeated polyA sequences, and two repeated mRNA cleavage sequences was inserted upstream of *npr-1:SL2:GFP* under the control of the *flp-21* promoter (*flp-21::LoxStopLox::npr-1 cDNA)*. Transgenic animals containing this plasmid were crossed with animals expressing *nCre* under the *ncs-1* promoter (*ncs-1::nCre)*. Bottom, GFP expression in L4 larval stage animal expressing both *ncs-1::nCre* and *flp-21::LoxStopLox::GFP*. Strong and consistent expression is observed in RMG and M2; ADL, ASJ, and ASK are seen weakly and inconsistently. **b,** Aggregation and related behaviors of *npr-1(ad609)* animals carrying either or both of the *ncs-1::nCre* and *flp-21:: LoxStopLox::npr-1 cDNA* transgenes. Asterisk, different from *npr-1(ad609)* ($P < 0.01$, Student's t-test). **c**, Images of mock-ablated (left) or RMG-ablated (right) *npr-1(ad609)* animals (mock-ablated: 97.1% bordering, 40% aggregating. RMG-ablated: 17% bordering, 0% aggregating. $\chi^2 = 43.05$, $P < 0.001$). **d,** Quantification of the rate of locomotion on food of *N2* and *npr-1(ad609)* animals that have been either mock-ablated or RMG ablated. Asterisk, different from mock-ablated *npr-1(ad609)* ($P < 0.01$, Student's t-test). All error bars indicate s.d.

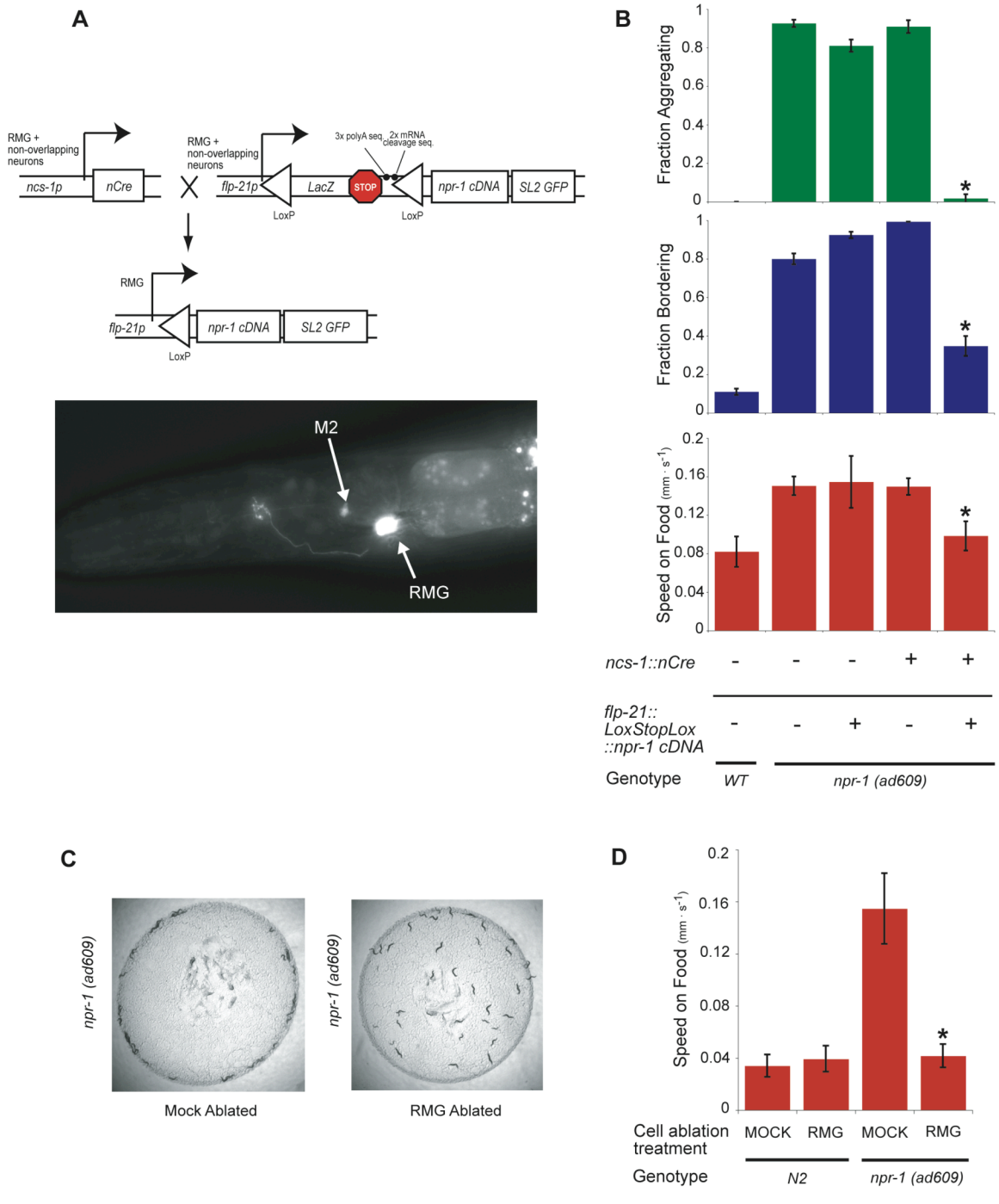
A
RMG +
non-overlapping
neurons
ncs-1p
nCre
RMG +
non-overlapping
neurons
flp-21p
LacZ
STOP
3x polyA seq.
2x mRNA
cleavage seq.
LoxP
LoxP
npr-1 cDNA
SL2 GFP
RMG
flp-21p
LoxP
npr-1 cDNA
SL2 GFP
M2
RMG
B
Fraction Aggregating
Fraction Bordering
Speed on Food (mm · s-1)
ncs-1::nCre
flp-21::
LoxStopLox
::npr-1 cDNA
Genotype
WT
npr-1 (ad609)
C
npr-1 (ad609)
npr-1 (ad609)
Mock Ablated
RMG Ablated
D
Speed on Food (mm · s-1)
Cell ablation
treatment
MOCK
RMG
MOCK
RMG
Genotype
N2
npr-1 (ad609)

Figure 3-2

Figure 3-3. ASK and ASJ sensory neurons contribute to aggregation behavior. **a**, Circuit diagram of neurons with gap junctions to RMG[85]. Arrow, chemical synapses; H, gap junctions. **b,** RMG-ablated *npr-1(ad609)* animals avoid solutions of high osmolarity. Animals were tested using the dry drop test with 1M glycerol. *osm-10(n1602)* control animals are strongly defective in osmotic avoidance. Avoidance Index = Average number of responses of 8-10 animals in 8-10 trials. Asterisk, different from *WT* ($P < 0.01$, t-test). Error bars indicate s.d. **c,** Rescue of aggregation and related behaviors in *tax-4(p678); npr-1(ad609)* mutant animals by expression of a *tax-4* cDNA. Asterisk, different from *tax-4; npr-1*. **d,** Aggregation and related behaviors of *npr-1(ad069)* animals expressing tetanus toxin light chain (TeTx) in specific neurons. (1), different from *npr-1(ad609)*. (2), different from *npr-1 (ad609);RMG::TeTx*, *npr-1 (ad609);URX::TeTx* and *npr-1(ad609)*. (3), different from *npr-1 (ad609);RMG::TeTx* , *npr-1 (ad609);ASJ+ASK::TeTx,* and *npr-1(ad609)*. (4), different from *npr-1 (ad609);RMG::TeTx, npr-1 (ad609);URX::TeTx, npr-1 (ad609);ASJ+ASK::TeTx,* and *npr-1(ad609)*. **e,** TeTx light chain inhibits aggregation and related behaviors through synaptobrevin cleavage. Cleavage resistant synaptobrevin (crSNB) was expressed in all neurons, and crossed into animals expressing TeTx light chain in RMG. Asterisk, different from *npr-1(ad609);RMG::TeTx* ($P<0.01$, student's t-test). Error bars indicate s.d.

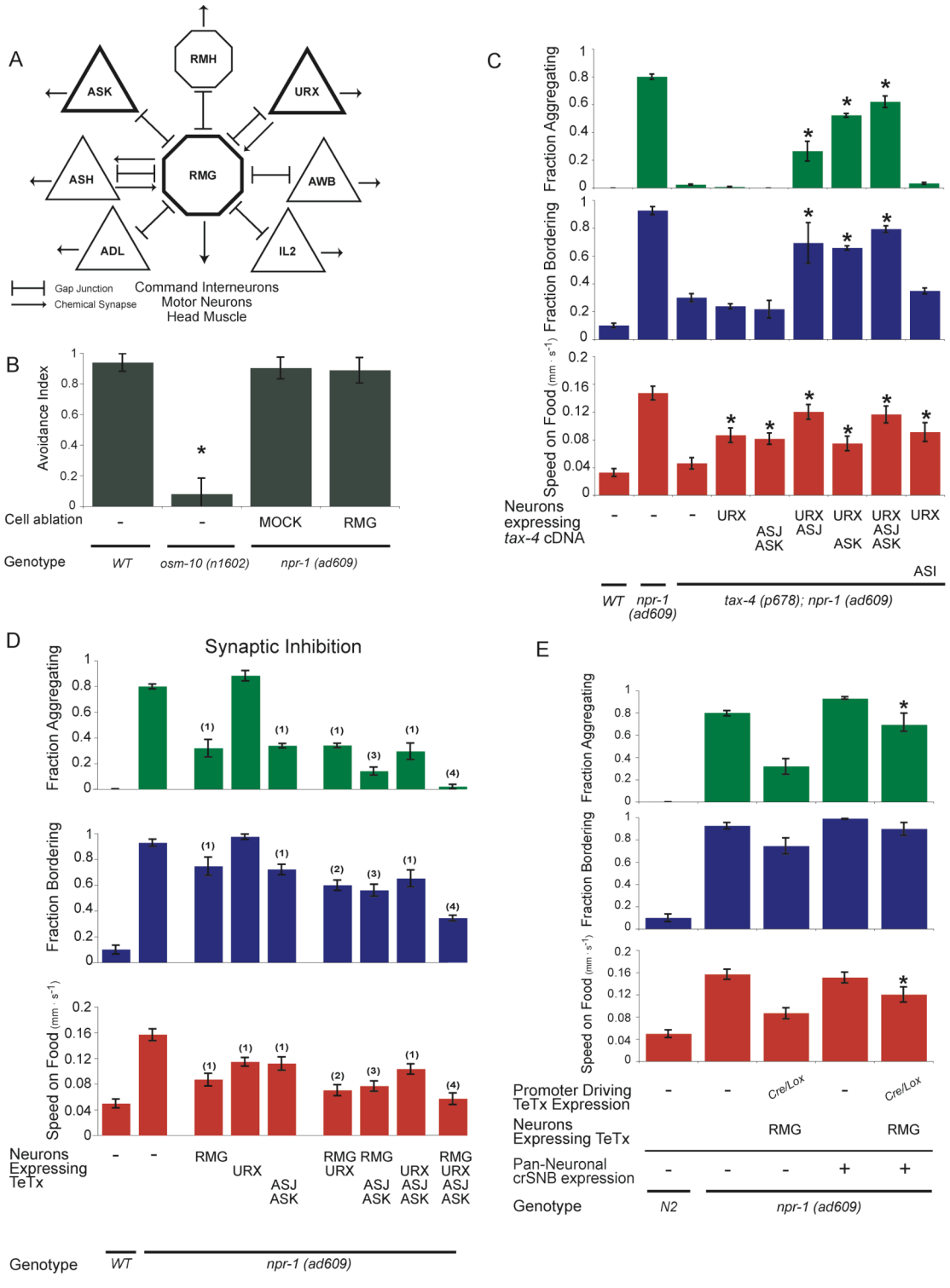
A
RMH
ASK
URX
ASH
RMG
AWB
ADL
IL2
Gap Junction
Chemical Synapse
Command Interneurons
Motor Neurons
Head Muscle
B
Avoidance Index
Cell ablation
-
-
MOCK
RMG
Genotype
WT
osm-10 (n1602)
npr-1 (ad609)
C
Fraction Aggregating
Fraction Bordering
Speed on Food (mm · s-1)
Neurons expressing tax-4 cDNA
-
-
-
URX
ASJ ASK
URX ASJ
URX ASK
URX ASJ ASK
URX
ASI
WT
npr-1 (ad609)
tax-4 (p678); npr-1 (ad609)
D
Synaptic Inhibition
Fraction Aggregating
Fraction Bordering
Speed on Food (mm · s-1)
Neurons Expressing TeTx
-
-
RMG
URX
ASJ ASK
RMG URX
RMG ASJ ASK
URX ASJ ASK
RMG URX ASJ ASK
Genotype
WT
npr-1 (ad609)
E
Fraction Aggregating
Fraction Bordering
Speed on Food (mm · s-1)
Promoter Driving TeTx Expression
-
-
Cre/Lox
-
Cre/Lox
Neurons Expressing TeTx
RMG
RMG
Pan-Neuronal crSNB expression
-
-
-
+
+
Genotype
N2
npr-1 (ad609)

Figure 3-3

Figure 3-4. **a,** Aggregation and related behaviors of *WT* animals expressing a gain-of-function novel protein kinase C (*pkc-1(gf))* in specific neurons. (1), different from WT. (2), different from *RMG::pkc-1(gf)*, *URX::pkc-1(gf),* and *npr-1(ad609)*. (3), different from *RMG::pkc-1(gf), URX::pkc-1(gf)*, *ASJ+ASK::pkc-1(gf),* and *npr-1(ad609)*. **b,** Bordering behavior of animals expressing *pkc-1(gf)* and/or *TeTx* in URX. **c,** Suppression of high locomotion on food by ablating RMG in N2 animals expressing *flp-21::pkc-1(gf)* (third lane in panel). Asterisk, different from mock ablated *flp-21::pkc-1(gf)* ($P < 0.01$, student's t-test). Suppression of bordering was observed in RMG(-) animals, but because of the small number of ablated worms, neither aggregation nor bordering was quantified. All error bars indicate s.d.

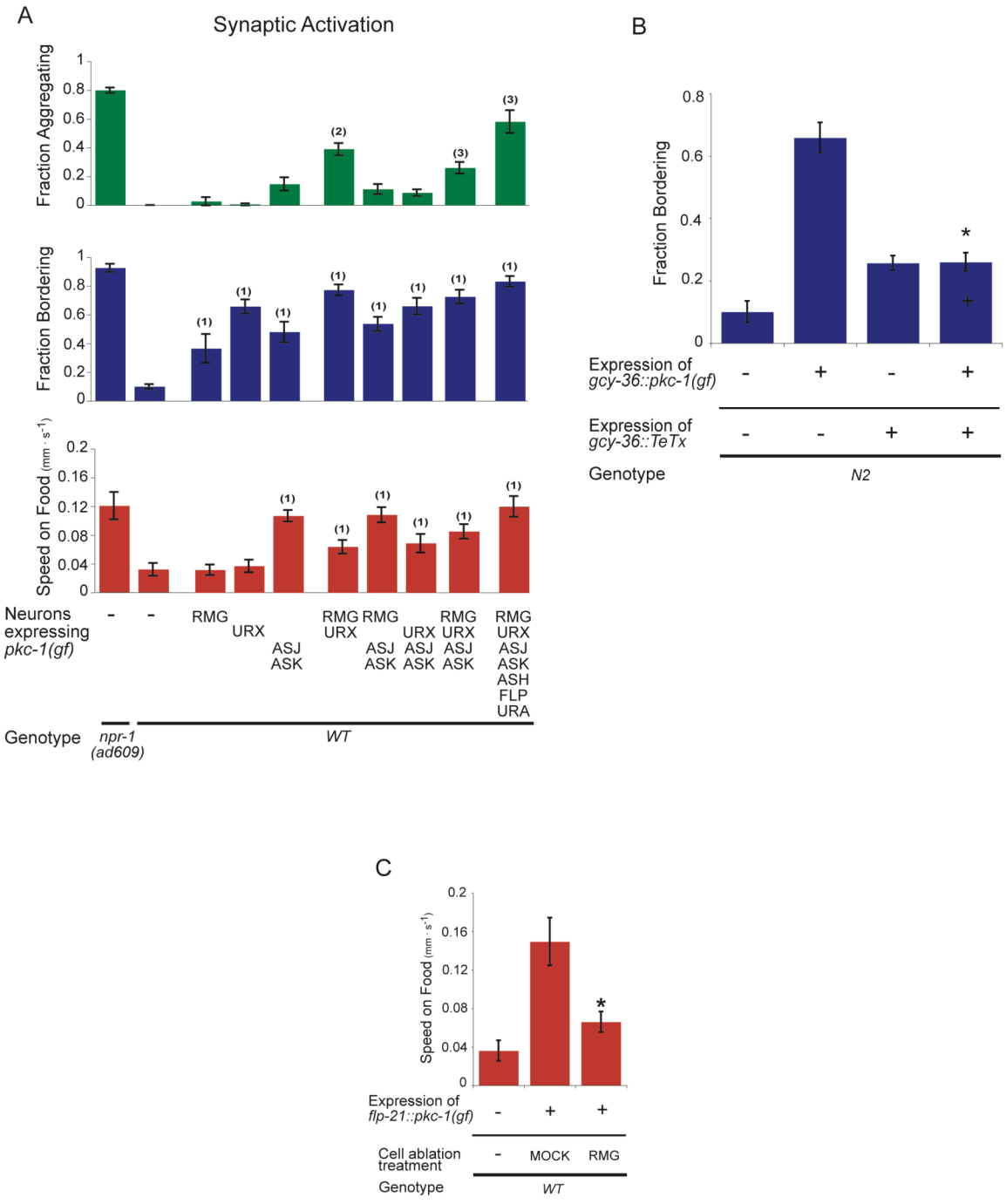
A
Synaptic Activation
Fraction Aggregating
Fraction Bordering
Speed on Food (mm · s⁻¹)
Neurons expressing pkc-1(gf)
RMG
URX
ASJ
ASK
ASH
FLP
URA
Genotype
npr-1 (ad609)
WT
B
Fraction Bordering
Expression of gcy-36::pkc-1(gf)
Expression of gcy-36::TeTx
Genotype
N2
C
Speed on Food (mm · s⁻¹)
Expression of flp-21::pkc-1(gf)
Cell ablation treatment
MOCK
RMG
Genotype
WT

Figure 3-4

Figure 3-5. **a**, Chemical structures of the three synthetic ascarosides. **b,** Schematic diagram of the pheromone chemotaxis assay. Washed animals were placed in the center of a 4-quadrant plate with ascarosides in alternating quadrants and scored after ten minutes. A chemotaxis index (C.I.) was calculated as (# on pheromone - # on buffer)/(total #). In the cartoon C.I. = -0.6**.** **c**, Ascaroside chemotaxis index of male and hermaphrodite animals. Asterisk, different from *npr-1(ad609)*. **d**, Expression of the *tax-4* cDNA in ASK restores pheromone attraction of *tax-4; npr-1* animals. Asterisk, different from *tax-4; npr-1*. **e**, Expression of TeTx in RMG or ASJ and ASK eliminates pheromone attraction in *npr-1(ad609)*. Asterisk, different from *npr-1(ad609).* **f**, Expression of *tax-4* cDNA in ASI partially restores repulsion to *tax-4* animals. Asterisk, different from *tax-4*. **g,** Chemotaxis of *npr-1(ad609)* and wild-type animals to various combinations of 10 nM ascarosides. **h**, Chemotaxis 10 nM ascaroside combinations of *tax-4(p678);npr-1(ad609)* and the same strain expressing *tax-4* in ASK. **i,** Chemotaxis to 10 nM ascaroside combination of *tax-4(p678);npr-1(ad609)* and the same strain rescued by expressing *tax-4* in ASI, ASK, or both. **j,** Chemotaxis to 10 nM ascaroside combination of *ocr-2(ak47)* and the same strain rescued by expressing *ocr-2* in ADL using the *srh-220* promoter. For all statistical tests, $P<0.01$ by Bonferroni's multiple comparison test. Error bars in b-d indicate standard error of the mean (s.e.m.).

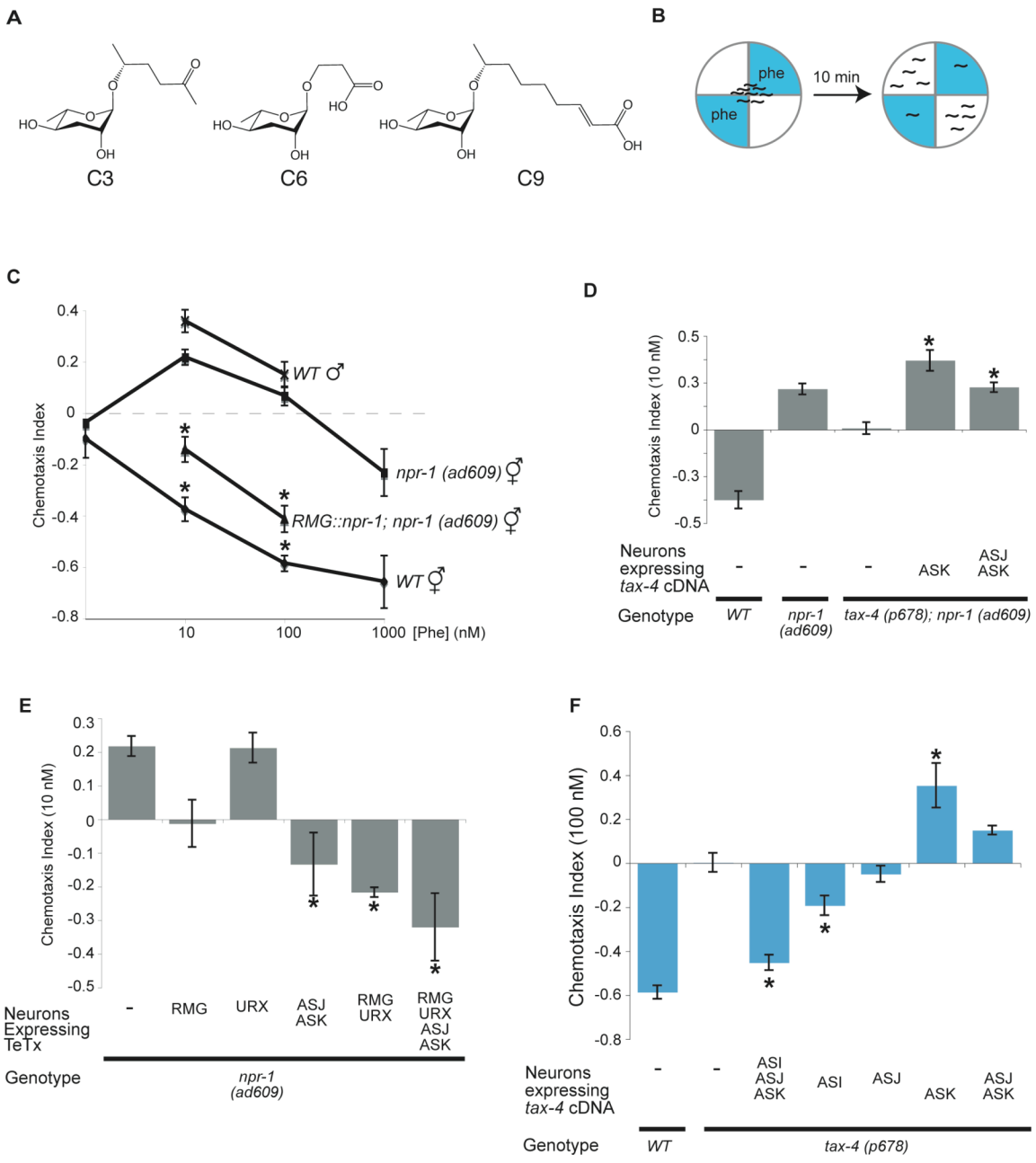
A
C3
C6
C9
B
phe
phe
10 min
C
Chemotaxis Index
WT ♂
npr-1 (ad609) ♀
RMG::npr-1; npr-1 (ad609) ♀
WT ♂
[Phe] (nM)
D
Chemotaxis Index (10 nM)
Neurons expressing tax-4 cDNA
Genotype
WT
npr-1 (ad609)
tax-4 (p678); npr-1 (ad609)
E
Chemotaxis Index (10 nM)
Neurons Expressing TeTx
RMG
URX
ASJ ASK
RMG URX
RMG URX ASJ ASK
Genotype
npr-1 (ad609)
F
Chemotaxis Index (100 nM)
Neurons expressing tax-4 cDNA
ASI ASJ ASK
ASI
ASJ
ASK
ASJ ASK
Genotype
WT
tax-4 (p678)

Figure 3-5 (A-F)

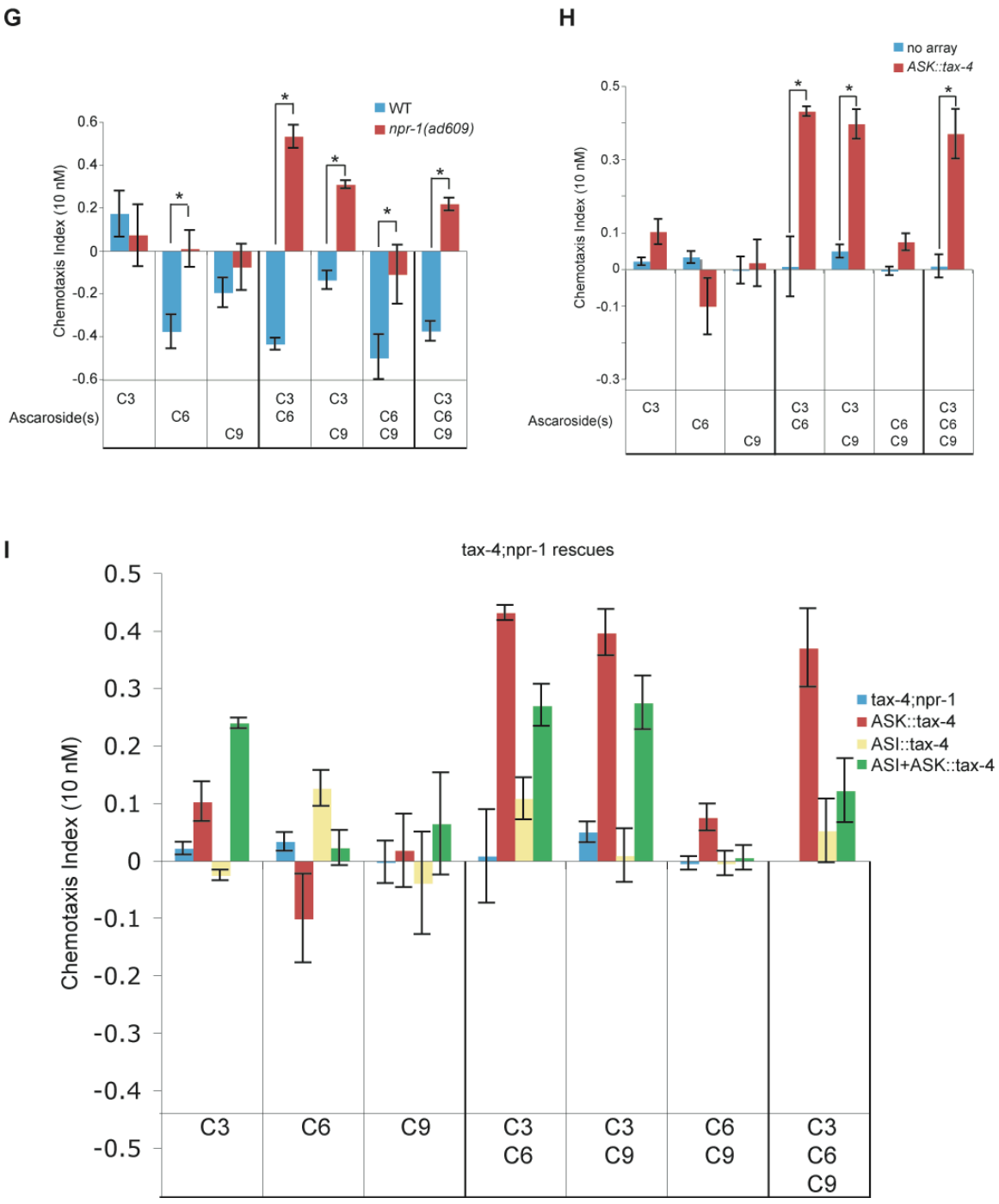
G
WT
npr-1(ad609)
Chemotaxis Index (10 nM)
0.6
0.4
0.2
0
-0.2
-0.4
-0.6
Ascaroside(s)
C3
C6
C9
C3 C6
C3 C9
C6 C9
C3 C6 C9
H
no array
ASK::tax-4
0.5
0.3
0.1
-0.1
-0.3
I
tax-4;npr-1 rescues
tax-4;npr-1
ASK::tax-4
ASI::tax-4
ASI+ASK::tax-4
0.5
0.4
0.3
0.2
0.1
0
-0.1
-0.2
-0.3
-0.4
-0.5

Figure 3-5 (G-I)

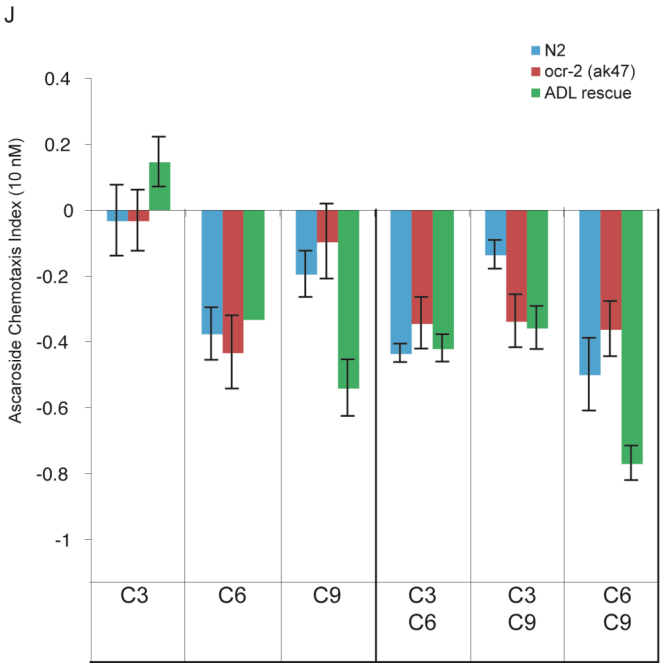
J
N2
ocr-2 (ak47)
ADL rescue
Ascaroside Chemotaxis Index (10 nM)
0.4
0.2
0
-0.2
-0.4
-0.6
-0.8
-1
C3
C6
C9
C3 C6
C3 C9
C6 C9

Figure 3-5 (J)

Figure 3-6. Calcium imaging of pheromone responses in ASK and AIA. **a,** 100 nM ascaroside-induced calcium decreases in the ASK sensory neurons of wild-type (n = 17) and *npr-1(ad609)* animals (n=17). **b**, ASK calcium responses to stimulation in mock-ablated (n = 10) and RMG-ablated (n = 9) *npr-1*(*ad609)* animals. Dark gray shading indicates presence of ascarosides (5s pulses of 1 μM pheromone cocktail). Light gray shading indicates s.e.m. **c**, Ascaroside-induced calcium increases in the AIA interneurons of *npr-1(ad609)* animals (mock, n=16; RMG ablated, n = 10; ASK ablated, n = 10; ASK+RMG ablated, n = 10). In a, b, and c, dark gray shading indicates presence of ascarosides (1 μM each). Light gray shading indicates s.e.m. **d**, Left, average responses of traces in **f** from the first 5 seconds after ascaroside stimulation. Right, average time to half-maximal response after pheromone addition. Asterisk, different from mock ablated ($P<0.01$ by Bonferroni's multiple comparison test). **e**, Plots of AIA calcium responses in mock ablated (left) and RMG-ablated (right) animals that are averaged in 3-6c. Each row is an individual animal. **f,** Model of a potential pheromone chemotaxis circuit based upon the *C. elegans* wiring diagram.[85] AIA is part of a circuit involved in odor chemotaxis and therefore could be a direct effector of pheromone chemotaxis. The ASI peptide DAF-7 suppresses aggregation[138], a function antagonistic to the ASK and ASJ functions defined here. These relationships between ASI, ASK and ASJ are analogous to the antagonistic functions of ASI and ASJ/ASK in dauer larva formation[84]. All of these neurons make or receive synapses from additional neurons not shown in this diagram.

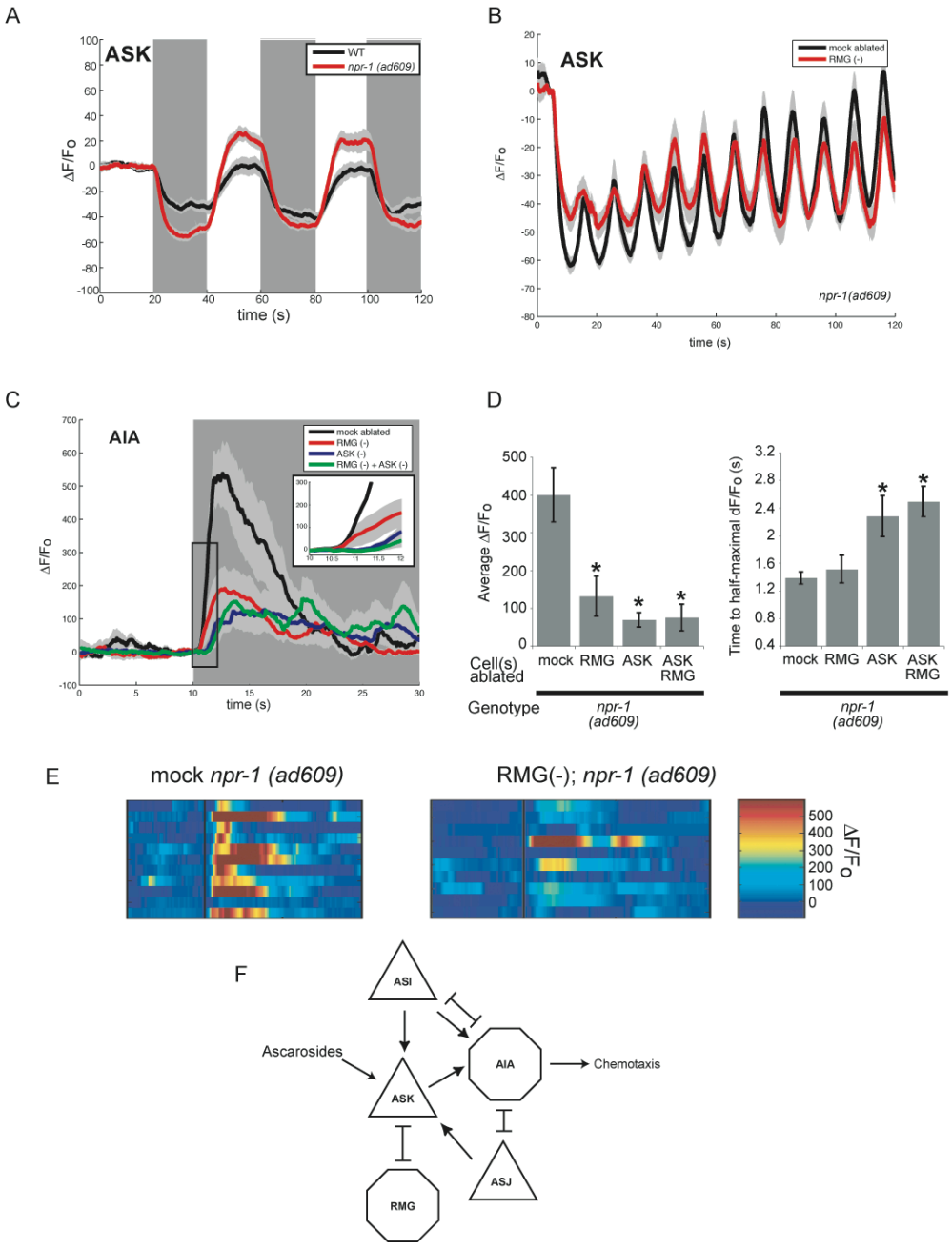
A
ASK
WT
npr-1 (ad609)
ΔF/Fo
time (s)
B
ASK
mock ablated
RMG (-)
ΔF/Fo
npr-1(ad609)
time (s)
C
AIA
mock ablated
RMG (-)
ASK (-)
RMG (-) + ASK (-)
ΔF/Fo
time (s)
D
Average ΔF/Fo
Cell(s) ablated
mock RMG ASK ASK RMG
Genotype
npr-1 (ad609)
Time to half-maximal dF/Fo (s)
mock RMG ASK ASK RMG
npr-1 (ad609)
E
mock npr-1 (ad609)
RMG(-); npr-1 (ad609)
ΔF/Fo
F
ASI
Ascarosides
ASK
AIA
Chemotaxis
ASJ
RMG

Figure 3-6 (A-E)

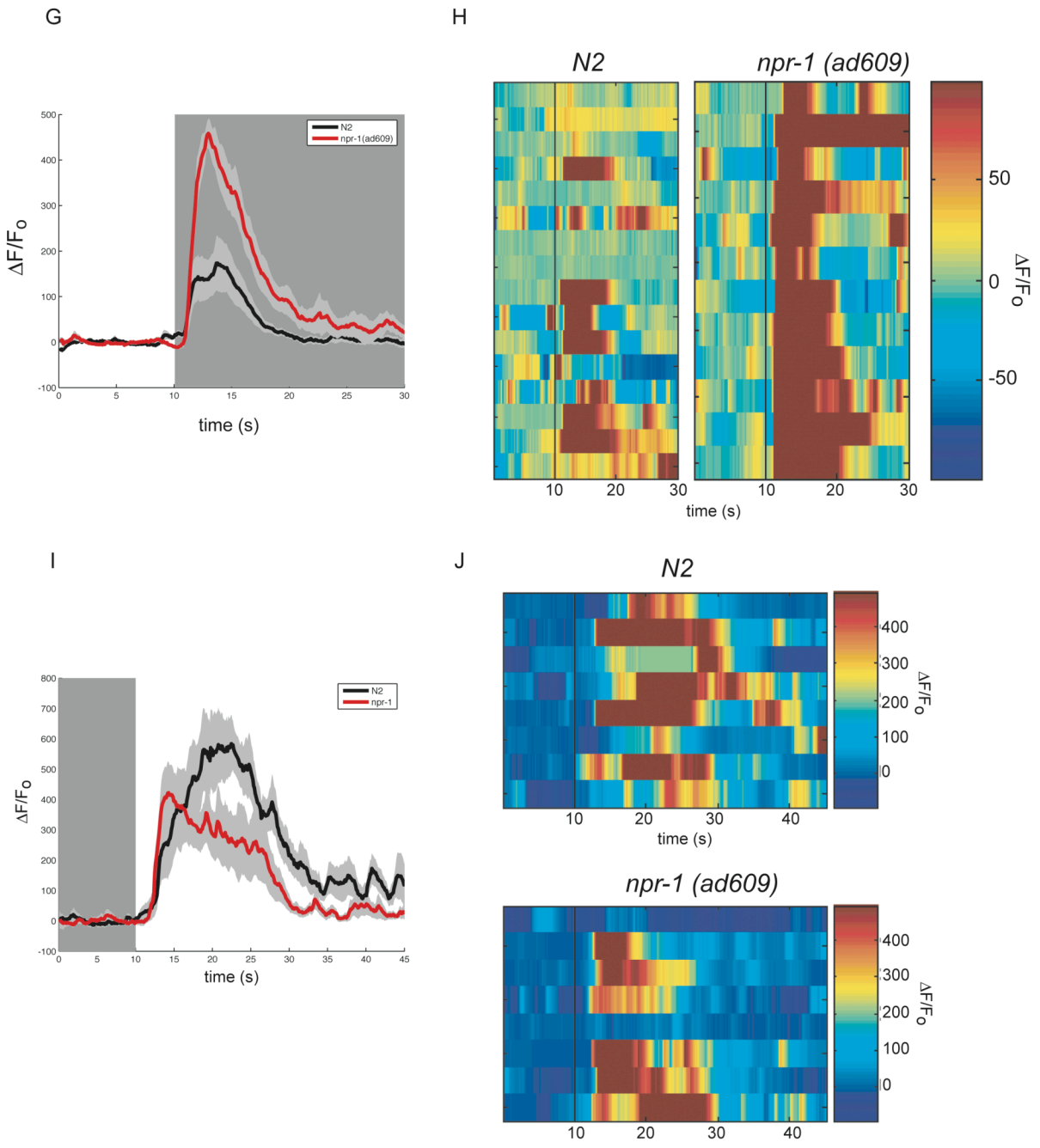

Figure 3-6 (G-J)

Figure 3-7. Genetic screen for suppressors of social feeding. **a,** Oxygen speed responses, on food, of *npr-1* and RMG-ablated *npr-1* animals (in collaboration with M. Zimmer). **b,** Oxygen response of wild-type *N2* animals. **c,** Oxygen response of *npr-1; arl-3(ky891)* resembles *N2*. **d,** Oxygen response of *npr-1;ky893* resembles RMG-ablated animals. **e,** *arl-3* and *pdl-1* suppress bordering and aggregation in *npr-1* animals. Asterisk, different from *npr-1(ad609)*. **f,** Pan-neuronal expression of *egl-21* cDNA rescues bordering and aggregation in *npr-1; egl-21(ky893)* animals. Asterisk, different from *npr-1 (ad609)*. Double asterisk, different from *egl-21(ky893); npr-1(ad609)*. For e and f, Bonferroni's t-test was used, $P < 0.05$. Error bars in e and f are standard errors of the mean (s.e.m.)

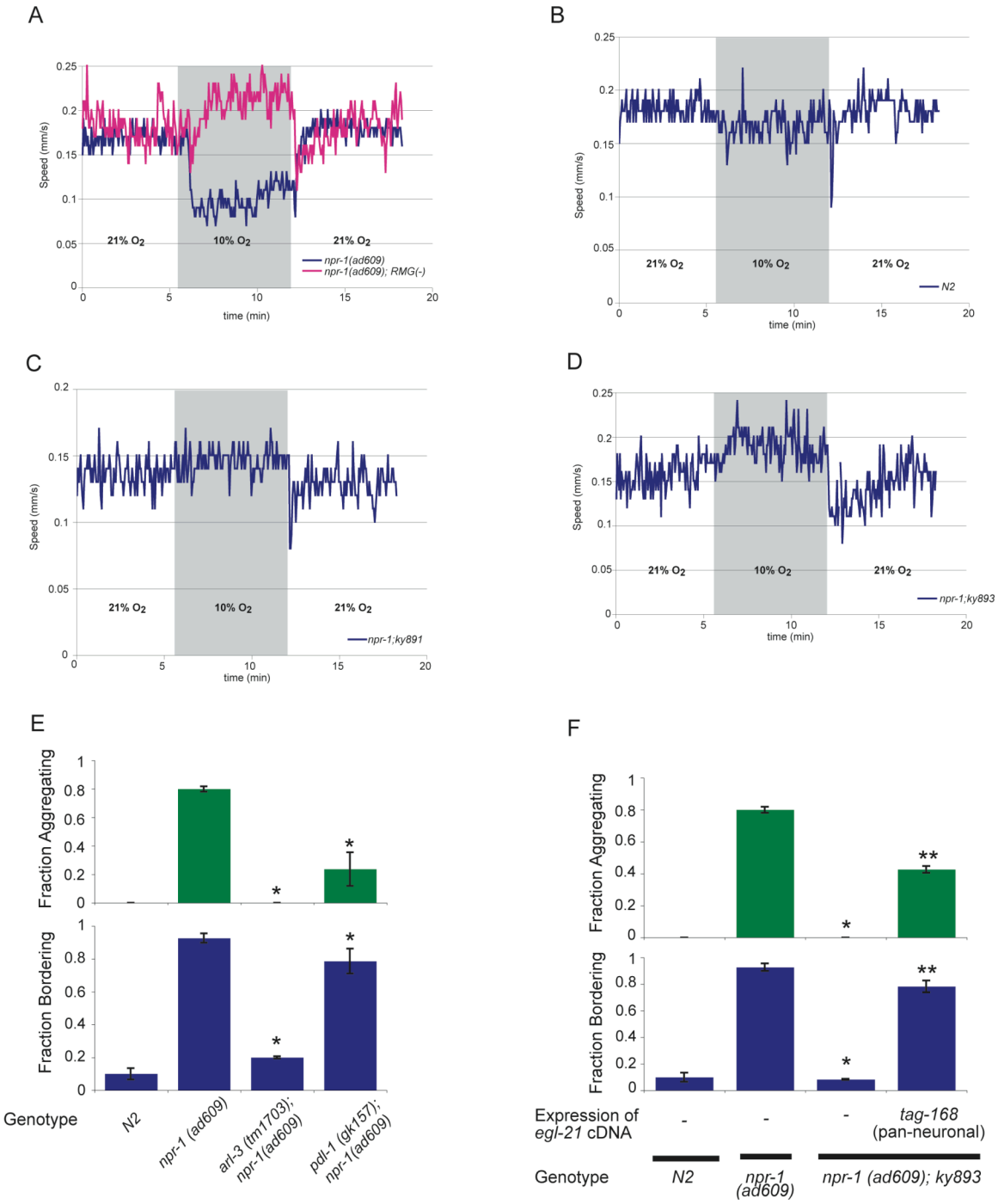
A
Speed (mm/s)
time (min)
21% O2
10% O2
21% O2
npr-1(ad609)
npr-1(ad609); RMG(-)
B
N2
C
npr-1;ky891
D
npr-1;ky893
E
Fraction Aggregating
Fraction Bordering
Genotype
N2
npr-1 (ad609)
arl-3 (tm1703); npr-1(ad609)
pdl-1 (gk157); npr-1(ad609)
F
Expression of egl-21 cDNA
tag-168 (pan-neuronal)
Genotype
N2
npr-1 (ad609)
npr-1 (ad609); ky893

Figure 3-7

Figure 3-8. Additional ascaroside chemotaxis experiments. **a,** Ascaroside chemotaxis in *npr-1(ad609);ocr-2(ak47)*, *ocr-2(ak47)*, and *ocr-2(ak47)* rescued strains. For ADL rescue the promoter *srh-220* was used; ASH+ASI rescue used the *sra-6* promoter. **b**, Ascaroside chemotaxis in the *pkc-1(gf)* strains from Figure 3-4A.

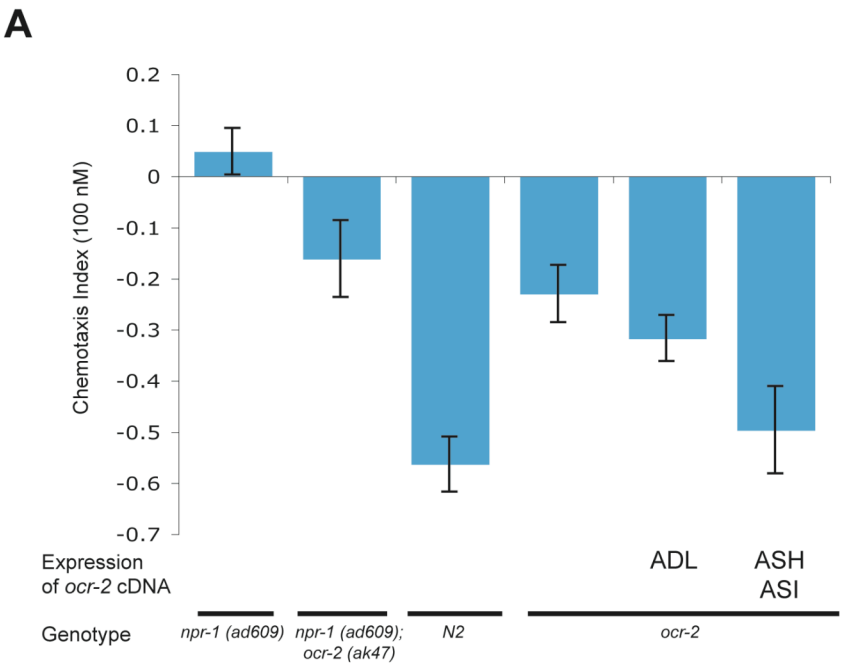

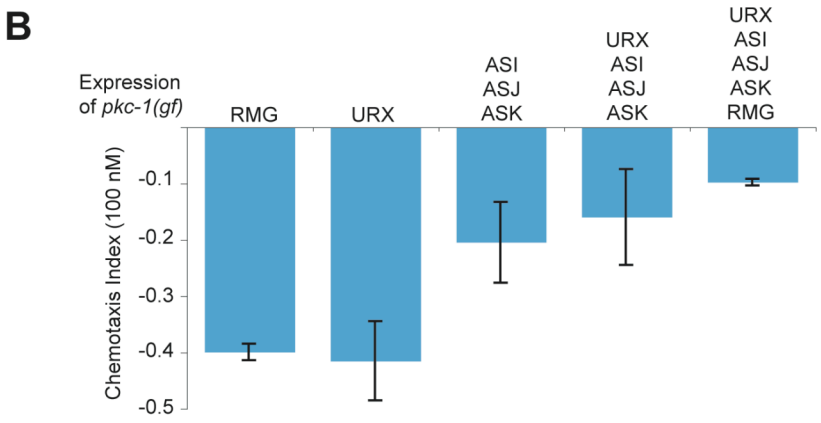

Figure 3-9. Additional aggregation and bordering experiments. **a,** Expression of TeTx in the ASH and ADL neurons using the *sra-6* and *srh-220* promoters does not affect the social feeding behavior of *npr-1(ad609)* mutants. **b,** *osm-3;odr-4;npr-1* triple mutants are social, unlike *odr-4;npr-1* double mutants[99]. Social feeding could be eliminated by pan-neuronal expression of the *osm-3* cDNA, but only partial suppression was observed when *osm-3* was expressed in most amphid gustatory neurons (*gpa-3*). These data do not provide a clear indication of how *osm-3* suppresses the *npr-1;odr-4* double mutant. **c,** Social feeding behavior is not strongly suppressed when an *npr-1* cDNA containing the 215F allele is expressed.

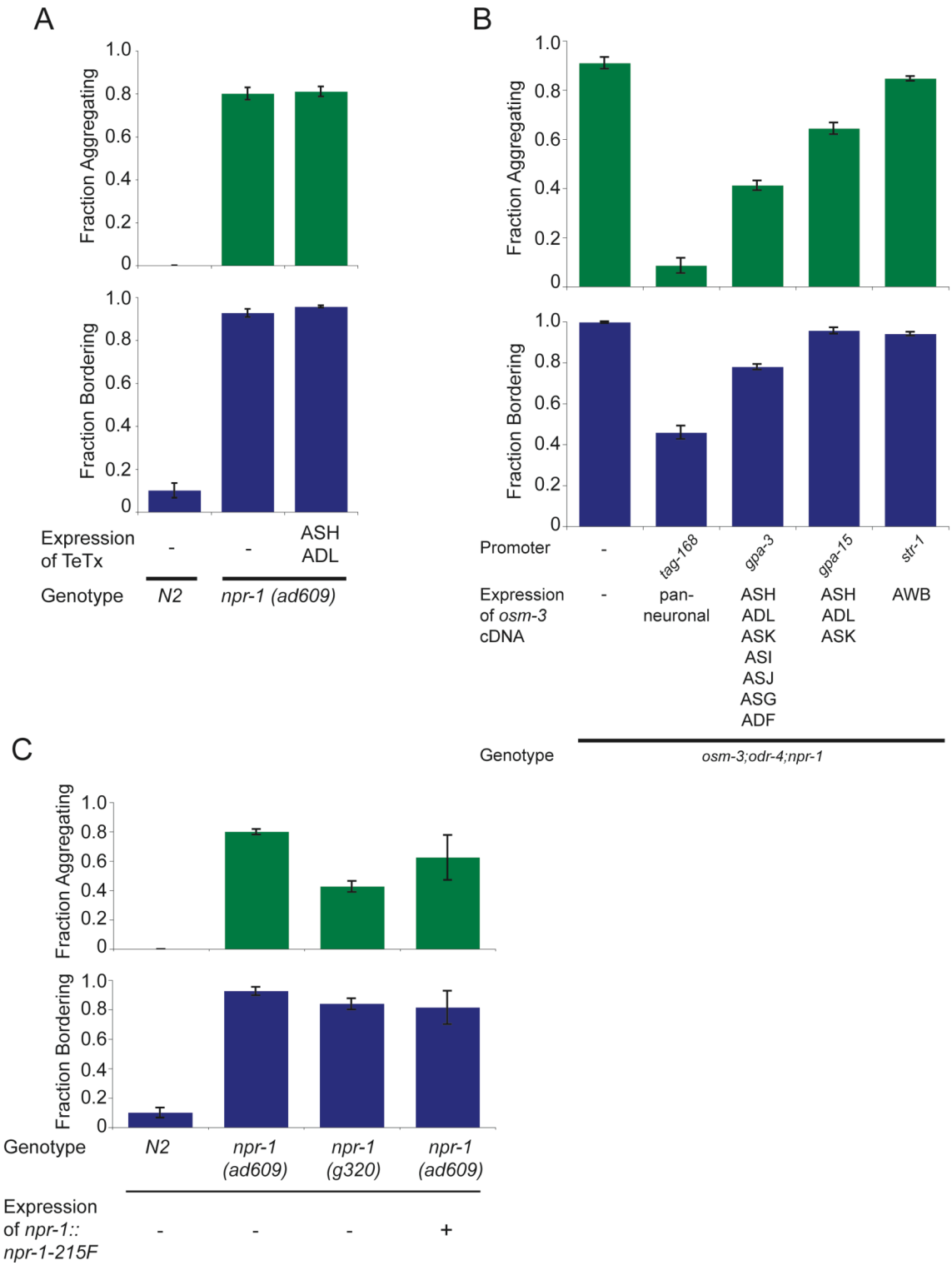
A
Fraction Aggregating
1.0
0.8
0.6
0.4
0.2
0
Fraction Bordering
Expression of TeTx
-
-
ASH ADL
Genotype
N2
npr-1 (ad609)
B
Promoter
-
tag-168
gpa-3
gpa-15
str-1
Expression of osm-3 cDNA
-
pan-neuronal
ASH ADL ASK ASI ASJ ASG ADF
ASH ADL ASK
AWB
Genotype
osm-3;odr-4;npr-1
C
Genotype
N2
npr-1 (ad609)
npr-1 (g320)
npr-1 (ad609)
Expression of npr-1:: npr-1-215F
-
-
-
+

Figure 3-9

Chapter 4:

Studies of a Vasopressin Peptide Homologue in C. elegans

Introduction

The studies of social behavior in previous chapters began with behavioral observations that were subsequently studied at the cellular and genetic levels. Early in my graduate career, I sought an alternative approach: to find *C. elegans* homologues of gene products known to affect social behaviors in other species. The most interesting candidate was the gene F39C12.4, which encodes a peptide with homology to the vasopressin and oxytocin neuropeptides of vertebrates. There is strong and abundant evidence that these two neuropeptides, which differ only slightly in sequence, control social behavior. For example, polymorphic expression of the vasopressin receptor V1a determines whether male voles are monogamous or polygamous[139]. Oxytocin has been shown in numerous species to be important for pair bonding between parents and progeny, and recently was found to shape trust responses to social interactions in humans[28]. Both peptides also play important physiological roles. Vasopressin, for example, is a regulator of blood pressure and osmolarity, and body temperature[140]. I sought to understand the behavioral role of the vasopressin/oxytocin homologue in *C. elegans*.

Results

F39C12.4 Gene Encodes a Vasopressin Homologue

I performed a blast search of the human vasopressin (huVP) gene product against the *C. elegans* genome. Only the gene *F39C12.4* returned a significant hit. Sequence

alignment of huVP with *F39C12.4* is shown in Figure 4-1A. The cysteines in the propeptide are conserved, suggesting that the two gene products fold similarly. Further, there is some homology between the huVP mature peptide sequence (red line) and the *F39C12.4* sequence. Taken together, these observations suggest that *F39C12.4* (ceVP) is the *C. elegans* homologue of vasopressin/oxytocin.

Several classes of vasopressin and oxytocin receptors exist in vertebrate genomes. *C. elegans* has many 7-transmembrane receptors, several of which have homology to these vasopressin/oxytocin receptors. I focused specifically on the *C. elegans* genes *T07D10.2* and *F14F4.1*, which have the strongest homology to the vasopressin V1a receptor (V1aR). In vertebrates, V1aR is responsible for many of the behavioral effects of vasopressin[27].

ceVP and its Candidate Receptors are Expressed in Specific Neuronal Subsets

To further understand the role of ceVP in the *C. elegans* nervous system, I fused GFP to 3 kb of promoter sequence upstream of the ceVP translational start site. Strong expression was seen specifically in the thermosensory neuron AFD. Next, the expression patterns of the two V1aR homologues were determined. *T07D10.2* drove strong expression in the sensory neurons ASH and ADF, as well as other cells less strongly and frequently, while ASH and ADL expression was seen in *F1414.1* (Table 4-1). These data suggest that ceVP is an AFD-specific peptide that likely modulates the activity of other amphid sensory neurons, such as ASH, ADL, and AFD.

ceVP Regulates Thermotaxis Behavior

When cultivated at a fixed temperature, worms will return to that temperature when placed in a temperature gradient off of food[141]. This behavior, known as thermotaxis, was found to require the AFD sensory neurons and downstream RIA, AIZ, and AIY interneurons[54]. Using electrophysiological methods, AFD activity was observed to fluctuate with temperature[142]. Since ceVP is expressed specifically in AFD, I asked whether it might regulate thermotaxis behavior. Animals were placed in a linear temperature gradient from 18° C to 26° C for 45 minutes, after which their distribution across the plate was counted (Figure 4-1B). When wild-type *N2* animals were cultivated at 20° C, they accumulated at the center of the plate, where the temperature was near 20° C (Figure 4-1C). A loss-of-function *ceVP* mutant obtained from the National BioResource Project of Japan, *tm2385*, showed cryophilic behavior, accumulating in the coldest region of the plate. A transgenic worm overexpressing *ceVP* also was cryophilic. A loss of function mutation in the V1aR homologue *F14F4.1, tm2243,* did not affect thermotaxis behavior when animals were cultivated at 20° C, but did show an athermotactic phenotype when cultivated at 25° C, distributing evenly throughout the termperature gradient (Figure 4-1D). These data demonstrate that *ceVP*, and at least one of its receptors, *F14F4.1*, regulate thermotaxis behavior.

Thermotaxis and Pathogenic Bacteria

In vertebrates, injection of vasopressin into the cerebrospinal fluid causes a strong reduction of fever in cases of infection or other inflammatory-mediated pyresis[143]. *C.*

elegans has previously been used as a model system to understand the behavioral responses to infection by several pathogenic bacteria, including *Pseudomonas aeruginosa*[144,145]. Growth of *C. elegans* on the PA14 strain of *P. aeruginosa* results in an intestinal infection that leads to avoidance of the bacterium and nutritional deficiency. I asked whether thermotaxis was affected by *P. aeruginosa* exposure. Growth of animals at 20° C on the standard *E. coli* OP50 strain resulted in accumulation of animals at the center of the thermal gradient. By contrast, when animals were exposed to PA14 during cultivation, their thermotaxis behavior became cryophilic (Figure 4-1E). This behavior was a consequence of pathogenicity because a related, non-pathogenic *Pseudomonas* species, *P. fluorescens*, did not strongly affect thermotactic behavior.

The avoidance of pathogenic bacteria was previously found to be dependent on serotonin signaling[145]. I asked whether serotonin is required for PA14-induced cryophilia. Cultivation of *cat-1*, a monoamine transporter mutant that eliminates both dopamine and serotonin signaling, on OP50 at 20°C resulted in a mild thermotaxis defect in which animals accumulated at slightly lower temperatures than 20°C (Figure 4-1F). No increase in cryophilic behavior was observed when *cat-1* animals were cultivated in the presence of PA14. The serotonin receptor *mod-1* was found to be required for learned avoidance of PA14 by *C. elegans*[145]; however, *mod-1* was indistinguishable from *N2* in its thermotaxis behavior when cultivated on either OP50 or PA14. These data suggest that serotonin—or perhaps another biogenic amine—regulate thermotactic responses to pathogenic bacteria through receptors other than *mod-1*.

Discussion

Although I showed above that *C. elegans* becomes cryophilic when grown on pathogenic bacteria, I was not able to show a functional connection between *ceVP* and the pathogenic response. This was because both *ceVP* loss-of-function and overexpression caused cryophilia, preventing me from testing whether the gene was required for the PA14 response. It is surprising that *ceVP* deletion and overexpression cause the same phenotype. One possibility is that the *ceVP* promoter used in the overexpression study is causing toxicity in AFD. SAGE expression data of AFD indicates that the *ceVP* promoter is very strong[146]. Perhaps the multi-copy array used to generate overexpression caused deleterious transcription defects in AFD that led to impaired function. Indeed, AFD-ablated animals and mutants that show AFD cell fate defects are cryophilic[54,147].

The involvement of monoamine signaling in the thermotactic response to PA14 is consistent with the role of serotonin in the regulation of other behavioral responses to pathogenic bacteria. Intriguingly, one of the V1aR receptors, *T07D10.2*, is expressed in ADF, a serotonergic neuron involved in the response to PA14[145]. Examination of a *T07D10.2* mutant in thermotaxis could prove interesting, as would crossing it into a serotonin-deficient background. Such experiments could help connect *ceVP* signaling with the pathogenic bacterial response.

These studies also provide some interesting evolutionary context for vasopressin and oxytocin, neuropeptides with numerous roles in physiology and behavior in vertetbrates. Specifically, it appears that the thermoregulatory activity of this

neuropeptide family evolved very early, and perhaps was its original function. Careful thermal sensation and control are essential for the proper maintenance of a myriad of physiological processes, such as energy homeostasis[148] and synaptic transmission[149]. It remains to be seen whether *ceVP* has other effects on *C. elegans* behavior and physiology.

Table 4-1. Expression patterns of the vasopressin ligand homologue F39C12.4 and neuropeptide receptor homologues. Most consistent expression is listed in bold; less frequently seen cells are in normal type. The less consistent cells are listed in order of descending frequency seen.

Gene Name	Description	Expression Pattern
F39C12.4	Vasopressin ligand homologue	**AFD**, tail cell (rarely seen)
T07D10.2	V1aR homologue	**ASH, ADF**, AWC, RIC, ASI, AWB, AUA, PQR, DVC
F14F4.1	V1aR homologue	**ASH, ADL**, other identified cells
F54D7.3	GnRH receptor homologue	**ADF, ASI, other unidentified neurons anterior to nerve ring, RIC, ventral nerve cord,** ASI, RMG, PVQ, RIB, SAAV
ZK455.3	Galanin receptor homologue	**AIB**, AVJ (faint), AIY (faint)
W05B5.2	Orexin receptor homologue	**AVE, AIY, two unidentified cells posterior to AIY, RIV, SIBV/GLR, AIZ, AVB**, RIM, RIC, ASG, AVA

Figure 4-1. **a**, Protein sequence of human vasopressin (human VP) with the *F39C12.4* gene of *C. elegans* (*ceVP*). Gray boxes indicate similarity; black boxes indicate identity or gaps in the alignment. The red bar designates the mature human vasopressin peptide sequence. **b,** Diagram of thermotaxis using a linear gradient system. Peltier devices on either side of a conductive metal surface generate a linear temperature gradient. Water is run below in order to cool the system. Animals are placed at the center of an unseeded NGM plate atop the metal surface, and allowed to move through the gradient for 45 minutes before counting. **c,** Thermotactic behavior of the loss-of-function *ceVP* mutant *tm2385*, the V1aR homologue *F14F4.1 (tm2243)* and a *ceVP* overexpression transgenic line. All animals were cultivated at 20 degrees. Asterisk: different from *N2* in bin #1 ($P < 0.05$ by Bonferoni's t-test). **d,** *F14F4.1(tm2243)* is athermotactic when cultivated at 25 degrees. Asterisk: different from *N2* in bin #6 ($P < 0.05$ by student's t-test). **e,** Cultivation on pathogenic PA14 bacteria causes cryophilia. Asterisk, different from *N2* in bin #1 ($P < 0.05$ by student's t-test). **f,** Thermotactic behavior of *cat-1* and *mod-1* mutants cultivated at 20 degrees.

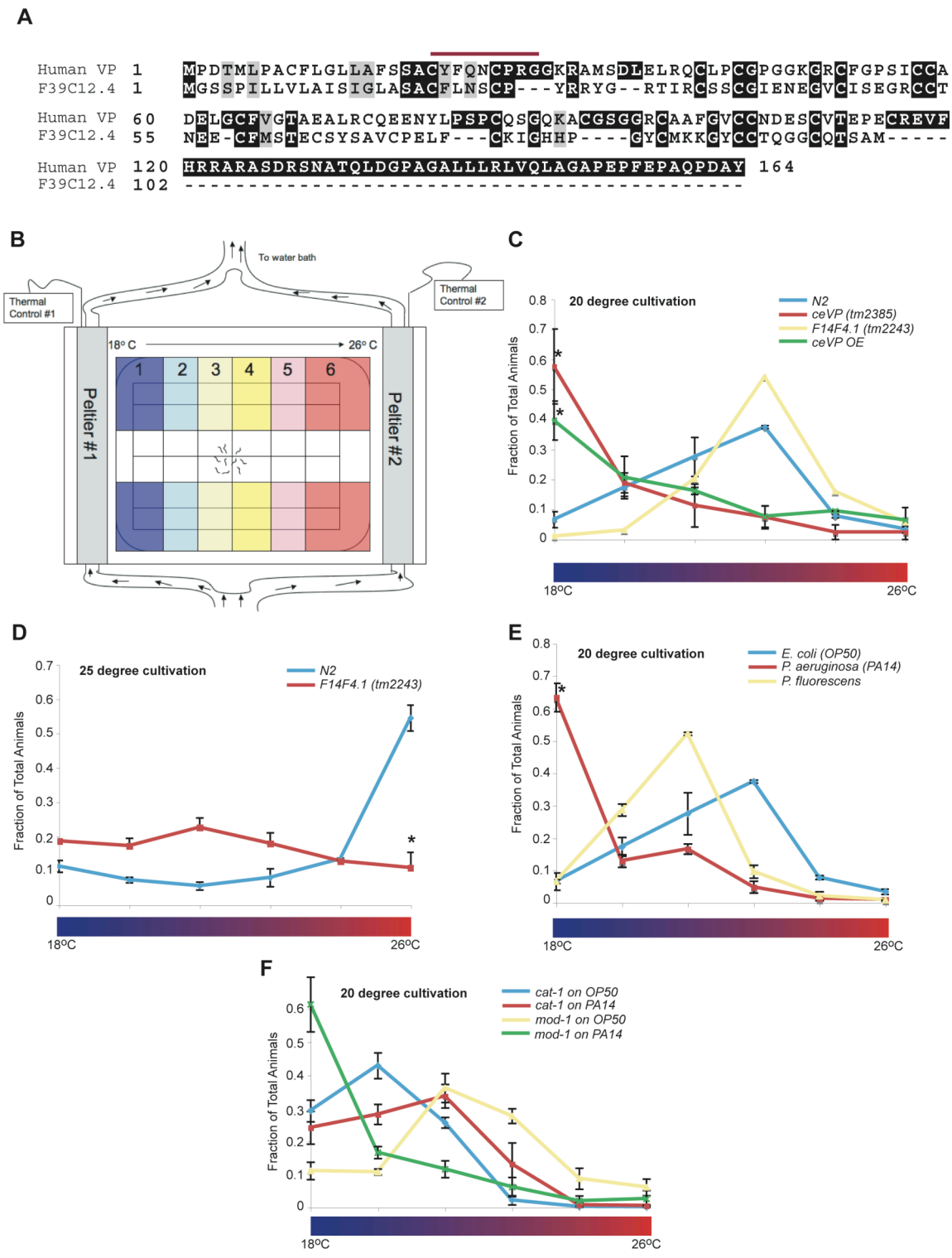
A
Human VP 1 MPDTMLPACFLGLLAFSSACYFQNCPRGGKRAMSDLELRQCLPCGPGGKGRCFGPSICCA
F39C12.4 1 MGSSPILLVLAISIGLASACFLNSCP---YRRYG--RTIRCSSCGIENEGVCISEGRCCT
Human VP 60 DELGCFVGTAEALRCQEENYLPSPCQSGQKACGSGGRCAAFGVCCNDESCVTEPECREVF
F39C12.4 55 NEE-CFMSTECSYSAVCPELF---CKIGHHP----GYCMKKGYCCTQGGCQTSAM-----
Human VP 120 HRRARASDRSNATQLDGPAGALLLRLVQLAGAPEPFEPAQPDAY 164
F39C12.4 102 ----------
B
To water bath
Thermal Control #1
Thermal Control #2
18° C
26° C
1 2 3 4 5 6
Peltier #1
Peltier #2
C
20 degree cultivation
N2
ceVP (tm2385)
F14F4.1 (tm2243)
ceVP OE
Fraction of Total Animals
18ºC
26ºC
D
25 degree cultivation
N2
F14F4.1 (tm2243)
Fraction of Total Animals
18ºC
26ºC
E
20 degree cultivation
E. coli (OP50)
P. aeruginosa (PA14)
P. fluorescens
Fraction of Total Animals
18ºC
26ºC
F
20 degree cultivation
cat-1 on OP50
cat-1 on PA14
mod-1 on OP50
mod-1 on PA14
Fraction of Total Animals
18ºC
26ºC

Figure 4-1

Chapter 5:

Conclusions and Future Experiments

Ascaroside sensation

The molecular machinery by which *C. elegans* senses pheromone is completely unknown. Studies of pheromone sensation in *Drosophila* have produced interesting insights into olfactory signal transduction pathways,[38] and elucidated important molecular differences between male and female flies that could help account for unique behavioral responses to pheromones[39]. The identification of ascaroside-dependent calcium changes in ASK neurons (Chapter 3) provides a system to begin to understand how pheromone sensation occurs in *C. elegans*. First, determining the contribution of each of the three components used in my studies—C3, C6, and C9—will be important, as my data indicate that these ascarosides have different behavioral affects (Chapters 2 and 3). In male mating behavior, C9 and C6 act cooperatively[16]. Calcium imaging experiments could help determine whether this cooperativity is a consequence solely of augmentation of ASK signaling, or whether circuit components—like the sensory neurons ASI and ASJ or the interneurons RMG or AIA—are required.

The imaging of pheromone responses in ASI and ASJ will also prove interesting. ASI has a clear role in pheromone-induced behaviors: ASI-ablated animals constitutively dwell in the exploration assay (Chapter 2), regardless of the presence of ascarosides. Furthermore, ASI rescue of *tax-4* promotes pheromone avoidance (Chapter 3). In addition, ASI appears to influence social feeding based on the effects of *daf-7*, a gene with ASI-selective expression: *daf-7* animals show a modest aggregation phenotype and, like *npr-1*, they avoid high oxygen levels on a bacterial lawn[113]. These data indicate that

ASI, in contrast to ASK, inhibits social feeding and promotes pheromone avoidance. Calcium imaging of ASI would help uncover whether this opposing activity is encoded at the level of chemosensation, or whether ASI synaptic output to other neurons causes this switch. ASJ is also thought to be involved in dauer pheromone sensation[84], and, when *tax-4* is rescued in both URX and ASJ, social feeding is restored in an *npr-1;tax-4* double mutant (Chapter 3). ASJ may also respond to ascaroside stimulation.

The study of pheromone chemosensation by calcium imaging is somewhat hampered by the response of the ASJ and ASK neurons to blue light[150]. This necessitated pre-exposure of the animals to a period of blue light before beginning ASK calcium imaging experiments (see methods); without pre-exposure, pheromone-induced changes were erratic and small in magnitude (data not shown). Presumably, pre-exposure induces light-specific adaptation in ASK that allows it to respond to other stimuli, like pheromone. Animals in this adapted state, however, may be different from those that are tested in behavior, which could result in discrepancies between genetic requirements in the two systems. Technical improvements in calcium imaging, such as two-photon imaging could help alleviate this problem.

Further Characterization of Deathmone Components

Using the drop test, I found that deathmone was an acute repellent (Chapter 2); however, the active substances in this mix have yet to be identified. Although the ascaroside C7 also causes avoidance, it appears to act through different sensory pathways than deathmone (Figure 2-1D). Specifically, deathmone avoidance is completely dependent on *osm-9* activity and the neurons ASH and ADL (J.H. Thomas, unpublished),

while the C7 ascaroside acts only partially through *osm-9* in neurons other than ASH. The four other ascarosides (C3, C5, C6, and C9) should be tested for repellent activity, and assayed for dependence on the TRP channel *osm-9*. ASH is the main nociceptive neuron in *C. elegans*, so identification of repellents that act independently of this neuron could illuminate new sensory signaling pathways in the worm.

A mix of ascaroside and tryptophan-like small molecules appears to account for the dwelling activity of deathmone (Chapter 2). Nematodes produce a variety of indole-containing molecules, including serotonin and derivatives such as N-acetylserotonin[151]. Further chemical analysis of deathmone, combined with behavioral studies of these candidate small molecules, will be important for determining the exact identity of the tryptophan-like compound. Additionally, it was found that deathmone from a distantly related nematode, PS512, is active on *C. elegans*. This PS512 deathmone should be subjected to a dilution series in order to compare its activity with *C. elegans* deathmone. Chemical analysis may uncover whether these two nematodes produce similar behaviorally active compounds.

The AIY and AIZ Connection

Laser ablation analysis of amphid interneurons suggest that AIY and AIZ have opposite roles in exploratory behavior: AIY promotes roaming while AIZ induces dwelling. Although it receives input from many well-studied amphid sensory neurons, AIZ's role in behavior is poorly understood. AIY and AIZ were found to have opposite effects in thermotaxis[54], a behavior in which animals off of food move towards the temperature at which they had previously been cultivated. It is possible that the synaptic

connections between AIZ and other neurons are important for both thermotaxis and exploratory behavior. The simplicity of the exploration assay, and the ability to obtain reliable data from a small number of individual animals, could enable thorough examination of AIZ connectivity through laser ablation. Killing AIZ in combination with other neurons could help identify its important inputs and outputs; these cells, in turn, would be candidate effectors of thermotaxis behavior.

Pheromones, Social Feeding, and Mating

My work shows that pheromone sensation and social feeding both involve the ASK neurons, with the cooperation of ASI and ASJ, both of which are presynaptic to ASK. Previous reports have implicated these neurons, particularly ASK, in male pheromone chemotaxis[16], and the aggregating *npr-1* strain has a pheromone response more similar to wild-type males than wild-type hermaphrodites (Chapter 3). Furthermore, males show hyperactivity on food and aggregation, albeit milder than *npr-1,* and wild-type males, like *npr-1* hermaphrodites, engage in aerotaxis on a bacterial lawn (Macosko and Jang, unpublished). Together, these data provide suggestive evidence that male behavior and social feeding share overlapping neuronal circuitry. Most of the intensely studied social behaviors from other systems—courtship and aggression in flies, birdsong in finches, colony structure of fire ants—are related to reproduction or mating. Therefore, it is not surprising that *C. elegans* social feeders and males share similar behaviors that may be executed by the same neuronal circuitry.

Are similar molecular mechanisms at work in males and social feeders to transform the circuit's responses? In particular, is RMG hyperactive in males, resulting

in an activation of ASK and downstream neurons, as is postulated for *npr-1* social feeders (Chapter 3)? Quantitative imaging of AIA in wild-type males in combination with RMG ablations, as was performed on *npr-1* animals, could help answer this question. Recently, it was found that *fem-3* overexpression in the nervous system of *C. elegans* hermaphrodites caused male-like pheromone responses[77], much as *fruitless*^{M} expression in flies can induce male neuronal fates in female animals. I am currently generating animals expressing *fem-3* in specific cells within the aggregation circuit to determine which neurons need to be re-programmed in order to produce male-like pheromone and oxygen responses.

egl-21 and social feeding

I isolated *egl-21* as a strong social feeding inhibitor with intact, wild-type oxygen responses (Chatper 3). Although it appears that RMG expression is not required, it will nonetheless be interesting to identify the *egl-21* site of action. Based on the preliminary data, I suspect that ASI, ASJ, and ASK, in cooperation with other as-yet unidentified neurons, are the important players. Recently, mass spectrometry was used to compare the neuropeptide profile of wild-type animals with *egl-21* mutants, and indicated that a subset of neuropeptides in the *C. elegans* genome require *egl-21* for proper processing[152]. This technique could be employed to determine which *egl-21*-dependent neuropeptides are necessary for social feeding behavior, by analyzing *egl-21;npr-1* mutants rescued in a cell-specific manner. Loss-of-function mutants could then be used to confirm which are required for social feeding.

At present, although several neuropeptide mutants have been found to display behavioral phenotypes[97,114,153], we still know relatively little about how individual neuropeptides work at specific sites in a *C. elegans* neuronal circuit. The identification of a particular neuropeptide, acting in a specific neuronal cell-type to execute social feeding behavior, would be a powerful system in which to study how neuropeptides alter neuronal circuitry, and how their secretion and activity is regulated by other nervous system components.

Behavioral Dissection of Social Feeding

The data presented in Chapter 3 indicate that social feeding is a complex amalgam of behavioral components—high speed on food, bordering, and aggregation—that have different neural dependencies. Within these broad behavioral component definitions, there may be even finer behavioral subclasses. For example, aggregation likely requires separate aerotactic, chemotactic, and other as-yet unidentified cues. When screening for suppressors of social feeding, it may be more informative to study mutants that are defective in only one of these behavioral components.

The generation of microfluidic devices to carefully control the spatial navigation of individual animals[67] could help to dissect social feeding into finer components. For example, these devices could be used to evaluate the effects of pheromone gradients, oxygen shifts, and other controlled stimuli on social feeding. This, in turn, could help inform the design of new genetic screens.

Gap Junction Studies

Electrophysiological analysis will ultimately be necessary to deomonstrate the functionality of RMG gap junctions *in vivo*, and uncover the exact mechanism by which NPR-1 alters circuit dynamics. Several genetic experiments could, however, offer some insights. First, 25 gap junction subunit (innexin) genes are known in *C. elegans*[154], and there are deletion mutants available for most. I crossed many of these mutants into *npr-1*, and did not see suppression of social feeding (Figure 5-1, Table 5-1). There are many possible explanations for the lack of a phenotype: some innexin alleles are lethal, while others may not be complete nulls. Alternatively, innexins could function redundantly in RMG. It would be useful to have a list of innexin genes that are expressed in RMG. SAGE profiling techniques have been used to obtain expression data from specific neuronal cell types in *C. elegans*[155]. The adaptation of the intersectional Cre-Lox method to *C. elegans* has made possible RMG-specific expression; it may therefore be possible to generate SAGE expression information on RMG. An alternative model is that RMG gap junctions are not themselves the conduit by which the cell exerts its effects; rather, they may promote spatial proximity to other important neurons, facilitating the transmission of extrasynaptic signals like neuropeptides or small molecules.

Conclusion

The molecular and cellular dissection of social behavior is a major goal of neurobiology. The results above demonstrate the utility of a simple, genetically tractable organism like *C. elegans* in this endeavor. In addition to understanding the evolutionary

origins of social behaviors, the neuronal circuit I uncovered has anatomical and functional features that are distinct from others that have been studied intensively. It will therefore be a useful system for studying circuit motifs that have otherwise remained poorly understood.

Table 5-1. Innexin mutants crossed to npr-1 (ad609). None significantly suppressed social feeding. unc-7 and unc-9 result in uncoordinated phenotypes that impair social feeding. The locomotion defects and social behavior defect of unc-7;npr-1 can be rescued by expressing unc-7 in the body motorneurons using the oig-1 promoter (not shown).

Strain Name	Genotype
CX10173	*eat-5 (ad464); npr-1 (ad609)*
CX10040	*inx-2 (ok376); npr-1 (ad609)*
CX10042	*inx-7 (tm2738); npr-1 (ad609)*
CX10044	*inx-8 (gk42); npr-1 (ad609)*
CX10028	*inx-9 (ok1502); npr-1 (ad609)*
CX10023	*inx-20 (ok681); npr-1 (ad609)*
CX10195	*inx-22 (tm1661); npr-1 (ad609)*
CX10001	*unc-7 (e5); npr-1 (ad609)*
CX10173	*unc-9 (e101); npr-1 (ad609)*

Figure 5-1. **a**, RNAi against various innexin subunits in an *npr-1;eri-1;lin-15* triple mutant background. No significant social feeding suppression was observed.

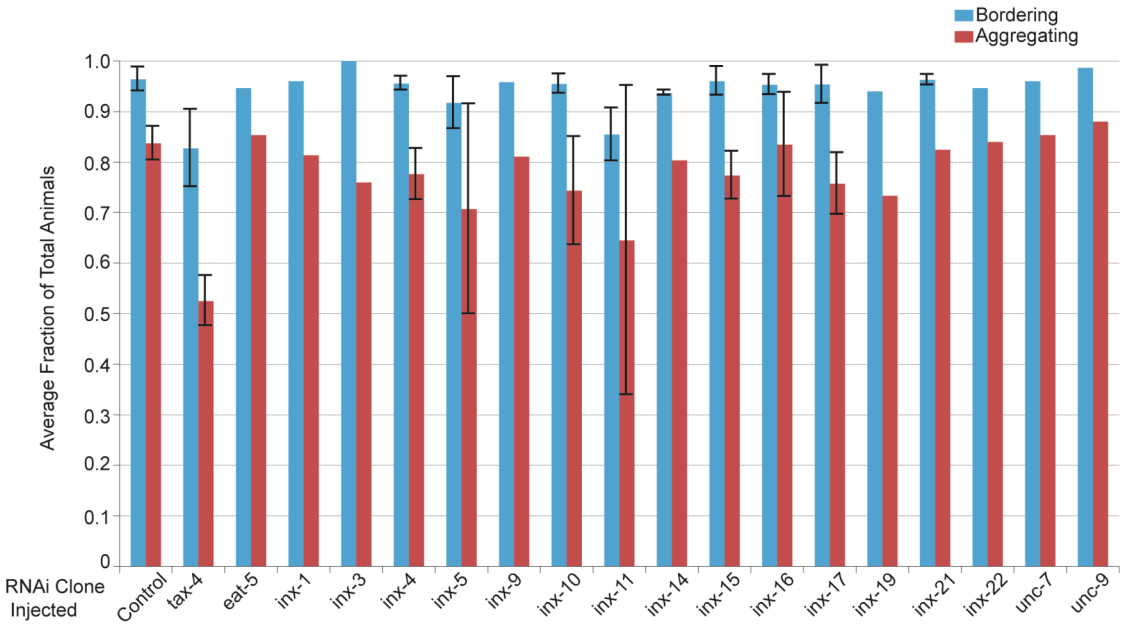

Methods

Behavioral analysis

Exploratory behavior was assayed as described[79]. Individual L4 animals were placed on 35 mm NGM agar plates seeding overnight with OP50 bacteria. 18 hours later, tracks could be seen in the bacteria where the animal had explored. A transparency with 5x5 mm grid squares was superimposed on the plate, and the number of squares in which the animal entered was counted. For a typical experimental condition, five individual animals were assayed and the average exploration was recorded.

Aggregation and bordering behaviors were measured essentially as described[7], using NGM plates seeded with 200 µl OP50 for 48 hours and 150 adult animals per assay. Behaviors were scored two hours after picking the animals to the assay plates. An animal was scored as aggregating if it touched two or more other animals, and bordering if it was less than 2 mm from the edge of the bacterial lawn. To determine the rate of locomotion on food, 10 cm NGM agar plates were seeded with a thin layer of OP50 bacteria and allowed to grow overnight at 25 degrees. A filter paper soaked in 20 mM copper chloride was placed around the perimeter of the plate to avoid animals escaping from view. 20 animals were then picked to the center of the plate, allowed to rest for 1 hour, and filmed for 10 minutes. Average speed was calculated from speed values determined every ten seconds by an automated worm tracker (http://wormsense.stanford.edu/tracker)[156].

Chemotaxis to pheromone was assayed using quadrant plates as described for salt chemoattraction[157], except that a 1:1:1 cocktail of three ascarasides (Supplemental Figure

4A)[19] was added to alternating quadrants instead of NaCl. For each assay, 200 worms were picked to a seeded plate for 2-3 hrs. The worms were then washed three times with chemotaxis buffer, and placed in the center of the assay plate. The population of worms in each quadrant was counted 10 minutes after the start of the assay. A chemotaxis index (C.I.) was calculated as (# of animals on pheromone quadrants - # of animals on buffer quadrants)/(total # of animals).

Osmotic or acute deathmone avoidance was measured using the dry drop test[95]. 8-10 animals per condition were placed on individual NGM plates without food. After 10 min, a small drop of 1M glycerol or 1:1000 diluted deathmone, dispensed from a micropipette, was placed in the path of a forward-moving animal, so that the drop soaked into the agar as the animal reached the drop. A reversal away from the glycerol or deathmone was scored as an avoidance event. Each animal was tested 8-10 times, from which a fractional response was calculated. The avoidance index is the average fractional response for all animals tested in a given condition.

Thermotaxis was assayed as described[60]. Briefly, animals were raised at fixed cultivation temperatures of either 20^{o}C and 25^{o}C. Animals were washed three times in S-basal and placed at the center of a square NGM plate. The plate was affixed to a conductive metal surface using glycerol, under which two Peltier devices created a linear thermal gradient (Figure 4-1B). After 45 minutes, the plate was inverted over chloroform to freeze the position of the worms. The plate was divided into 6 sections, and the number of animals in each of the sections was counted.

Laser Ablation

Cells were ablated at the L1 stage as described[158], and behavior was assayed 48 hours (if L4s were needed, for exploratory behavior) or 72 hours later (if adults were used, for social feeding experiments).

RMG Ablations: For behavioral assays, the RMG inter/motor neurons were targeted for laser killing using a transgenic strain expressing GFP in RMG (*ncs-1::GFP*) and a MicroPoint laser system. Individual ablated animals were examined for the absence of RMG fluorescence to confirm cell death. For calcium imaging experiments, the RMG neurons were identified using Normarski optics based on their position and morphology, then killed with a laser. Adult animals were visually scored for aggregation-related behaviors to confirm the death of RMG.

Other ablations: Most other neurons were identified using Nomarski optics. The AIY neurons were targeted using a *ttx-3::GFP* reporter strain, which marks AIY neurons specifically[105].

Calcium Imaging

Calcium imaging of the AIA and ASK neurons was performed essentially as described[68]. For ASK imaging, the strain CX10982 was used, containing *GCaMP3*.1 (gift from Loren Looger) expressed under the *sra-9* promoter in *npr-1 (ad609)*. For AIA imaging, the strain CX11346 was used, containing *GCaMP3.1* expressed under the T01A4.2 promoter. ASK fluorescence was recorded in the neuronal cell body, and AIA fluorescence was measured in the dorsal AIA process in the nerve ring. The near-uv light wavelengths

used to excite the G-CaMP fluorophore elicited fluorescence changes in ASK; therefore, as described for other light-sensitive neurons[63], the uv-response was desensitized by a two minute light pre-exposure before the beginning of all experiments monitoring ASK and AIA activity. Previous studies are consistent with a possible light-sensitive function of ASK[150], and with a demonstrated light-sensitive activity of the synaptically connected ASJ neurons[150]. All imaging experiments used a 1:1:1 ratio of three ascarosides (Figure 3-5A), each at 1 μM. Behavioral responses to pheromones were examined in strains used for imaging, and resembled those of the parental *npr-1* strains.

To quantify differences in the AIA responses, the average change in fluorescence during the first 5 seconds after presentation of the ascaroside stimulus was calculated for each recording; these values were then averaged together to generate Figure 3-6D**.** Time to half maximal response was calculated using 90% of the highest recorded value as "maximal"; the use of 90% rather than 100% eliminated effects of small fluctuations around the peak value.

Molecular biology

Coding Sequences

The *daf-1* cDNA was amplified by RT-PCR from *C. elegans* mixed stage RNA using the oligonucleotides 5'- agctatcgctagcatgaggatacggcacgtgg-3' and 5'-agctatcggtaccctaaccaagaagtgggcgtg-3' and cloned into the NheI and KpnI sites of pSM-SL2GFP.

The *egl-4f* cDNA was amplified by RT-PCR from *C. elegans* mixed stage RNA using the oligonucleotides 5'- agctagctactagtatgaagaaggtttatgtggtat-3' and 5'-

agctagctggtaccgttcgtatcaataattcattcc-3' and cloned into pSM-SL2GFP using the NheI and KpnI sites.

The *npr-1* cDNA, including 5' and 3' UTRs sequences, was amplified by RT-PCR from *C. elegans* mixed stage RNA using the oligonucleotides 5'-agctacctgctagcacataggccaaatggaagttg-3' and 5'-agctaggtggtaccaaaaaaagatcataaaaactatttcagcaa-3' and cloned into the vector *pSM-SL2GFP* via the NheI and KpnI sites.

The *pkc-1* cDNA was amplified by RT-PCR from *C. elegans* mixed stage RNA using the oligonucleotides 5'-ctgttcacaggcaccgtgcgcgttc-3' and 5'-gtaggtaaaatgcggattgataaatg-3' and cloned into *pSM-SL2GFP* via the NheI and KpnI sites. The gain-of-function A160E mutation was introduced by QuickChange (Stratagene).

Tetanus toxin light chain (TeTx) was amplified from the *Drosophila* tetanus toxin light chain expression vector pTNT (courtesy S. Sweeney, Univ. of York[159]) using the oligonucleotides 5'-gcgatcggatcgctagcatgccgatcaccatcaacaacttcc-3' and 5'-cgcgatccgatggtaccctagcggtacggttgtacaggttt-3'and cloned into the *pSM-mCherry* vector using the NheI and KpnI sites to generated an mCherry fusion protein .

The cleavage-resistant synaptobrevin (crSNB) coding sequence was amplified from a plasmid generously provided by Michael Nonet using the oligonucleotides 5'-agctgcttgctagcggaacagccggataagacc-3' and 5'-agctgcttggtaccgagttttcaacaccattttattcgc-3' and cloned into the *pSM* vector using the NheI and KpnI sites.

The *tax-4* cDNA was amplified by RT-PCR from *C. elegans* mixed stage RNA using the oligonucleotides 5'-agctgcttgctagcatgtcaacggcggaacctg-3' and 5'-

agctgcttggtaccctatttgagcaaggattcagat-3' and cloned into the vector *pSM-SL2GFP* via the NheI and KpnI sites.

A NcoI-SacI fragment containing nCre (Gift of R. Axel) was introduced into the NcoI and SacI sites of *pSM* to generate *pSM-Cre*.

To generate *pSM-LoxPLacZLoxP*, a ~3.5 kb LacZ cDNA fragment from *pJM67* was amplified with oligonucleotides 5'-taccgttcgtatagcatacattatacgaagttatatggtcgttttacaacgtcgtg-3' and 5'-agtagtggatcctattatttttgacaccagac-3' and 5'-gagagagctagctaccgttcgtatagcatacattatacg-3'. The stop sequence was amplified using oligonucleotides 5'-gcgcagagatctaataaagaataaagaataaattt-3' and 5'-gagagagctagctaccgttcgtataatgtatgctat-3' from template oligonucleotides with the sequence 5'-gatctaataaagaataaagaataaatttttttttgaaacatgaaacataacttcgtatagcatacattatacga agttata-3' and 5'-ccggtataacttcgtataatgtatgctatacgaagttatgtttcatgtttcaaaaaaaatt tattctttattctttatta-3'. The LacZ and stop fragments were digested with BglII, ligated with T4 DNA ligase, and used as template for PCR with oligonucleotides 5'-gagagagctagcgataacttcgtatagcatacat-3' and 5'-gagagagctagcgataacttcgtataatgtatgc-3'. The resulting PCR product was digested with NheI and ligated into the NheI site of *pSM-GFP*.

The *egl-21* cDNA was amplified by RT-PCR from *C. elegans* mixed stage RNA using the oligonucleotides 5'-agtcatgcgctagcacacagacaactagagagtcca-3' and 5'-agtcatgcggtaccttaacgacgacgggcaatctc-3' and cloned into pSM-SL2GFP using the NheI and KpnI sites.

The *F39C12.4* genomic sequence was amplified from genomic *N2* DNA using the oligonucleotides 5'- agctgcttgctagcatgggctcctcacctatcct - 3' and 5'- agctgcttggtaccttaacacattgcacttgttt-3' and cloned into the NheI and KpnI sites of pSM-SL2GFP.

A Not-I-Not-I fragment containing GCaMP3.1 (gift from Loren Looger) was introduced into pSM-NOT to generate pSMNOT-GCaMP3.1.

Promoters

All promoters were amplified from N2 wild-type genomic lysates. The sequences of the promoter ends are shown below, along with the concentration at which they were injected for generation of transgenic lines:

nhr-79: cacgatcattttaagccaag, ttttatgctaaaaatgcataaa 10 ng/µl

gcy-27: gtaaactgggagtgaaagcatctcc, tatgctttcagctgtactccttttg 50 ng/µl

gpa-3: ttgaaaattgcataagatctacga, ttgttctttggctaataattttctg 50 ng/µl

tdc-1: gcgcaggaaatcatgctcta, tcgccaagcccgtaaac 50 ng/µl

gpa-15: atttcttcgcatcgattgattc, atcccattctctgtttttc 40 ng/µl

tag-168: aaaaagcaggcttctccttgaagct, tgcaggcgcccacacccagctttct 20 ng/µl

flp-21: tgaggtcacgcaacttgatgatcat, ctccaaaatccaaaaagtcattttc 40 ng/µl

npr-1: ctcgagttctcgtgtttgtgtccgt, ctccattagactaaaaaaatttcag 75 ng/µl

ncs-1: ccaatctgcaataagctttactgtt, agagagaatcaagttgcaaatcaaa 20 ng/µl

sax-7: gacatggatttgggtaaattggtct, ctagatcacgtcgaaagaccaccat 75 ng/µl

gcy-32: atttccattccactgatgatgtgat, attcgaaagcggaaaggaaaatata 50 ng/µl

gcy-36: tggatgttggtagatggggtttgga, aaattcaaacaagggctacccaaca 2 ng/µl

flp-8: gcaatgagtgctcaaatggagtctg, tcagtccacacttttcaagtagaaa 40 ng/µl

r09f10.6: gggcaaggacaatgttgccgcagaa, ttcatacgtcgttattttattccca 50 ng/µl

sra-9: gcatgctatattccaccaaaagaaa, tagcttgtgcatcaatcatagaaca 50 ng/µl

f39c12.4: tcatgtttgcataaactccaaa, gaggagcccctagttggaat 20 ng/µl

Strains

Strains were grown and maintained under standard conditions[43]. Wild-type animals were *C. elegans* Bristol strain N2.

CX4537 *osm-9 (ky10) IV;*

VM384 *ocr-2 (ak47) IV;*

CX7265 *osm-9 (ky10) IV; kyExz053 ["ASH::osm-9" osm-10::osm-9, elt-2::GFP]*

CX9192 *egl-4 (n479) IV;*

CX9579 *egl-4 (n479) IV; kyEx2050 ["ASH+ADL+ASK::egl-4" gpa-15::egl-4f SL2 GFP, ofm-1::dsRed]*

CX9694 *egl-4 (n479) IV; kyEx2121 ["ASI+ASJ+ASK+ASH+ADL::egl-4"nhr-79::egl-4f SL2 GFP, gcy-27::egl-4f SL2 GFP, ofm-1::dsRed]*

DR40 *daf-1 (m40) IV;*

CX9132 *daf-1 (m40) IV*; *kyEx1814 [tdc-1::daf-1 SL2 GFP, elt-2::GFP]*

DA609 *npr-1 (ad609)* X

CX9390-CX9391 *npr-1 (ad609)* X; *kyEx1960-kyEx1961 ["pan-neuronal::npr-1" tag-168::npr-1 SL2 GFP, ofm-1::dsRed]*

CX9395, CX9586 *npr-1 (ad609)* X; *kyEx1965 ,kyEx2057 [gcy-32::npr-1 SL2 GFP, ofm-1::dsRed]*

CX9396, CX9695, CX9777 *npr-1 (ad609)* X; *kyEx1966, kyEx2158, kyEx2122 [flp-21::npr-1 SL2 GFP, ofm-1::dsRed]*

CX9592-CX9594 *npr-1 (ad609)* X; *kyEx2061-kyEx2063 ["endogenous npr-1 promoter::npr-1" npr-1::npr-1 SL2 GFP, ofm-1::dsRed]*

CX9633-CX9634 *npr-1 (ad609)* X; *kyEx2096-kyEx2097 [flp-8::npr-1 SL2 GFP, ofm-1::dsRed]*

CX9641-CX9643 *npr-1 (ad609)* X; *kyEx2104-kyEx2106 [sax-7::npr-1 SL2 GFP, ofm-1::dsRed]*

CX9644-CX9645 *npr-1 (ad609)* X; *kyEx2107-kyEx2108 [ncs-1::npr-1 SL2 GFP, ofm-1::dsRed]*

CX10114 *npr-1 (ad609)* X; *kyEx2295 [ncs-1::nCre, ofm-1::dsRed]*

CX10116 *kyEx2295; kyEx2296 [flp-21::LoxStopLox::GFP, elt-2::mCherry]*

CX10189-CX10190 *npr-1 (ad609)*; *kyEx2295; kyEx2352-kyEx2353 [flp-21::LoxStopLox::npr-1 SL2 GFP, elt-2::mCherry]*

CX9741 *npr-1 (ad609); kyEx2144 [ncs-1::GFP]*

CX10645-CX10646 *kyEx2695-kyEx2696 ["ASI+ASJ+ASK+URX+flp-21::LoxStopLox::pkc-1(gf)" gcy-36::pkc-1(gf), gcy-27::pkc-1(gf), flp-21::LoxStopLox::pkc-1(gf), elt-2::mCherry]*

CX10252-CX10254 *kyEx2385-kyEx2387 [flp-21::pkc-1(gf) SL2 GFP, ofm-1::dsRed]*

CX10386 *kyEx2491 ["URX::pkc-1(gf)" gcy-36::pkc-1(gf) SL2 GFP, ofm-1::dsRed]*

CX4819 *tax-4(p678)* III; *npr-1 (ad609)* X

CX10544-CX10546 *tax-4(p678)* III; *npr-1 (ad609)* X; *kyEx2603-kyEx2605 ["ASJ+URX::tax-4" srh-11::tax-4 SL2 GFP, gcy-36::tax-4 SL2 GFP, elt-2::GFP*]

CX10547-CX10549 *tax-4(p678)* III; *npr-1 (ad609)* X; *kyEx2606-kyEx2608 ["ASK+URX::tax-4" sra-9::tax-4 SL2 GFP, gcy-36::tax-4 SL2 GFP, elt-2::GFP]*

CX10550-CX10552 *tax-4(p678)* III; *npr-1 (ad609)* X; *kyEx2609-kyEx2611 ["ASK+ASJ::tax-4" srh-11::tax-4 SL2 GFP, sra-9::tax-4 SL2 GFP, elt-2::GFP]*

CX10553-CX10555 *tax-4(p678)* III; *npr-1 (ad609)* X; *kyEx2612-kyEx2614 ["ASK+ASJ+URX::tax-4" srh-11::tax-4 SL2 GFP, sra-9::tax-4 SL2 GFP, gcy-36::tax-4 SL2 GFP, elt-2::GFP]*

CX10556 *tax-4(p678)* III; *npr-1 (ad609)* X; *kyEx2615 ["URX::tax-4" gcy-36::tax-4 SL2 GFP, elt-2::GFP]*.

CX11110-CX11112 *tax-4(p678)* III; *kyEx2925-kyEx2927 ["ASJ+ASK::tax-4" srh-11::tax-4 SL2 GFP, sra-9::tax-4 SL2 GFP, elt-2::GFP]*

CX11115-CX11117 *tax-4(p678)* III; *kyEx2930-kyEx2932 ["ASK::tax-4" sra-9::tax-4 SL2 GFP, elt-2::GFP]*

CX11118-CX11120 *tax-4(p678)* III; *kyEx2933-kyEx2935 ["ASJ::tax-4" srh-11::tax-4 SL2 GFP , elt-2::GFP]*

CX10982 *npr-1 (ad609) X; kyEx2866 ["ASK::GCaMP3.1" sra-9::GCaMP3.1 SL2 GFP, ofm-1::GFP]*.

CX11346 *npr-1 (ad609) X; kyEx2916 ["AIA:GCaMP3.1" T01A4.2::GCaMP3.1 SL2 GFP, ofm-1::GFP]*.

CX10007 *npr-1 (ad609)*; *kyEx2257 [gcy-36::TeTx::mCherry, ofm-1::dsRed]*

CX10008-CX10009 *npr-1 (ad609)*; *kyEx2258-kyEx2259 [flp-8::TeTx::mCherry, ofm-1::dsRed]*

CX10191-CX10192 *npr-1 (ad609); kyEx2295; kyEx2354-kyEx2355 [flp-21::LoxStopLox::TeTx::mCherry, elt-2::mCherry]*

CX10388 *kyEx2493 ["pan-neuronal::crSNB" TAG-168::snb-1(Q68V), elt-2::GFP]*

CX10806 npr-1 (ad609); kyEx2295; kyEx2771 ["RMG+ASJ+ASK::TeTx" flp-21::LoxP::TeTx, srh-11::TeTx, sra-9::TeTx, elt-2::mCherry]

CX10809-CX10810 *npr-1 (ad609);kyEx2295;kyEx2774-kyEx2775 ["URX+RMG::TeTx" flp-21::LoxP::TeTx, gcy-36::TeTx, elt-2::mCherry]*

CX10807 *npr-1 (ad609); kyEx2295; kyEx2771; kyEx2772-kyEx2773 [gcy-36::TeTx, elt-2::GFP]*

CB4856 [Hawaiian wild isolate for SNP mapping]

CX10867 *arl-3 (ky891)* II*; npr-1 (ad609)* X

FX01703 *arl-3 (tm1703)* II

CX11011 *pdl-1 (gk157)* II; *npr-1 (ad609)* X

CX10869 *egl-21 (ky893)* IV; *npr-1 (ad609)* X

CX10043 *unc-31 (e928)* IV; *npr-1 (ad609)* X

MT1241 *egl-21 (n611) IV;*

CX8634 *F39C12.4 (tm2385)* X

CX8633 *F14F4.1 (tm2243)* X.

CX7943-CX7944 *kyEx1177-kyEx1178 ["ceVP OE" F39C12.4::F39C12.4 SL2 CFP, elt-2::CFP]*

CB1111 *cat-1 (e1111)* X

MT9668 *mod-1 (ok103)* V.

References

[1] *Wilson, E. O., Sociobiology: The New Synthesis, Twenty-fifth Anniversary Edition. (Harvard University Press, Cambridge, 2000).*

[2] *Ayre, D.J., Inter-genotype aggression in the solitary sea anemone Actinia tenebrosa. Marine Biology 68, 199-205 (1982).*

[3] *Howe, N.R. and Sheikh, Y.M., Anthopleurine: A sea anemone alarm pheromone. Science 189, 386-388 (1975).*

[4] *Borden, J.H., Aggregation pheromones. (University of Texas Press, Austin, 1982).*

[5] *Raffa, K.F., Mixed messages across multiple trophic levels: the ecology of bark beetle chemical communication systems. Chemoecology 11, 49-65. (2001).*

[6] *Hansen, K., Reception of the bark beetle pheromone in the predacious clerid beetle, Thanasimus formicarius. Journal of Comparative Physiology 150 (1983).*

[7] *de Bono, M. and Bargmann, C. I., Natural variation in a neuropeptide Y receptor homolog modifies social behavior and food response in C. elegans. Cell 94, 679-689 (1998).*

[8] *Wertheim, B., van Baalen, E.A., Dicke, M., and Vet, L.E., Pheromone-mediated aggregation in nonsocial arthropods. Annual Review of Entomology 50, 321-346. (2004).*

[9] *Croll, N.A., Components and patterns in the behavior of the nematode Caenorhabditis elegans. J. Zool. (London) 176, 159-176 (1975).*

[10] *Mayr, E., What Evolution Is. (Basic Books, New York, 2001).*

[11] *Vander Meer, R.K. and Alonso, L.E., Pheromone Directed Behavior in Ants. (Westview Press, Boulder, CO, 1998).*

[12] *Obin, M.S. and Vander Meer, R.K., Alate semiochemicals release worker behavior during fire ant nuptial flights. Journal of Entological Science 29, 143-151 (1994).*

[13] *Barr, M. M. and Garcia, L. R., Male mating behavior. WormBook, 1-11 (2006).*

[14] *Liu, K. S. and Sternberg, P. W., Sensory regulation of male mating behavior in Caenorhabditis elegans. Neuron 14, 79-89 (1995).*

[15] *Simon, J. M. and Sternberg, P. W., Evidence of a mate-finding cue in the hermaphrodite nematode Caenorhabditis elegans. Proc Natl Acad Sci U S A 99, 1598-1603 (2002).*

[16] *Srinivasan, J. et al., A blend of small molecules regulates both mating and development in Caenorhabditis elegans. Nature 454, 1115-1118. (2008).*

[17] *Jeong, P.Y. et al., Chemical structure and biological activity of the Caenorhabditis elegans dauer-inducing pheromone. Nature 433, 541-545 (2005).*

[18] *Butcher, R.A., Fujita, M., Schroeder, F.C., and Clardy, J., Small-molecule pheromones that control dauer development in Caenorhabditis elegans. Nature Chemical Biology 3, 420-422. (2007).*

[19] *Butcher, R.A., Ragains, J.R., Kim, E., and Clardy, J., A potent dauer pheromone component in Caenorhabditis elegans acts synergistically with other components. Proceedings of the National Academy of Sciences 105, 14288-14292. (2008).*

[20] *Godin, J.J., Behavioural Ecology of Teleost Fishes. (Oxford University Press, 1997).*

[21] *Pitcher, T.J. and Parrish, J.K., Functions of Shoaling Behavior in Teleosts. (Chapman and Hall, London, 1993).*

[22] *Gray, J.M. et al., Oxygen sensation and social feeding mediated by a C. elegans guanylate cyclase homologue. Nature 430, 317-322 (2004).*

[23] *Osborne, K. A. et al., Natural behavior polymorphism due to a cGMP-dependent protein kinase of Drosophila. Science 277, 834-836 (1997).*

[24] *Ben-Shahar, Y., Robichon, A., Sokolowski, M. B., and Robinson, G. E., Influence of gene action across different time scales on behavior. Science 296, 741-744 (2002).*

[25] *Grozinger, C. M., Sharabash, N. M., Whitfield, C. W., and Robinson, G. E., Pheromone-mediated gene expression in the honey bee brain. Proc Natl Acad Sci U S A 100 Suppl 2, 14519-14525 (2003).*

[26] *Leng, G. and Ludwig, M., Neurotransmitters and peptides: whispered secrets and public announcements. J Physiol 586, 5625-5632 (2008).*

[27] *Lim, M. M., Bielsky, I. F., and Young, L. J., Neuropeptides and the social brain: potential rodent models of autism. Int J Dev Neurosci 23, 235-243 (2005).*

[28] *Baumgartner, T., Heinrichs, M., Vonlanthen, A., Fischbacher, U., and Fehr, E., Oxytocin shapes the neural circuitry of trust and trust adaptation in humans. Neuron 58, 639-650 (2008).*

[29] *Nishimori, K. et al., Oxytocin is required for nursing but is not essential for parturition or reproductive behavior. Proc Natl Acad Sci U S A 93, 11699-11704 (1996).*

[30] *Bielsky, I. F., Hu, S. B., Szegda, K. L., Westphal, H., and Young, L. J., Profound impairment in social recognition and reduction in anxiety-like behavior in vasopressin V1a receptor knockout mice. Neuropsychopharmacology 29, 483-493 (2004).*

[31] *Clarke, A. and File, S. E., Selective neurotoxin lesions of the lateral septum: changes in social and aggressive behaviours. Pharmacol Biochem Behav 17, 623-628 (1982).*

[32] *Dickson, B.J., Wired for Sex: The Neurobiology of Drosophila Mating Decisions. Science 322, 904-909 (2008).*

[33] *Sturtevant, A.H., Experiments on sex recognition and the problem of sexual selection in Drosophila. Animal Behavior 5, 351-366. (1915).*

[34] *Bartelt, R.J., Schaner, A.M., and Jackson, L.L., cis-Vaccenyl acetate as an aggregation pheromone in Drosophila melanogaster. Journal of Chemical Ecology 11, 1747-1756 (1985).*

[35] *Kurtovic, A., Widmer, A., and Dickson, B.J. , A single class of olfactory neurons mediates behavioural responses to a Drosophila sex pheromone. Nature 446, 542-546 (2007).*

[36] *Benton, R., Vannice, K. S., and Vosshall, L. B., An essential role for a CD36-related receptor in pheromone detection in Drosophila. Nature 450, 289-293 (2007).*

[37] *Jin, X., Ha, T. S., and Smith, D. P., SNMP is a signaling component required for pheromone sensitivity in Drosophila. Proc Natl Acad Sci U S A 105, 10996-11001 (2008).*

[38] *Laughlin, J. D., Ha, T. S., Jones, D. N., and Smith, D. P., Activation of pheromone-sensitive neurons is mediated by conformational activation of pheromone-binding protein. Cell 133, 1255-1265 (2008).*

[39] *Datta, S. R. et al., The Drosophila pheromone cVA activates a sexually dimorphic neural circuit. Nature 452, 473-477 (2008).*

[40] *Stockinger, P., Kvitsiani, D., Rotkopf, S., Tirian, L., and Dickson, B.J., Neural circuitry that governs Drosophila male courtship behavior. Cell 121, 795-807 (2005).*

[41] *Demir, E. and Dickson, B. J., fruitless splicing specifies male courtship behavior in Drosophila. Cell 121, 785-794 (2005).*

[42] *Kimura, K., Hachiya, T., Koganezawa, M., Tazawa, T., and Yamamoto, D., Fruitless and doublesex coordinate to generate male-specific neurons that can initiate courtship. Neuron 59, 759-769 (2008).*

[43] *Brenner, S., The genetics of Caenorhabditis elegans. Genetics 77, 71-94 (1974).*

[44] *Stiernagle, T., Maintenance of C. elegans. WormBook, 1-11 (2006).*

[45] *Mello, C. and Fire, A., DNA transformation. Methods Cell Biol. 48, 451-482 (1995).*

[46] *Fire, A. et al., Potent and specific genetic interference by double-stranded RNA in Caenorhabditis elegans. Nature 391, 806-811 (1998).*

[47] *Kennedy, S., Wang, D., and Ruvkun, G., A conserved siRNA-degrading RNase negatively regulates RNA interference in C. elegans. Nature 427, 645-649 (2004).*

[48] *Sulston, J. E. and Horvitz, H. R., Post-embryonic cell lineages of the nematode, Caenorhabditis elegans. Dev. Biol. 56, 110-156 (1977).*

[49] *White, J. G., Southgate, E., Thomson, J. N., and Brenner, S., The structure of the nervous system of Caenorhabditis elegans. Philos Trans R Soc Lond B Biol Sci 314, 1-340 (1986).*

[50] *Chalfie, M. et al., The neural circuit for touch sensitivity in Caenorhabditis elegans. J Neurosci 5, 956-964 (1985).*

[51] *Chalfie, M. and Sulston, J., Developmental genetics of the mechanosensory neurons of Caenorhabditis elegans. Dev. Biol. 82, 358-370 (1981).*

[52] *de Bono, M. and Maricq, A. V., Neuronal substrates of complex behaviors in C. elegans. Annu Rev Neurosci 28, 451-501 (2005).*

[53] *Bargmann, C. I., Hartwieg, E., and Horvitz, H. R., Odorant-selective genes and neurons mediate olfaction in C. elegans. Cell 74, 515-527 (1993).*

[54] *Mori, I. and Ohshima, Y., Neural regulation of thermotaxis in Caenorhabditis elegans. Nature 376, 344-348 (1995).*

[55] *Komatsu, H., Mori, I., Rhee, J. S., Akaike, N., and Ohshima, Y., Mutations in a cyclic nucleotide-gated channel lead to abnormal thermosensation and chemosensation in C. elegans. Neuron 17, 707-718 (1996).*

[56] *Barr, M. M. and Sternberg, P. W., A polycystic kidney-disease gene homologue required for male mating behaviour in C. elegans. Nature 401, 386-389 (1999).*

[57] *Rankin, C. H., Beck, C. D., and Chiba, C. M., Caenorhabditis elegans: a new model system for the study of learning and memory. Behav Brain Res 37, 89-92 (1990).*

[58] *L'Etoile, N.D. and Bargmann, C.I., Olfaction and odor discrimination are mediated by the C. elegans guanylyl cyclase ODR-1. Neuron 25, 575-586 (2000).*

[59] *Zhang, Y., Lu, H., and Bargmann, C., Pathogenic bacteria induce aversive olfactory learning in Caenorhabditis elegans. Nature 438, 179-184 (2005).*

[60] *Ryu, W. S. and Samuel, A. D., Thermotaxis in Caenorhabditis elegans analyzed by measuring responses to defined Thermal stimuli. J Neurosci 22, 5727-5733 (2002).*

[61] *Pierce-Shimomura, J. T., Morse, T. M., and Lockery, S. R., The fundamental role of pirouettes in Caenorhabditis elegans chemotaxis. J Neurosci 19, 9557-9569 (1999).*

[62] *Berg, H. C. and Brown, D. A., Chemotaxis in Escherichia coli analysed by three-dimensional tracking. Nature 239, 500-504 (1972).*

[63] *Hilliard, M.A. et al., In vivo imaging of C. elegans ASH neurons: cellular response and adaptation to chemical repellants. Embo J 24, 63-72 (2005).*

[64] *Kerr, R. et al., Optical imaging of calcium transients in neurons and pharyngeal muscle of C. elegans. Neuron 26, 583-594 (2000).*

[65] *Raizen, D. M. and Avery, L., Electrical activity and behavior in the pharynx of Caenorhabditis elegans. Neuron 12, 483-495 (1994).*

[66] *Goodman, M. B., Hall, D. H., Avery, L., and Lockery, S. R., Active currents regulate sensitivity and dynamic range in C. elegans neurons. Neuron 20, 763-772 (1998).*

[67] *Chronis, N., Zimmer, M., and Bargmann, C.I., Microfluidics for in vivo imaging of neuronal and behavioral activity in Caenorhabditis elegans. Nature Methods 4, 727-731 (2007).*

[68] *Chalasani, S.H. et al., Dissecting a circuit for olfactory behaviour in Caenorhabditis elegans. Nature 450, 63-70. (2007).*

[69] *Lockery, S. R. et al., Artificial dirt: microfluidic substrates for nematode neurobiology and behavior. J Neurophysiol 99, 3136-3143 (2008).*

[70] *Davis, R.B., Herreid, C.F., and Short, H.L., Mexican free-tailed bat in Texas. Ecological Monographs 32, 311-346 (1962).*

[71] *Stevens, D.A. and Saplikoski, N.J., Rats' reactions to conspecific muscle and blood: evidence for an alarm substance. Behavioral Biology 8, 75-82. (1973).*

[72] *Von Fisch, K. , Zur psychologie des Fische-Schwarmes. Naturewissenschafen 26, 601-606. (1938).*

[73] *Stowe, M.K., Turlings, T.C., Loughrin, J.H., Lewis, W.J., and Tumlinson, J.H., The chemistry of evesdropping, alarm, and deceit. Proceedings of the National Academy of Sciences 92, 23-28. (1995).*

[74] *Snyder, N. and Snyder, H., Alarm response of Diadema antillarum. Science 168 (1970).*

[75] *Smith, R.J., Alarm signals in fishes. Reviews in Fish Biology and Fisheries 2, 33-63. (1992).*

[76] *Winslow, J.T., Infant vocalization, adult aggression, and fear behavior of an oxytocin null mutant. Hormones and Behavior 35, 144-155 (2000).*

[77] *White, J.Q. et al., The sensory circuitry for sexual attraction in C. elegans males. Current Biology 17, 1847-1857. (2007).*

[78] *Perry, G. and Pianka, E.R., Animal foraging: past, present and future. Ecology and Evolution 12, 360-364 (1997).*

[79] *Fujiwara, M., Sengupta, P., and McIntire, S. L., Regulation of body size and behavioral state of C. elegans by sensory perception and the EGL-4 cGMP-dependent protein kinase. Neuron 36, 1091-1102 (2002).*

[80] *Shtonda, B. B. and Avery, L., Dietary choice behavior in Caenorhabditis elegans. J Exp Biol 209, 89-102 (2006).*

[81] *Albert, P. S., Brown, S. J., and Riddle, D. L., Sensory control of dauer larva formation in Caenorhabditis elegans. J Comp Neurol 198, 435-451 (1981).*

[82] *Bargmann, C. I. and Horvitz, H. R., Control of larval development by chemosensory neurons in Caenorhabditis elegans. Science 251, 1243-1246 (1991).*

[83] *Ren, P. et al., Control of C. elegans larval development by neuronal expression of a TGF-beta homolog. Science 274, 1389-1391 (1996).*

[84] *Schackwitz, W.S., Inoue, T., and Thomas, J.H., Chemosensory neurons function in parallel to mediate a pheromone response in C. elegans. Neuron 17, 719-728 (1996).*

[85] *White, J.G., Southgate, E., Thomson, J.N., and Brenner, S., The structure of the nervous system of the nematode Caenorhabditis elegans. Phil. Transact. R. Soc. Lond. B 314, 1-340 (1986).*

[86] *Tomioka, M. et al., The insulin/PI 3-kinase pathway regulates salt chemotaxis learning in Caenorhabditis elegans. Neuron 51, 613-625 (2006).*

[87] *Gray, J.M., Hill, J.J., and Bargmann, C.I., A circuit for navigation in Caenorhabditis elegans. Proc Natl Acad Sci USA 102, 3184-3191 (2005).*

[88] *Zheng, Y., Brockie, P. J., Mellem, J. E., Madsen, D. M., and Maricq, A. V., Neuronal control of locomotion in C. elegans is modified by a dominant mutation in the GLR-1 ionotropic glutamate receptor. Neuron 24, 347-361 (1999).*

[89] *Greer, E.R., Perez, C.L., Van Gilst, M.R., Lee, B.H., and Ashrafi, K., Neural and molecular dissection of a C. elegans sensory circuit that regulates fat and feeding. Cell Metabolism 8, 118-131 (2008).*

[90] *Daniels, S. A., Ailion, M., Thomas, J. H., and Sengupta, P., egl-4 acts through a transforming growth factor-beta/SMAD pathway in Caenorhabditis elegans to regulate multiple neuronal circuits in response to sensory cues. Genetics 156, 123-141 (2000).*

[91] *L'Etoile, N.D. et al., The cyclic GMP-dependent protein kinase EGL-4 regulates olfactory adaptation in C. elegans. Neuron 36, 1079-1089 (2002).*

[92] *Available at www.wormbase.org.*

[93] *Bishop, N. A. and Guarente, L., Two neurons mediate diet-restriction-induced longevity in C. elegans. Nature 447, 545-549 (2007).*

[94] *Bilgrami, A.L., Gaugler, R., and Brey, C., Prey preference and feeding behaviour of the diplogastrid predator Mononchoides gaugleri. Nematology 7, 333-342 (2005).*

[95] *Hilliard, M. A., Bargmann, C. I., and Bazzicalupo, P., C. elegans responds to chemical repellents by integrating sensory inputs from the head and the tail. Curr Biol 12, 730-734 (2002).*

[96] *Hodgkin, J. and Doniach, T., Natural variation and copulatory plug formation in Caenorhabditis elegans. Genetics 146, 149-164 (1997).*

[97] *Rogers, C. et al., Inhibition of Caenorhabditis elegans social feeding by FMRFamide-related peptide activation of NPR-1. Nat Neurosci. 6, 1178-1185 (2003).*

[98] *Hammock, E.A. and L.J., Young, Oxytocin, vasopressin and pair bonding: implications for autism. Philosophical Transactions of the Royal Society of London (B) 361, 2187-2198. (2006).*

[99] *de Bono, M., Tobin, D. M., Davis, M. W., Avery, L., and Bargmann, C. I., Social feeding in Caenorhabditis elegans is induced by neurons that detect aversive stimuli. Nature 419, 899-903 (2002).*

[100] *Cheung, B.H., Cohen, M., Rogers, C., Albayram, O., and de Bono, M., Experience-dependent modulation of C. elegans behavior by ambient oxygen. Curr. Biol. 15, 905-917 (2005).*

[101] *Davies, A. G., Bettinger, J. C., Thiele, T. R., Judy, M. E., and McIntire, S. L., Natural variation in the npr-1 gene modifies ethanol responses of wild strains of C. elegans. Neuron 42, 731-743 (2004).*

[102] *Coates, J. C. and de Bono, M., Antagonistic pathways in neurons exposed to body fluid regulate social feeding in Caenorhabditis elegans. Nature 419, 925-929 (2002).*

[103] *Sze, J.Y., Zhang, S., Li, J., and Ruvkun, G., The C. elegans POU-domain transcription factor UNC-86 regulates the tph-1 tryptophan hydroxylase gene and neurite outgrowth in specific serotonergic neurons. Development 129, 3901-3911 (2002).*

[104] *Etchberger, J.F. and Hobert, O., Vector-free DNA constructs improve transgene expression in C. elegans. Nature Methods 5, 3 (2008).*

[105] *Hobert, O. et al., Regulation of interneuron function in the C. elegans thermoregulatory pathway by the ttx-3 LIM homeobox gene. Neuron 19, 345-357 (1997).*

[106] *Plummer, M.R., Rittenhouse, A., Kanevsky, M., and Hess, P., Neurotransmitter modulation of calcium channels in rat sympathetic neurons. Journal of Neuroscience 11, 2339-2348 (1991).*

[107] *Toth, P.T., Bindokas, V.P., Bleakman, D., Colmers, W.F., and Miller, R.J., Mechanism of presynaptic inhibition of neuropeptide Y at sympathetic nerve terminals. Nature 364, 635-639 (1993).*

[108] *Bargmann, C. I., Thomas, J. H., and Horvitz, H. R., Chemosensory cell function in the behavior and development of Caenorhabditis elegans. Cold Spring Harb Symp Quant Biol 55, 529-538 (1990).*

[109] *Mori, I., Genetics of chemotaxis and thermotaxis in the nematode Caenorhabditis elegans. Annu Rev Genet 33, 399-422 (1999).*

[110] *Schiavo, G. et al., Tetanus and botulinum-B neurotoxins block neurotransmitter release by proteolytic cleavage of synaptobrevin. Nature 359, 832-835 (1992).*

[111] *Sweeney, S.T., Broadie, K., Keane, J., Niemann, H., and O'Kane, C.J., Targeted expression of tetanus toxin light chain in Drosophila specifically eliminates synaptic transmission and causes behavioral defects. Neuron 14, 341-351 (1995).*

[112] *Nakashiba, T., Young, J.Z., McHugh, T.J., Buhl, D.L., and Tonegawa, S., Transgenic inhibition of synaptic transmission reveals role of CA3 output in hippocampal learning. Science 319, 1260-1264 (2008).*

[113] *Chang, A.J., Chronis, N., Karow, D.S., Marletta, M.A., and Bargmann, C.I., A distributed chemosensory circuit for oxygen preference in C. elegans. PLoS Biology 4, e274 (2006).*

[114] *Sieburth, D. et al., Systematic analysis of genes required for synapse structure and function. Nature 436, 510-517 (2005).*

[115] *Sieburth, D., Madison, J.M., and Kaplan, J.M., PKC-1 regulates secretion of neuropeptides. Nature Neuroscience 10, 49-57 (2007).*

[116] *Okochi, Y., Kimura, K.D., Ohta, A., and Mori, I., Diverse regulation of sensory signaling by C. elegans nPKC-epsilon/eta TTX-4. Embo J 24, 2127-2137 (2005).*

[117] *Nakai, J., Ohkura, M., and Imoto, K., A high signal-to-noise Ca(2+) probe composed of a single green fluorescent protein. Nat. Biotechnol. 19, 137-141 (2001).*

[118] *Suzuki, H. et al., Functional asymmetry in Caenorhabditis elegans taste neurons and its computational role in chemotaxis. Nature 454, 114-117 (2008).*

[119] *Linari, M., Hanzal-Bayer, M., and Becker, J., The delta subunit of rod specific cyclic GMP phosphodiesterase, PDE delta, interacts with the Arf-like protein Arl3 in a GTP specific manner. FEBS Letters 458, 55-59 (1999).*

[120] *Zhang, H. et al., Photoreceptor cGMP phosphodiesterase delta subunit functions as a prenyl-binding protein. Journal of Biological Chemistry 279, 407-413 (2004).*

[121] *Zhang, H. et al., Deletion of PrBP/delta impedes transport of GRK1 and PDE6 catalytic subunits to photoreceptor outer segments. Proceedings of the National Academy of Sciences 104, 8857-8862 (2007).*

[122] *Jacob, T. C. and Kaplan, J. M., The EGL-21 carboxypeptidase E facilitates acetylcholine release at Caenorhabditis elegans neuromuscular junctions. J Neurosci 23, 2122-2130 (2003).*

[123] *Kim, K. and Li, C., Expression and regulation of an FMRFamide-related neuropeptide gene family in Caenorhabditis elegans. Journal of Comparative Neurology 475, 540-550 (2004).*

[124] *Ribelayga, C., Cao, Y., and Mangel, S.C., The circadian clock in the retina controls rod-cone coupling. Neuron 59, 790-801 (2008).*

[125] *Thompson, R.J., Zhou, N., and MacVicar, B.A., Ischemia opens neuronal gap junction hemichannels. Science 312, 924-927 (2006).*

[126] *Adermark, L. and Lovinger, D.M, Ethanol effects on electrophysiological properties of astrocytes in striatal brain slices. Neuropharmacology 51, 1099-1108 (2006).*

[127] *Berger, A. J., Hart, A. C., and Kaplan, J. M., G alphas-induced neurodegeneration in Caenorhabditis elegans. J Neurosci 18, 2871-2880 (1998).*

[128] *Maricq, A. V., Peckol, E., Driscoll, M., and Bargmann, C. I., Mechanosensory signalling in C. elegans mediated by the GLR-1 glutamate receptor. Nature 378, 78-81 (1995).*

[129] *Chen, B. L., Hall, D. H., and Chklovskii, D. B., Wiring optimization can relate neuronal structure and function. Proc Natl Acad Sci U S A 103, 4723-4728 (2006).*

[130] *Karl, T. et al., Y1 receptors regulate aggressive behavior by modulating serotonin pathways. Proceedings of the National Academy of Sciences 101, 12742-12747 (2004).*

[131] *Marchant, E.G., Watson, N.V., and Mistlberger, R.E., Both neuropeptide Y and serotonin are necessary for entrainment of circadian rhythms in mice by daily treadmill running schedules. Journal of Neuroscience 17, 7974-7987 (1997).*

[132] *Kalra, S.P., Clark, J.T., Sahu, A., Dube, M.G., and Kalra, P.S., Control of feeding and sexual behaviors by neuropeptide Y: physiological implications. Synapse 2, 254-257 (1988).*

[133] *Stanley, B.G. and Leibowitz, S.F., Neuropeptide Y injected in the paraventricular hypothalamus: a powerful stimulant of feeding behavior. Proceedings of the National Academy of Sciences 82, 3940-3943 (1985).*

[134] *Gehlert, D.R., Role of hypothalamic neuropeptide Y in feeding and obesity. Neuropeptides 33, 329-338. (1999).*

[135] *Klauber, L.M., Rattlesnakes, their habits, life histories, and influenceon mankind. (University of California Press, Berkley, 1972).*

[136] *Graves, B.M., Halpern, M., and Friesen, J.L., Snake aggregation phermones: Source and chemosensory mediation in western ribbon snakes (Thamnophis proximus). Journal of Comparative Psychology 105, 140-144. (1991).*

[137] *Lockery, S.R. et al., Artificial dirt: microfluidic substrates for nematode neurobiology and behavior. Journal of Neurophysiology 99, 3136-3143 (2008).*

[138] *Thomas, JH, Birnby, DA, and Vowels, JJ, Evidence for parallel processing of sensory information controlling dauer formation in Caenorhabditis elegans. Genetics 134, 1105-1117 (1993).*

[139] *Hammock, E. A. and Young, L. J., Microsatellite instability generates diversity in brain and sociobehavioral traits. Science 308, 1630-1634 (2005).*

[140] *Daikoku, R. et al., Body water balance and body temperature in vasopressin V1b receptor knockout mice. Auton Neurosci 136, 58-62 (2007).*

[141] *Hedgecock, E. M. and Russell, R. L., Normal and mutant thermotaxis in the nematode Caenorhabditis elegans. Proc Natl Acad Sci U S A 72, 4061-4065 (1975).*

[142] *Ramot, D., MacInnis, B. L., and Goodman, M. B., Bidirectional temperature-sensing by a single thermosensory neuron in C. elegans. Nat Neurosci 11, 908-915 (2008).*

[143] *Kozak, W. et al., Molecular mechanisms of fever and endogenous antipyresis. Ann N Y Acad Sci 917, 121-134 (2000).*

[144] *Mahajan-Miklos, S., Tan, M. W., Rahme, L. G., and Ausubel, F. M., Molecular mechanisms of bacterial virulence elucidated using a Pseudomonas aeruginosa-Caenorhabditis elegans pathogenesis model. Cell 96, 47-56 (1999).*

[145] *Zhang, Y., Lu, H., and Bargmann, C. I., Pathogenic bacteria induce aversive olfactory learning in Caenorhabditis elegans. Nature 438, 179-184 (2005).*

[146] *Colosimo, M.E. et al., Identification of thermosensory and olfactory neuron-specific genes via expression profiling of single neuron types. Curr Biol. 14, 2245-2251 (2004).*

[147] *Satterlee, J. S. et al., Specification of thermosensory neuron fate in C. elegans requires ttx-1, a homolog of otd/Otx. Neuron 31, 943-956 (2001).*

[148] *Andrews, Z. B., Diano, S., and Horvath, T. L., Mitochondrial uncoupling proteins in the CNS: in support of function and survival. Nat Rev Neurosci 6, 829-840 (2005).*

[149] *Sabatini, B. L. and Regehr, W. G., Timing of neurotransmission at fast synapses in the mammalian brain. Nature 384, 170-172 (1996).*

[150] *Ward, A., Liu, J., Feng, Z., and Xu, X.Z., Light-sensitive neurons and channels mediate phototaxis in C. elegans. Nature Neuroscience 11, 916-922. (2008).*

[151] *Isaac, R. E., Eaves, L., Muimo, R., and Lamango, N., N-acetylation of biogenic amines in Ascaridia galli. Parasitology 102 Pt 3, 445-450 (1991).*

[152] *Husson, S. J. et al., Impaired processing of FLP and NLP peptides in carboxypeptidase E (EGL-21)-deficient Caenorhabditis elegans as analyzed by mass spectrometry. J Neurochem 102, 246-260 (2007).*

[153] *Nelson, L. S., Rosoff, M. L., and Li, C., Disruption of a neuropeptide gene, flp-1, causes multiple behavioral defects in Caenorhabditis elegans. Science 281, 1686-1690 (1998).*

[154] *Starich, T., Sheehan, M., Jadrich, J., and Shaw, J., Innexins in C. elegans. Cell Commun Adhes 8, 311-314 (2001).*

[155] *Blacque, O.E. et al., Functional genomics of the cilium, a sensory organelle. Curr Biol. 15, 935-941 (2005).*

[156] *Ramot, D., Johnson, B.E., Berry, T.L., Carnell, L., Goodman, M.B., The Parallel Worm Tracker: a platform for measuring average speed and drug-induced paralysis in nematodes. PLoS ONE 3, e2208. (2008).*

[157] *http://www.wormbook.org/chapters/www_behavior/behavior.html.*

[158] *Bargmann, C. I. and Avery, L., Laser killing of cells in Caenorhabditis elegans. Methods Cell Biol 48, 225-250 (1995).*

[159] *Sweeney, S.T., Broadie, K., Keane, J., Niemann, H., O'Kane, C.J., Targeted expression of tetanus toxin light chain in Drosophila specifically eliminates synaptic transmission and causes behavioral defects. Neuron 14, 341-351 (1995).*